

MODELLING OF BIOBARRIER
OF REMEDIATION AT LEAD CONTAMINATED SITES

Miss Duangjai Khankruer



บทคัดย่อและแฟ้มข้อมูลฉบับเต็มของวิทยานิพนธ์ตั้งแต่ปีการศึกษา 2554 ที่ให้บริการในคลังปัญญาจุฬาฯ (CUIR)
เป็นแฟ้มข้อมูลของนิสิตเจ้าของวิทยานิพนธ์ ที่ส่งผ่านทางบัณฑิตวิทยาลัย

The abstract and full text of theses from the academic year 2011 in Chulalongkorn University Intellectual Repository (CUIR)
are the thesis authors' files submitted through the University Graduate School.

A Dissertation Submitted in Partial Fulfillment of the Requirements
for the Degree of Doctor of Philosophy Program in Environmental Management

(Interdisciplinary Program)

Graduate School

Chulalongkorn University

Academic Year 2014

Copyright of Chulalongkorn University

แบบจำลองคณิตศาสตร์ของตัววางก้นชีวภาพเพื่อศึกษาการชะของดินปนเปื้อนตะกั่ว



วิทยานิพนธ์นี้เป็นส่วนหนึ่งของการศึกษาตามหลักสูตรปริญญาวิทยาศาสตรดุษฎีบัณฑิต
สาขาวิชาการจัดการสิ่งแวดล้อม (สหสาขาวิชา)
บัณฑิตวิทยาลัย จุฬาลงกรณ์มหาวิทยาลัย
ปีการศึกษา 2557
ลิขสิทธิ์ของจุฬาลงกรณ์มหาวิทยาลัย

Thesis Title	MODELLING OF BIOBARRIER OF REMEDICATION AT LEAD CONTAMINATED SITES
By	Miss Duangjai Khankruer
Field of Study	Environmental Management
Thesis Advisor	Assistant Professor Thidarat Bunsri, Ph.D.
Thesis Co-Advisor	Associate Professor Muttucumaru Sivakumar, Ph.D.

Accepted by the Graduate School, Chulalongkorn University in Partial
Fulfillment of the Requirements for the Doctoral Degree

..... Dean of the Graduate School
(Associate Professor Sunait Chutintaranond, Ph.D.)

THESIS COMMITTEE

..... Chairman
(Assistant Professor Chantra Tongcumpou, Ph.D.)

..... Thesis Advisor
(Assistant Professor Thidarat Bunsri, Ph.D.)

..... Thesis Co-Advisor
(Associate Professor Muttucumaru Sivakumar, Ph.D.)

..... Examiner
(Associate Professor Jin Anotai, Ph.D.)

..... Examiner
(Assistant Professor Ekawan Luepromchai, Ph.D.)

..... Examiner
(Pichet Chaiwiwatworakul, Ph.D.)

..... External Examiner
(Pattanan Tarin, Ph.D.)





CONTENTS

	Page
THAI ABSTRACT	iv
ENGLISH ABSTRACT.....	v
ACKNOWLEDGEMENTS	vi
CONTENTS.....	vii
LIST OF TABLES	xii
LIST OF FIGURES	xiv
LIST OF SYMBOLS	xvi
LIST OF ABBREVIATIONS.....	xviii
CHAPTER 1 INTRODUCTION	1
1.1 Preamble	1
1.2 Justification of Research.....	1
1.3 Objectives	2
1.4 Hypotheses.....	3
1.5 Expected Outcomes	3
1.6 Structure of Theses	3
CHAPTER 2 THEORETICAL BACKGROUND AND LITERATURE REVIEWS.....	5
2.1 Theoretical background	5
2.1.1 Lead	5
2.1.1.1 Lead in environment.....	5
2.1.1.2 Lead-contaminated soil found in Kanchanaburi, Thailand	7
2.1.1.3 Lead and microbes.....	9
2.1.2 Transport	11
2.1.2.1 Distribution of Lead in Soils	11
2.1.2.2 Distribution of Lead in Groundwater	11
2.1.3 Lead remediation techniques.....	13
2.2.2.1 Permeable reactive barriers	13
2.2.2.2 Possible Occurrence Mechanisms	17

	Page
2.2.2.3 Biosorption	17
2.2.3.4 Bioaccumulation.....	18
2.2 Literature reviews	20
2.2.1 Biobarrier.....	20
2.2.1.1 Media.....	21
2.2.1.2 Microorganisms.....	23
2.2.1.3 Substrate Solution.....	23
Molasses	23
Phosphorus.....	24
2.2.2 Existing models for lead remediation/transport	24
CHAPTER 3 A CONCEPTUAL MODEL FOR BIOBARRIER.....	26
3.1 Development of conceptual model	26
3.2 Mass balance.....	27
3.3 Transport part.....	27
3.3.1 Saturated porous media	28
3.3.2 Variably saturated porous media.....	28
3.3.3 Consolidation of porous media.....	28
3.4 Soil hydraulic properties equation	29
3.5 Reaction part.....	29
3.5.1 Biosorption process	30
3.5.1.1 Langmuir isotherm	30
3.5.1.2 Freundlich isotherm.....	30
3.5.2 Bioaccumulation process.....	31
3.5.2.1 Modified Gompertz model	31
3.5.2.2 Monod kinetics equation	31
CHAPTER 4 MATERIALS AND THE EXPERIMENTAL SET-UP.....	33
4.1 Experimental framework	33
4.2 Materials	35
4.2.1 Sand–manure sample preparation	35

	Page
4.2.2 Zeolite preparation	35
4.2.3 Substrate preparation	36
4.2.3.1 Sand-manure column.....	36
4.2.3.2 Zeolite column.....	36
4.2.4 Contaminant preparation	36
4.2.5 Soil column fabrication	36
4.2.5.1 Sand-manure column.....	36
4.2.5.2 Zeolite column.....	37
4.3 Sand/Zeolite characterisation.....	37
4.4 Filtered water characterization.....	38
4.5 Adsorption isotherm test.....	39
4.6 Biosorption test.....	39
4.6.1 Sand-manure column.....	39
4.6.2 Zeolite column.....	39
4.7 Bioaccumulation test	40
4.8 Development of synthetic biobarrier	40
4.8.1 Sand-manure column.....	40
4.8.2 Zeolite column.....	41
4.9 Microbial communities identification.....	41
4.9.1 DNA extraction and purification	41
4.9.2 PCR amplification	41
4.9.3 DGGE.....	42
4.9.4 Sequencing of DGGE bands.....	43
4.9.4.1 Amplification of DNA and purification of PCR products.....	43
4.9.4.2 Cloning of PCR products	43
4.9.4.3 Plasmid extraction	44
4.9.4.4 Digestion of recombinant plasmid by restriction enzyme	44
4.9.4.5 Nucleotide base sequencing	44
4.10 Pb species detection.....	44

	Page
CHAPTER 5 EXPERIMENTAL OBSERVATION	47
5.1 Sand-manure biobarrier	47
5.1.1 Properties of manure and substrate solution.....	47
5.1.2 Biofilm formation.....	48
5.1.3 Bioaccumulation test	51
5.1.4 Biosorption test.....	53
5.1.5 Mechanism between Pb(II) and microbial community	56
5.2 Zeolite Biobarrier.....	59
5.2.1 Inoculum and biobarrier properties	59
5.2.2 Adsorption of Pb onto zeolite.....	62
5.2.3 Biosorption and bioaccumulation of Pb onto biobarrier	62
5.2.4 Mechanism between Pb(II) and microbial community	70
CHAPTER 6 MODELLING OF DEVELOPED BIOBARRIER.....	72
6.1 Hydraulic properties curve.....	72
6.2 Zeolite column test	74
6.2.1 Gravitational infiltration system.....	74
6.2.2 Gravitational infiltration and capillary force system.....	79
6.2.3 Dispersion transport in the laboratory scale zeolite column	81
6.3 Quality of filtered effluent from zeolite column.....	83
6.4 Application of contaminant transport model	88
CHAPTER 7 CONCLUSION AND RECOMMENDATION	91
7.1 General approaches.....	91
7.2 Specific approaches	92
7.3 Recommendations for future research	93
REFERENCES	94
APPENDIX.....	94
APPENDIX A.....	95
APPENDIX B	144
APPENDIX C	150

	Page
APPENDIX D.....	153
APPENDIX E.....	156
APPENDIX F.....	161
VITA.....	168



LIST OF TABLES

TABLE	PAGE
Table 2.1 Acceptable level of lead in the natural resources.....	7
Table 2.2 Summary of pollutants removed by PRB.....	15
Table 2.3 Advantages and limitations of the PRB technology	16
Table 2.4 Summary of previous adsorption of Pb(II) at the different pH.	18
Table 2.5 The comparison between biosorption and bioaccumulation [41]	19
Table 2.6 Summary of previous biobarrier applications.	20
Table 2.7 Media use in PRB.....	22
Table 4.1 Parameters and analytical methods for testing of soil properties.....	38
Table 4.2 Nucleotide sequences of primers used in this study.....	42
Table 4.3 The reagents for five fractions of sequential extraction method.....	45
Table 5.1 Properties of manure and molasses	47
Table 5.2 Possible functional group at assigned wave number.....	50
Table 5.3 Functional group of biopolymer appeared in artificial biosorbent.....	50
Table 5.4 Constants for Monod equation	52
Table 5.5 Parameters of adsorption isotherm on manure and biosorbent	52
Table 5.6 Microbial communities profile determined with PCR-DGGE of partial 16S rRNA genes fragments in sand-manure biobarrier.....	57
Table 5.7 Adsorption constant rate of Pb(II) batch adsorption on sorbent	62
Table 5.8 Adsorption constant rate of Pb(II) column adsorption on sorbent.....	62
Table 5.9 Chemical forms of Pb in biomaterial based zeolite, zeolite column fed Pb(II) and Biosorbent based zeolite.....	68
Table 5.10 Chemical forms of Pb in biomaterial based zeolite, zeolite column fed Pb(II) and Biosorbent based zeolite.....	68

TABLE	PAGE
Table 5.11 Constants for Monod equation of biobarrier	70
Table 5.12 Microbial communities profile determined with PCR-DGGE of partial 16S rRNA genes fragments in zeolite biobarrier	71
Table 6.1 Constant empirical coefficients for van Genuchten equations	73
Table 6.2 Constants for hydraulic properties	74
Table 6.3 Inputs for Pb(II) movement pass through zeolite column	74
Table 6.4 Inputs for Pb(II) movement pass through zeolite column	79
Table 6.5 Average diffusion-dispersion coefficients for zeolite column	82
Table 6.6 Inputs parameters for Pb(II) movement pass through zeolite column.....	83
Table 6.7 Inputs parameters for Pb(II) movement pass through zeolite column (continued).....	84
Table 6.8 Constants for Pb(II) movement in zeolite biobarrier	87
Table 6.9 Inputs parameters for Pb(II) movement pass through sand-manure barrier ...	88
Table 6.10 Inputs parameters for Pb(II) movement pass through sand-manure barrier (continued).....	89

LIST OF FIGURES

FIGURE	PAGE
Figure 1.1 The Framework of this research	4
Figure 2.1 Principle controls on free trace metal concentration in soils solution	7
Figure 2.2 Cross-section illustrating the temporary landfill of lead tailing sediment and its surrounding area.....	8
Figure 2.3 Metal-microbe interactions impacting bioremediation.....	10
Figure 2.4 Depiction of various types of bacterial interaction with heavy metals polluted soils	10
Figure 2.5 The hydrologic.....	12
Figure 2.6 The concept of PRB.....	14
Figure 2.7 The solubility diagram for Pb in Nibley clay loam soil	24
Figure 3.1 Conceptual model of biobarrier	26
Figure 4.1 Experimental framework	34
Figure 4.2 Physical appearances of materials (a) sand; (b) manure; (c) sand- manure.....	35
Figure 4.3 Physical appearances of (a) clean zeolite; (b) zeolite after seived	35
Figure 4.4 The experiment set up.....	37
Figure 4.5 Experimental setup	40
Figure 5.1 Physical appearance of biofilm on the top layer of biosorbent	48
Figure 5.2 FT-IR spectra of biosorbent and biomaterial.....	49
Figure 5.3 Biosorbent is fitted with modified Gompertz model	51
Figure 5.4 Specific substrate utilisation rate fitted by Monod model	53
Figure 5.5 The sequential extraction of sand-manure biobarrier	55

FIGURE	PAGE
Figure 5.6 Bands for sequencing to identify the species of microbial	56
Figure 5.7 Scanning electron microscopy (SEM) images of (a) Sand-manure (b,c,d) Sand-manure Biobarrier	58
Figure 5.8 Removal efficiencies of (a) COD and (b) Pb(II) in suspended growth SBR and attached growth on column A-1	60
Figure 5.9 Removal efficiencies of (a) COD and (b) Pb(II) in biobarrier (column A-1) and fresh zeolite (column A-2).....	61
Figure 5.10 FTIR results of zeolite and biobarrier.....	63
Figure 5.11 XRD peaks in (a) zeolite	65
Figure 5.12 XRD peaks in biofilm layer at middle of biobarrier.....	66
Figure 5.13 XRD peaks in (c) upper biofilm layer of zeolite biobarrier	67
Figure 5.14 Sequential extraction of zeolite biobarrier.....	69
Figure 5.15 Scanning electron microscopy (SEM) images of (a,b) Zeolite (c,d) Zeolite Biobarrier	71
Figure 6.1 Water retention curve on zeolite sample	73
Figure 6.2 Pressure Head (cmH ₂ O) of zeolite column at 1, 2, 4, 8 12 and 24 hours...	75
Figure 6.3 Pressure Head (cmH ₂ O) of zeolite column at 48, 60 and 72 hours	76
Figure 6.4 Volumetric water content (θ) of zeolite column at 1, 2, and 4 hours	76
Figure 6.5 Volumetric water content (θ) of zeolite column at 8,12, 24, 48, 60 and 72 hours.....	77
Figure 6.6 Simulation of time series of elevated pressure head in zeolite column using Richards' and van Genuchten equations (datum at the column test).....	78
Figure 6.7 Pressure Head (cmH ₂ O) versus time	80
Figure 6.8 Volumetric water content (θ) of zeolite column.....	81
Figure 6.9 Pb(II) concentration profiles in zeolite biobarrier	85
Figure 6.10 Pb(II) concentration profiles in sand-manure biobarrier	89

LIST OF SYMBOLS

C	Mass concentration of Pb(II) (M/L^3)
C/C_0	Refers to the reduction of substrate and Pb(II)
C_e	Concentration of Pb(II) at equilibrium (M/L^3)
C_0	Initial concentration of Pb(II) (M/L^3)
C_s	Amount of Pb(II) adsorbed (M/M) at equilibrium
D	Diffusivity coefficient (M/L^2)
D_z	Parameter determined by using Richards' equation
e	Euler Number (2.718)
g	Magnitude of gravitational acceleration (L/T^2)
I_{pb}	Empirical term for Pb(II) inhibition
K	Fully saturation permeability (L/T)
K_s	Half saturate concentration constant (mg COD/L)
K_F	Freundlich constant related to adsorption capacity of adsorbent
k_{rw}	Relative hydraulic conductivity [unitless]
K_z	Fully saturated hydraulic conductivity [$L T^{-1}$]
p	Empirical parameters yielded from the hydraulic properties curve [unitless]
q	Darcy's velocity (L/T)
q_z	Parameter determined by using Richards' equation
m	Empirical parameters yielded from the hydraulic properties curve [unitless]
n	Porosity
$R_{\text{biosorption}}$	Net rates of Pb(II) by biosorption and bioaccumulation reaction (M/L^3-T)
$R_{\text{bioaccumulation}}$	Net rates of Pb(II) by biosorption and bioaccumulation reaction (M/L^3-T)
S_s	Specific storativity (1/L)
t	Time interval [T]
x	Distance of flow path (L), elevation head [L]
μ_{max}	Maximum specific growth rate (1/h)

GREEK LETTERS

ψ	Pressure head [L]
ρ	Fluid density (M/L ³)
$\frac{\partial \psi}{\partial x}$	Hydraulic gradient (unitless)
μ	Fluid viscosity (M/L-T)
μ_m	Specific substrate consumption rate
λ	Delay reaction time (T)
θ	Volumetric water content [cm ³ /cm ³]
θ_r	Residual moisture content [cm ³ /cm ³]
θ_s	Saturated moisture content [cm ³ /cm ³]
θ_{10}	Volumetric moisture content at 10 kPa [cm ³ /cm ³]
ρ_B	Soil bulk density [g/cm ³]
ρ_w	Density of water [g/cm ³]

LIST OF ABBREVIATIONS

APHA	American Public Health Association
ASTM	American Society for Testing and Materials International
COD	Chemical oxygen demand
MATLAB	MATrix LABoratory programme
MO	Microorganism
ODE	Ordinary differential equation
PDE	Partial differential equation
R^2	Residual square
USDA	United States Department of Agriculture
VG	van Genuchten's hydraulic properties model

CHAPTER 1

INTRODUCTION

1.1 Preamble

The problem of lead, Pb(II) contamination in groundwater is being seriously concerned as a major source of metal(loid)s reaching food chain, mainly through plant uptake and animal transfer [1]. The slag or residual lead contained high concentration, which can be flushed by precipitation to surface and groundwater resource. The species of free lead ion are predominantly observed at the contaminated sites and these ions can transport and pose the risk on ecological and human health [2]. In order to prevent the movement of lead at source, the in-situ remediation technique might be employed. A permeable reactive barrier (PRB) or biobarrier is a novel technology for remediating lead ions. The biobarrier involves the media and active microbial communities, which can separate the ionic Pb from aqueous solution by biosorption and bioaccumulation. The media can act as the habitat of biofilm producing microbes, the common media are included the zero-valence iron, limestone, granular activated carbon and zeolites [3, 4]. However, the growth of biofilm and the formation of PRB are little known [5, 6].the mechanisms between biofilm and ionic Pb are adsorption, ion-exchange, precipitation, oxidation/reduction, and complexation [7].

In order to access the stability of PRB, a mathematical model is developed to evaluate the retardation and migration of ionic lead through a constructed biobarrier. The unsaturated transport model is modified to determine the inflow-outflow of percolation wastewater. The growth of biofilm forming and their activities are involved in the model, the biosorption and bioaccumulation of Pb(II) on the synthesized biobarrier are included in the source/sink term.

1.2 Justification of Research

Lead contaminated soil is one of the serious environmental issues. It strongly retained with sorption, retardation and surface precipitation. As soils are heterogeneous; it consists of minerals, organic constituents and pore spaces. It can form complexes with other chemicals and have biological interactions including

oxidation-reduction, precipitation, dissolution and volatilization. Heavy metals are not biodegradable, they tend to accumulate in living organisms and many heavy metal ions are known to be toxic or carcinogenic such as zinc, copper, nickel, mercury, cadmium, lead and chromium. The heavy metals are widely distributed in air, water, surface, subsurface soils. Lead was accumulated into aquatic animals that consumed it, resulting in lead poisoning under natural condition [8, 9]. Biobarrier can remediate and stabilise lead in a long term period, if the optimum condition is known [10, 11]. The installation, operation and maintenance of biobarrier were estimated based on experience. The key parameters of biobarrier which can reduce the pore velocity are the microscopic flow and microbial metabolism processes presented in process of bioclogging and media consolidation.

The existing models of biobarrier can predict the remediation of considered contaminants; however, it might not exactly predict the effect of lead accumulated, bioclogging and consolidation of media on the bioremediation. Hence, current research is established to make a better tool for modelling the biobarrier for lead contaminated soil and groundwater.

1.3 Objectives

This study aimed to develop a mathematical model to evaluate the retardation and migration of ionic lead through a constructed biobarrier. Therefore, the major objectives for this research were established as follows.

1.3.1 To define the reaction terms relating the microbial activities and Pb(II) retardation.

1.3.2 To apply the numerical technique and to produce computational code by MATLAB technical language.

1.3.3 To calibrate and verify the model by using experimental result and historical data.

1.4 Hypotheses

The research was driven by the following hypotheses:

1.4.1 The acclimatised biofilm can actively reduce the migration of lead by biosorption and bioaccumulation.

1.4.2 Zeolite can be applied as the adsorbent, which microbes can adhere. Zeolite itself can also adsorb Pb(II), hence the zeolite based biobarrier can enhance the retardation of Pb migration.

1.4.3 The sorbed phosphorus on zeolite could increase the stabilisation of Pb(II) by forming the insoluble lead phosphate minerals.

1.5 Expected Outcomes

The developed mathematical model for predicting the transport of active species of Pb(II) in the biobarrier.

1.6 Structure of Theses

This dissertation consists of the following chapters.

Chapter 1	Introduction
Chapter 2	Theoretical background and literature reviews
Chapter 3	A conceptual model for biobarrier
Chapter 4	Materials and experimental set-up
Chapter 5	Experimental observation
Chapter 6	Modelling of developed biobarrier
Chapter 7	Conclusions and recommendation

The framework of this research is given in Figure 1.1.

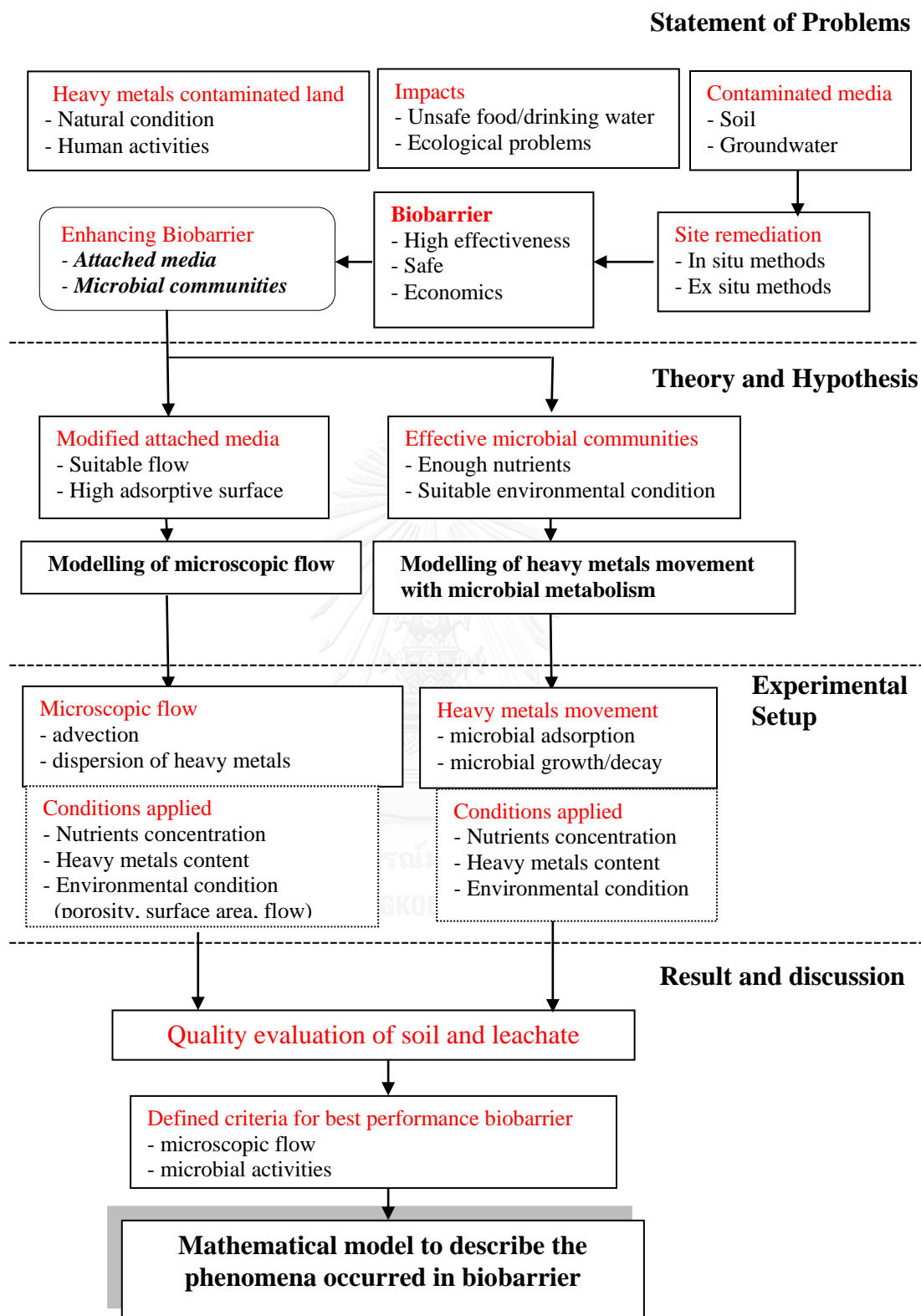


Figure 1.1 The Framework of this research

CHAPTER 2

THEORETICAL BACKGROUND AND LITERATURE REVIEWS

2.1 Theoretical background

2.1.1 Lead

Lead is one of the elements in carbon group (Group 14) with a symbol of Pb which derived from a Latin word of “*plumbum*”. It has an atomic number of 82. Lead is a post-transition metal, the metallic lead has a bluish white colour; however, it will change to gray when exposed to air. Lead in a liquid form will have a chrome silver luster. Lead's physical and chemical properties include high density, softness, ductility and malleability, poor electrical conductivity compared to other metals, high corrosion resistance, and ability to react with organic chemicals. Lead is the natural and heaviest non-radioactive element; it is often bounded with sulfide, carbonate and oxide compounds, it also combined with other elements in the ores. Lead was normally found in a form of galena (lead sulfide, PbS), cerrusite (lead carbonate, PbCO₃), anglesite (lead sulfate, PbSO₄) and lead oxide (Pb₃O₄). Lead is classified as a transition element with three various valence states that are 0, +2 and +4. The normal state of lead is +2 that can be written as Pb(II). The compounds of Pb (II) can be able to form an ionic bond with other elements, but the higher valence state of Pb(IV) compounds could create only covalent bonds with other elements.

2.1.1.1 Lead in environment

The release of Pb(II) into the environment is a real concern for humankind and environmental toxicologists. Because Pb(II) is not biodegradable and has a long biological half-life, it has the capability to accumulate within the organism and can cause poisoning, illnesses and neurological disorders to mankind and living creatures. Lead occurs naturally in the environment. However, most lead found in the environment are a result of human activities. Anthropogenic activities are the major

source of contaminants in soils and water including the use of pesticides, herbicides, and fertilizers in agriculture and mining. These activities add various organic and inorganic contaminants to the soil, which make the soil unsafe for humans, animals, plants, and microbes.

The accumulation of metals in sediments and land systems has increased continuously as a result of industrial emissions, mining activities, and other human activities. There were many possible pathways for the fate and moving of lead in natural system especially in soil and groundwater. The exposure of lead was varied depending on background concentration of lead in natural sources and human activities [12]. Groundwater was contaminated with lead because of industrial and agriculture activities, landfilling, mining and transportation system [13]. Most of lead found in the land often attached onto reactive soil particles. Soluble lead added to the soil reacts with clays, phosphates, sulfates, carbonates, hydroxides and organic matter [14].

Multiphase equilibria must be considered when defining metal behavior in soils (Figure 2.1) [15]. Metals in the soil solution are subjected to mass transfer out of the system by leaching to groundwater, plant uptake, or volatilization. At the same time, metals participate in chemical reactions with the soil solid phase. The concentration of metals in the soil solution, at any given time, is governed by a number of interrelated processes including inorganic and organic complexation, oxidation-reduction reactions, precipitation/dissolution reactions and adsorption/desorption reactions. Metals will form soluble complexes with inorganic and organic ligands. Common inorganic ligands are SO_4^{2-} , Cl^- , OH^- , PO_4^{3-} , NO_3^- , CO_3^{2-} . The primary processes influencing the fate of Pb in soil include adsorption, ion exchange, precipitation, and complexation with sorbed organic matter [5, 14].

Lead could be effectively entering human body through inhalation, ingestion, dermal contact or transfer via the placenta. In young children, lead intake was via hand to mouth and foods that could directly harm to ingestion system. Lead could be cumulated in the human body and it could chronically harm to human health. Lead could strictly affect the central nervous system [16]. The risk of lead on human health

was highly concerned so the standards and guidelines were established to limit the level of lead in water and soil, as summary in Table 2.1.

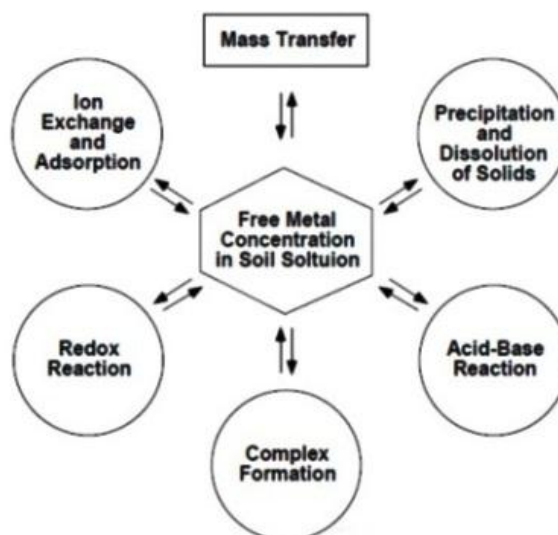


Figure 2.1 Principle controls on free trace metal concentration in soils solution

Table 2.1 Acceptable level of lead in the natural resources

Natural resources	EPA	WHO standards (2008)	Thailand standards By PCD*
Drinking water	0.015 mg/L	0.01 mg/L 10µg/L	0.05 mg/L
Agriculture soil	< 400 mg/kg	-	< 400 mg/kg
Effluent from Industry	-	-	< 0.2 mg/L
Surface water	-	-	0.05 mg/L
Groundwater	-	-	< 0.01 mg/L

* PCD: Pollution Control Department

2.1.1.2 Lead-contaminated soil found in Kanchanaburi, Thailand

Environmental issues related to mining activities can include erosion, formation of sinkholes, loss of biodiversity and the contamination of soil, groundwater and surface water by chemicals. Contamination resulting from leakage of chemicals can sequentially affect the health of the local population if not properly

controlled. An example of pollution from mining activities in Thailand which produced massive amounts of environmental damage that last for several years or even decades is located in the Lower Klity Village, Tongpaphoom District, Kanchanaburi Province. It was found out that the water in the village creek was contaminated with high levels of lead. The inorganic lead dissolved out from the creek and flowed into the floor sediments and resulted to a large amount of lead-tainted sediment.

There was a mineral mining processing plant up stream of the village which has been operated from more than 30 years with a provision of license-concession agreement. In the smelter site area, 8 pits of lead tailing sediment (closed temporary landfill of lead tailing sediment as shown in Figure 2.2) with 2 m depth and capacity size of 1,355 m³ or 2,886 ton were found. The tailing sediment was tested and found to contain 52,000 to 170,700 ppm of lead while the standard acceptable limit level in water must be approximately less than 200 ppm [17]. The geological test survey suggested that the deep soil sediment was contaminated with lead since the old ancient period of mining.

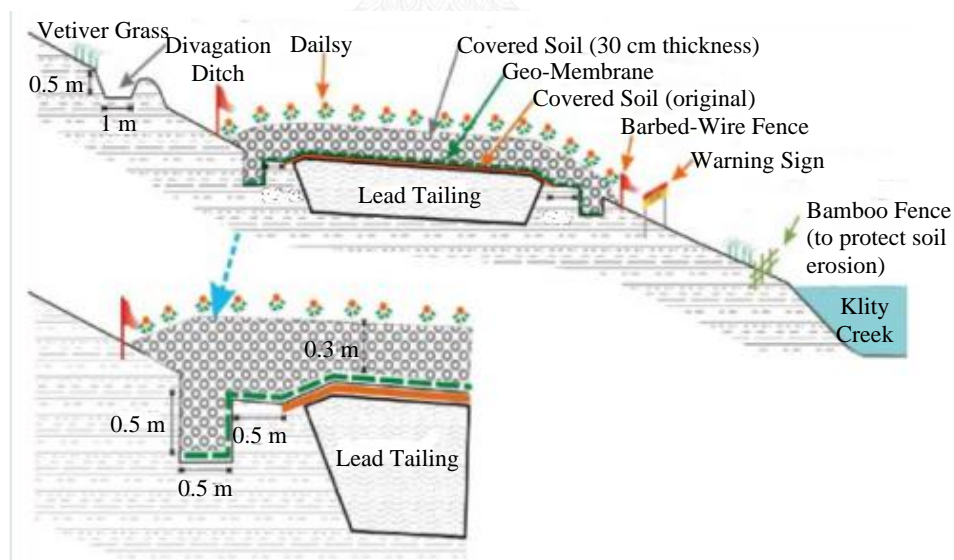


Figure 2.2 Cross-section illustrating the temporary landfill of lead tailing sediment and its surrounding area

Majority of people live at Lower Klity Creek are subsistence farmers growing rice, cassava, and vegetables. It was reported that the villagers and their pets consumed water directly from the creek, as the only source of water provided for their livelihood, both for livestock and irrigated cultivation, without the knowledge of water toxicity. Many of the plaintiffs suffer the symptoms of chronic lead poisoning, such as abdominal pain, fatigue, headaches, and mood changes. Some of their children have severe intellectual and developmental disabilities [2, 18].

2.1.1.3 Lead and microbes

Lead is difficult to remove from the environment because it cannot be degraded chemically or biologically. In addition, lead toxic is occurred at low concentration and its toxic effects last longer [19]. Furthermore, some metals may transform from less toxic species into more toxic forms under some environmental conditions [20]. The effects of lead to cell depend upon the type of lead concentration and substance in the environment of the cell. If lead is at high concentration, then it will completely destroy the cell [21]. Although high-concentration lead is highly toxic to microbes, scientists still believe that microbes can deal with lead toxic issue in the environment in which lead concentration is low [22]. Microorganisms are responsible for many diseases but they can play an important part and give some contribution to the ecosystems by removing environmental pollutants. Bacteria play a major role in modern medicine and agriculture, and have profound ecological impact. The mechanisms of metal-microbe interactions impacting bioremediation are shown in Figure 2.3[23] and Figure 2.4[19] shows the depiction of various types of bacterial interaction with heavy metals polluted soils.

The ability of the microbes to multiply rapidly can enhance the removal of lead since termination of lead is to enter the tissue or attach on the cell surface. With this advantage, it boosts the scientists to research the microbial cells that can be used to reduce the amount of lead in the environment. Nonetheless, when compared to the chemical usage method, these microbial alternatives were typically found to be less effective and more costly.

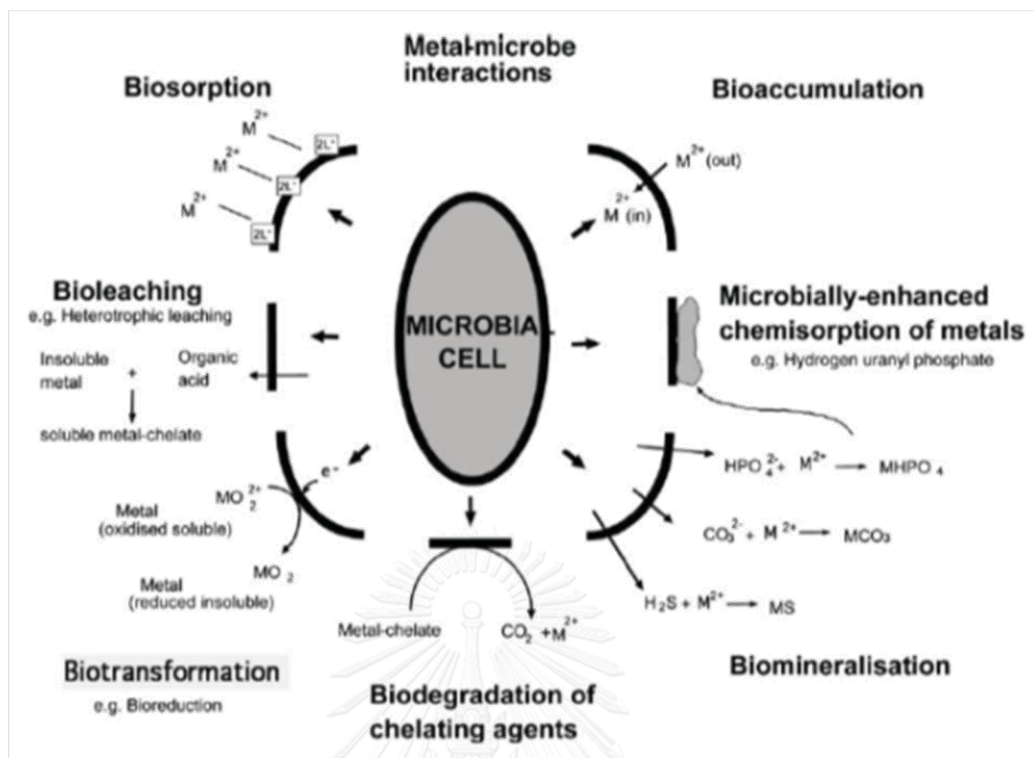


Figure 2.3 Metal-microbe interactions impacting bioremediation

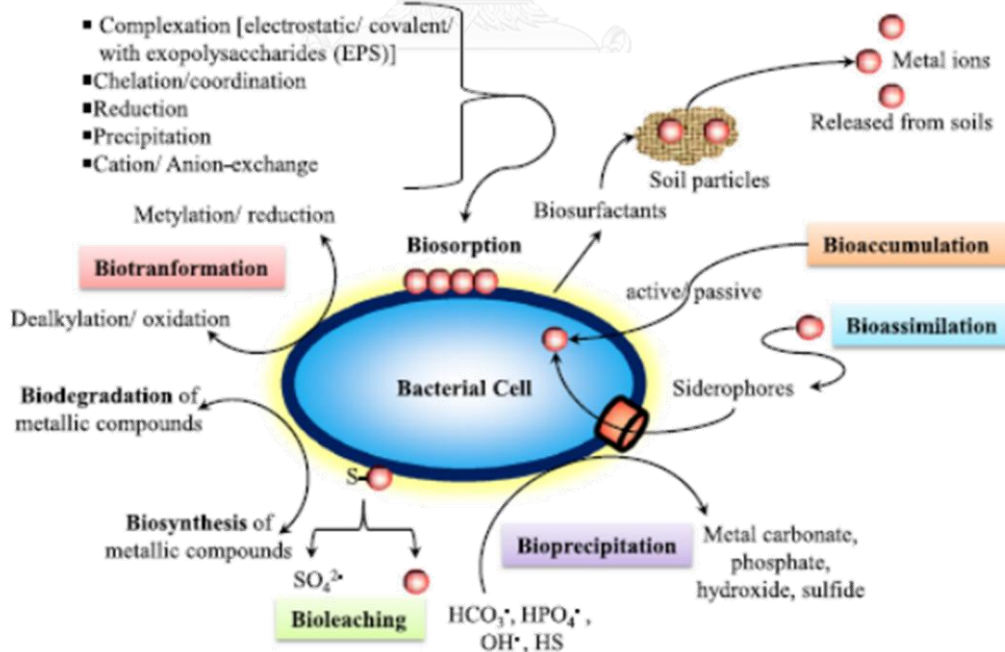


Figure 2.4 Depiction of various types of bacterial interaction with heavy metals polluted soils

2.1.2 Transport

2.1.2.1 *Distribution of Lead in Soils*

As Pb(II) migrated into soils, they can distribute in one or more of the following forms: (1) Solved in soil solution (pore water), (2) Inhabiting exchange sites on inorganic soil constituents, (3) Specifically adsorbed on inorganic soil constituents, (4) Related with insoluble soil organic matter, (5) Precipitated as pure or mixed solids, and (6) Present in the structure of minerals. The first four categories relate to the behavior of lead ions in the solution. Precipitation of lead (the fifth form) will occur only when it is present at the concentration higher than its solubility. The last fraction normally occurred, if metals were appeared in natural soils that had been subjected to various geological processes. The metal present in natural soil are able to be simply categorized into three phases: (1) aqueous phase, (2) adsorbed phase and (3) solid phase [14].

2.1.2.2 *Distribution of Lead in Groundwater*

Groundwater is one of the most important component and constitutes to human life and economic activity. It is accounted for about two thirds of the freshwater resources of the world and, if the polar ice caps and glaciers are not considered, groundwater accounts for nearly all usable freshwater. The dominant role of groundwater resources is clear of their use and protection. Fresh or underground water can be divided into two zones; the unsaturated zone and the saturated zone.

When rain falls, some infiltrates into the soil. Part of this moisture is taken up by the roots of plants and some moves deeper under the influence of gravity. In the rock nearest to the ground surface, the empty spaces are partly filled with water and partly with air. This is known as the unsaturated or vadose zone, and can vary in depth from nothing to tens of meters.

At greater depths, all the empty spaces are completely filled with water and this is called the saturated or phreatic zone. If a hole is dug or drilled down into the saturated zone, water will flow from the soil matrix into the hole and settle at the depth below which all the pore spaces are filled with water. This level is the water table and forms the upper surface of the saturated zone, at which the fluid pressure in

the pores is exactly atmospheric. Strictly speaking, the term groundwater refers only to the saturated zone below the water table. The water in the saturated zone is absorbed vertically or horizontally. Through discharge from the aquifers so called springs or seepage; then it evaporates back into the hydrologic cycle again cycle [24] Shown in Figure 2.5(<http://www.kgs.ku.edu/Publications/pic22>).

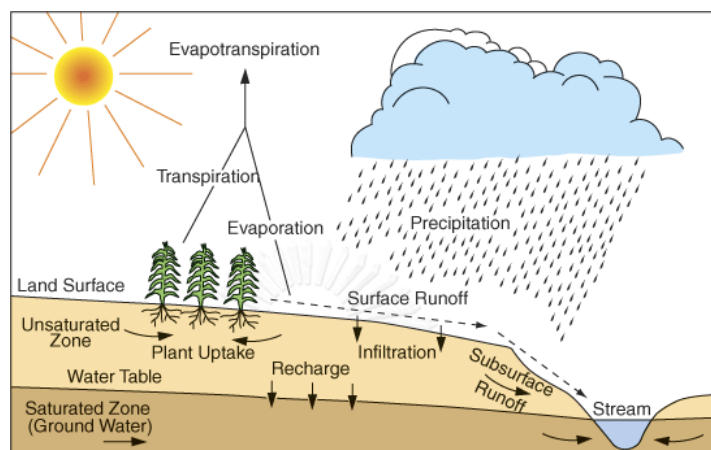


Figure 2.5 The hydrologic

The aqueous phase is referred to the metals remaining in soil solution as free metals ions, e.g., Cd^{2+} , Ni^{2+} , Zn^{2+} , Cr^{3+} and as several dissolved complexes, e.g., CdSO_4^0 , ZnCl^+ , CdCl_3^- . Metals are able to form soluble complexes with inorganic and organic ligands. The potential for migration (mobility) of metals in soils will possibly be higher, if higher amounts of metals are present in the aqueous phase. Metals in the aqueous phase are readily transported by advection and dispersion. The adsorbed phase is defined as the accumulation of metal ions at the interface between soil solids and aqueous phase. This phase is associated with the surface of soil solids such as organic matter, soil minerals, iron and manganese oxides and hydroxides, carbonates and amorphous aluminosilicates. The solid phase is implied to metals in a precipitate form. These precipitates could stay in solid phase and they may contain pure solids or mixed solids. Mixed solids are formed whenever several elements could be co-precipitated. The solids phase is perhaps present in which metal concentrations are significantly higher than their solubility limits. The metals that presented in solid phase could immobile in soils, meaning the solid phase metals are stagnantly occupied.

Almost tests of isotherms are subjected to simulate the probable levels of Pb either release from soil or adsorb onto soil under expected physiochemical environments covering the service life of soil. The classical tests of isotherm do not adequately simulate intermittent leaching and adsorption conditions at the long term. The Pb contaminated soil and Pb distribution are significant factors with respect to the leaching/adsorption rate of Pb onto soil. Pb adsorption may act either unbound Pb or bound Pb. In natural condition, free Pb could be adhered onto soil due to van de Waal force. The forecasting of groundwater flow is linked between soil hydraulic properties and hydrologic condition of natural surface water system [25].

2.1.3 Lead remediation techniques

Lead contamination is the accumulation of a substance, native or introduced, in soil at a level harmful for the growth and health of organisms, including microorganisms, plants, and animals. Lead can be removed by physical methods such as pump and treat, soil washing, encapsulation, and vitrification; chemical methods such as immobilization, precipitation, and oxidation; and biological methods such as phytoremediation and permeable reactive barrier (PRB) [26].

2.2.2.1 *Permeable reactive barriers*

Permeable reactive barriers (PRB) are a novel technology for remediating contaminated groundwater, particularly on industrial and mining sites. PRB are a sustainable technology that can operate over a long time scale with low maintenance. Over the past 10–15 years, there have been great strides in refining site characterisation techniques (i.e., geophysical techniques), developing/discovering reactive materials/sorbents (i.e., Fe^0 filings), and the installation and design of PRB (i.e., funnel-and-gate design) which have increased the cost-effectiveness of this technology. PRB are a sustainable site specific remediation technology that has the great potential to work well as a part of a larger scale integrated water resource management programme in developing countries [27].

The concept of PRB is relatively simple shown in Figure 2.6(<http://vertexenvironmental.ca/in-situ-remediation/permeable-reactive-barriers/>). A permeable reactive barrier material consisting of permanent, semi-permanent or replaceable reactive media is placed in the subsurface across the flow path of a plume of contaminated groundwater, which must move through it as it flows, typically under its natural gradient, thereby creating a passive treatment system. As the contaminant moves through the material, reaction occur that transform the contaminants into less harmful (non-toxic) or immobile species. PRB potentially have several advantages over conventional pump-and-treat methods for groundwater remediation. PRB can degrade or immobilise contaminants in-situ, hence no need for expensive above ground facilities for storage, treatment, transport, or disposal other than monitoring wells. After the installation the above ground can be re-used for other purposes. PRB do not require any input of energy, because a natural gradient of groundwater flow is used to carry contaminants through the reactive zone. The permeable wall may contain reactive substances, which could create the physical, chemical or biological or combination reactions [28].

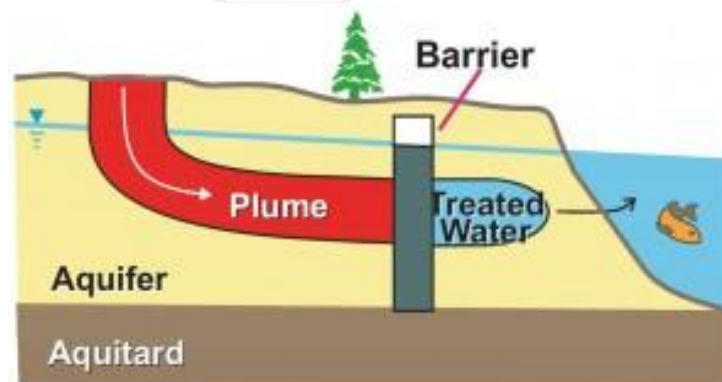


Figure 2.6The concept of PRB

Fundamental difference exists between organic and inorganic contaminant remediation as illustrated in Table 2.2. Organic contaminants can be broken down into innocuous elements and compounds, such as carbon dioxide and water because they are molecules consisting of carbon, hydrogen, halogens, oxygen, and sometimes sulphur, phosphorous and nitrogen. Conversely, most inorganic contaminants are themselves elements. They cannot be destroyed but can only change speciation.

Therefore remediation strategies must focus on transforming inorganics into forms that are non-toxic, immobile, or capable of being removed from the subsurface. The characteristics of these elements have in common is that they can undergo redox reactions and can form solid precipitates with carbonates, sulphide and hydroxide. These reactions are assessed to reduce the mobilisation and to detoxify the metals. To immobilise the metals, zeolite, hydroxyapatite, elemental iron and limestone are alternative materials that are properly added to improve the permeable treatment wall.

Table 2.2 Summary of pollutants removed by PRB

Treatment Material	Contaminants Treated
Zero-valent iron (granular iron)	Chlorinated solvents Reducible metals (Cr(VI), As)
Basic oxygen furnace slag	Arsenic Phosphorous
Solid organic amendments (wood chips, leaf compost)	Acid mine drainage (Fe, Zn, etc.) Nitrate Biologically degradable compounds
Liquid organic amendments (lactate, molasses, propylene glycol)	Biologically degradable compounds
Gas amendments (oxygen, hydrogen)	Biologically degradable compounds
Zeolites	Sr, Pb, Al, Ba, Cd, Mn, Ni, Hg
Phosphates	Mo, U, Tc, Pb, Cd, Zn, Sr

PRB are the continuous, in situ permeable treatment zone designed to intercept and remediate a contaminant plume. PRB are often intended as a remedy for a source-term management or as an on-site containment remedy. Over the past 10 years, the use of iron-based PRB has evolved from innovative to the acceptance of practical standard for containment and treatment as one of the variety of groundwater contaminants. Reactive media such as carbon sources (compost), limestone, granular activated carbon, zeolites, and others had also been deployed in recent years to treat metals and some organic compounds. Table 2.3 summarizes the advantages and disadvantages of PRB technology. Research and deployment of bio-barrier systems is

also growing in recent years, particularly for treatment of chlorinated solvents and petroleum hydrocarbon constituents [29].

Table 2.3 Advantages and limitations of the PRB technology

Advantages	Limitations
(a) Relatively cheap passive technology, i.e., inexpensive but effective reactive materials can be used; low energy cost; little or no disposal costs for treated wastes and; relatively low maintenance and monitoring costs with the exception of initial cost of installation	(a) Only contaminants flowing in the direction of the barrier can be treated
(b) Allows for treatment of multiple contamination plumes since more than one barrier can be used	(b) Requires proper characterization of the site, aquifer, hydrogeological conditions and accurate delineation of the contaminant plume prior to barrier installation
(c) Ability to treat a wide range of contaminants	(c) Restricted to plumes no deeper than 20 m beneath the ground surface
(d) The aboveground of the contaminated site can be put to profitable use while treatment is on-going	(d) Limited field data concerning longevity of barriers
(e) No cross-media contamination since contaminants are not brought to the surface	(e) Below ground structures (e.g. services, foundations) may present problems in construction and performance
(f) Require occasional monitoring to ensure that barriers are functioning properly	(f) Reactive media may have to be removed or be replaced during operation
(g) Obviates the handling and loss of large volumes of groundwater	(g) May require long-term monitoring, particularly in the case of persistent contaminants or very slow groundwater flow

2.2.2.2 Possible Occurrence Mechanisms

Metal mobility and bioavailability are the key risk factors for humans and animals. There are three main processes that control bioavailability and mobility of heavy metals: (1) removal of metals from the soil solution by solid particles, (2) release of metal from the soil surface to the solution – desorption, and (3) precipitation–dissolution as an independent phase in the soil matrix [30].

2.2.2.3 Biosorption

Biosorption of ionic metal is occurred under the passive binding of cations to biopolymers on the cell wall of dead organisms. On the other hand, the bioaccumulation is defined as the active binding substance, which cations adhere on the cell wall of living organisms. In fact, the cell wall of bacteria is composed of polymeric constituents that have negatively charge functional groups such as carboxyl, phosphate and sulfate. In the application prospect, the developed biobarrier must be applied to treat lead contaminated groundwater around the mining area. Hence, the biobarrier should be able to tolerate with an extremely acidic condition of the mining wastewater. In this study, the grounded cow dung mixed with fine sand is introduced as low cost biomaterial with appropriate permeability. The details of mechanisms between biomass and lead under acidic condition are investigated using the kinetic and isotherm models.

The potential use of a waste biosorbent material for the removal of Pb^{2+} ions from aqueous solutions was investigated by considering equilibrium and kinetic aspects. The relatively fast biosorption at all studied temperatures follows the pseudo-second-order kinetic model. Biosorption isotherm modeling showed that the equilibrium data fitted to the Langmuir model. The thermodynamic parameters indicated the biosorption of Pb^{2+} on the biomass was a spontaneous and endothermic process. Results of these work showed the suggested biosorbent could be an effective and eco-friendly alternative for the removal of Pb^{2+} ions from contaminated solutions [31]. Table 2.4 show the summary of previous adsorption of Pb(II) at the different pH.

Table 2.4 Summary of previous adsorption of Pb(II) at the different pH.

Experiment	Pollutants	pH	Media	References
Batch/ Column	Pb(II), Cu(II)	7	Activated sludge	[32]
Batch	Pb(II)+Cu(II)	5	<i>Rhizopus arrhizus</i>	[33]
Batch	Pb(II)	4-5.5,7-8	Anaerobically digested sludge	[34]
Batch	Pb(II)	4	Pine bark	[35]
Batch	Pb(II)	5	Modified quebracho tannin resin	[36]
Batch	Pb(II)	4.75	Zeolite	[37]
Batch	Zn(II), Pb(II)	7.5	Living non-growing filamentous fungus	[38]

2.2.3.4 Bioaccumulation

The sorption of Cd(II) and Pb(II) by exopolymeric substances (EPS) extracted from activated sludges and pure bacterial strains indicated that Pb(II) can form the complex compounds with EPS and be restrained for longer period. The EPS can retard Pb(II) more effectively than Cd(II) [39]. The natural fungal isolated from lead contaminated mine soils can restore some amount of heavy metals, even in the highly heavy metals contaminated sites [40].

The comparison between biosorption and bioaccumulation are mainly used for removal of metal cation from the solution which involve interactions, concentration of toxic metals or organic pollutants in the biomass, either living (bioaccumulation) or non-living (biosorption) shown in Table 2.5.

Table 2.5 The comparison between biosorption and bioaccumulation [41]

Biosorption	Bioaccumulation
Passive process	Active process
Biomass is not alive	Biomass is alive
Metals are bound with cellular surface	Metals are bound with cellular surface and interior
Adsorption	Absorption
Reversible process	Partially reversible process
Nutrients are not requires	Nutrients are required
Single-stage process	Double-stage process
The rate is quick	The rate is slow
Not controlled by metabolism	Controlled by metabolism
No danger of toxic effect	Danger of toxic effects caused by contaminants
No cellular growth	Cellular growth occurs
Intermediate equilibrium concentration of metal ions	Very slow equilibrium concentration of metal ions

2.2 Literature reviews

2.2.1 Biobarrier

Biobarrier is one of PRB attractive method for the future benefits due to its mechanisms. The biobarrier does enhance the bioactivity of natural microbes to perform self-purification processes. It involves biosorption and bioaccumulation. These mechanisms are presented in the active biomaterial that can separate the Pb(II) species from wastewater when it flows through. The development of biomaterial is remarkably a growing deal with environmental friendly cycle, cost effective, highly selective, high biosorption capacity and high efficiency in detoxifying. The biomaterial can be developed using low cost materials such as yeast biomass, clay and sawdust. Some previous experiments for remediation pollutants in various media are shown in Table 2.6

Table 2.6 Summary of previous biobarrier applications.

Pollutants	Media	Efficiency	References
Diesel	Peat moss, bentonite, and alginate	24.3%	[42]
TCE	The first column iron fillings as an iron-based barrier. The second column, sugarcane bagasse mixed with anaerobic sludge as an anaerobic barrier in. And a biofilm coated on oxygen carbon inducer releasing material as an aerobic barrier in the third column	42%, 16% and 25%,	[43]
Pb, Zn, Cu and Cd	Apatite and a commercial mixture of dolomite, diatomite, smectite basaltic tuff, bentonite, alginite and zeolite (Slovakite)	-	[44]
Cr(VI)	Green compost and siliceous gravel	>99%	[45]

2.2.1.1 Media

The media (both inorganic and organic) can act as the habitat of biofilm producing microbes, the common media such as sand, clay, zero-valent iron, compost, peat or organic compound, limestone, granular activated carbon, zeolites are widely employed to construct the permeable reactive biobarrier [46-52]. The highly surfactive media is normally applied as sorbent; this media acts as the habitat for the active microbes. The biofilm microbes play a significant role in controlling the propagation of Pb(II) in surface and subsurface systems. The biological mechanisms between biofilm and Pb are adsorption, ion-exchange, precipitation, oxidation/reduction and complexation [7, 37, 53-55]. However, the growth of biofilm and the formation of PRB are little known [56-58].

The compost and gypsum amendments significantly decreased dissolved Pb and Sb in pore water. The concentration of Pb in above ground plant tissues was 190 mg/kg in the control soil and was reduced to less than 20 mg/kg in the compost and gypsum-amended soils. Extended X-ray absorption fine structure (EXAFS) spectroscopy illustrated that Pb occurred as Pb sorbed on birnessite and/or ferrihydrite (Pb-Mn/Fe, ~ 60%) and Pb sorbed on organic matter (Pb-org, ~ 15%), and galena (PbS, ~ 10%) in the vegetated and unvegetated control soils. The compost amendment increased the proportion of organo-Pb by two folds higher than in the control soils. Galena and anglesite (PbSO₄) were not detected in compost-amended soils and even in gypsum-amended soils since a significant soil reduction to anoxic levels did not occur in the entire soil. The present study indicated that under flooding conditions, surface applications of compost and gypsum amendments reduced plant Pb uptake from the Pb contaminated soil [59]. Composts reduced soil solution potentially toxic element levels and raised soil pH and nutrient levels and are well suited to vegetation of contaminated sites. However, care must be taken to ensure correct pH management (pH 5–6) [60].

Contaminants in an aquifer and migrating through an installed reactive wall can be passively fixed in-situ by sorption onto the reactive materials contained at the treatment wall via ion exchange, surface complexation, surface precipitation or hydrophobic partitioning, sorption, chemical reaction and biological. For such a sorption technique to be effective, pH range of the barrier chemical needs to be

selected depending upon the metal to be removed and sorbents used, this technology is available for shallower depth of 3 to 12 m. The immobilised contaminants may be re-mobilised with changing environmental condition, sorption by means of zeolites, humic materials, oxides and precipitating media. Chemical reaction can also occur when zero-valent metals (Fe, As, etc.) and other reactive minerals are in barrier. Biological reactions by oxygen and nitrate release end-product compounds and organic materials. The media in the Table 2.7 are typically used for permeable reactive barrier.

Table 2.7 Media use in PRB


Pollutants	Media	References
Heavy Metal (Al, Cu,Zn)	A Mixture Of Limestone and Vegetal Compost	[61]
Boron	MgO and Sawdust	[62]
Pb(II)	Mulch	[54]
Heavy Metal (Cu, Cd, Co, Ni, and Zn)	Organic Carbon	[63]
Acid-Mine Drainage	Organic Matter	[64]
Cd(II)	Activated Carbon	[65]
Acid-Mine Drainage	Zero-Valent Iron and Municipal Compost	[66]
Acid Mine	Zero-Valent Iron	[67]
Heavy Metal(Cu,Ni)	Zero-Valent Iron (ZVI) and pumice	[68]
Nitrate	Carbonaceous Solid Materials and ZVI	[47]
As(III)	Iron Sulfide	[69]
Zn(II), Pb(II), Cd(II)	Reactive Medium Apatite II™	[55]
237U	Hydroxyapatite (HAP)	[70]
Zn(II)	Hydrated Sodium Zeolite-X	[71]
Ammonium and Cu(II)	Zeolites	[72]
Cu(II)	Zeolite	[73]

2.2.1.2 Microorganisms

The Pb(II) biosorption on *Bacillus sp.* (ATS-2) was investigated in the fixed-bed column test. The maximum Pb(II) biosorption capacity was obtained when the pH of system was at 4. The Pb(II) biosorption behavior can be explained by Langmuir, Freundlich and Dubinin–Radushkevich (D–R) isotherm models [74]. In another study, the sorption of Pb(II) on loamy sand had been investigated. Soil samples were collected from Oporto, Portugal. The adsorption behavior in soil column at pH 2 and 5 could be fitted by Redlich–Peterson and Khan models, respectively [75].

2.2.1.3 Substrate Solution

Molasses



Molasses is thick and dark brown syrup from the final crystallization stage of sugar production process. Therefore, it cannot be crystallized as a sugar again. Molasses contains sucrose, invert sugar and water. At this modern times, molasses is a very important to industrial sector; it can be used as a raw material for many various industries, such as the ethanol industry, food and beverages industry, beer and whisky industry, yeast production, pet food products, vinegar, soy sauce and so on.

Molasses does not just only consist of one chemical compound, but it is a mixture of many substances. The main content is sugar (sucrose) ($C_{12}H_{22}O_{11}$). The rest is complex and will vary depending on the source of molasses either from sugar beets, cane sugar (the two most common sources), or other. The total sugar content in molasses is approximately 50 %. Minor carbohydrates are glucose, fructose, raffinose and some other oligo- or polysaccharides. Their concentrations are below 1% and depend to a significant extent on the manufacturing process. Some of the minerals found in molasses are potassium followed by sodium, calcium and magnesium. Their content depends mainly on soil type and water availability. Additionally, the calcium and sodium contents are influenced by processing practices. About 20 % of the total mass consists of non-sucrose organic matter, in particular of non-protein nitrogen (NPN) containing substances such as betaine. In addition, molasses contains free and bound amino acids and pyrrolidone carboxylic acid (a conversion product of

glutamine). In the manufacturing process most of the amino acids undergo changes so that less than the amounts expected from beet roots are found in molasses.

Phosphorus

The stability diagram (Figures 2.6) [76] illustrates the decrease in Pb solubility with increasing pH, which is the usual trend with cationic metals. Lead phosphate will form at lower pH and a mixed Pb compounds are present at pH greater than 7.5. The formation of a solid phase may not be an important mechanism compared to adsorption in native soils because of the low concentration of trace metals in these systems. Precipitation reactions may be of much greater importance in waste systems where the concentration of metals may be exceedingly high.

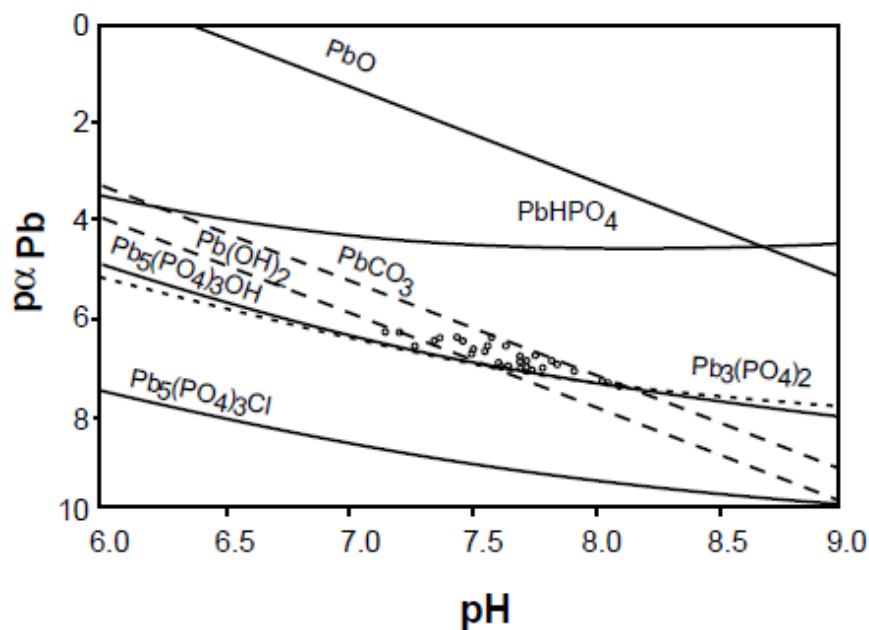


Figure 2.7 The solubility diagram for Pb in Nibley clay loam soil

2.2.2 Existing models for lead remediation/transport

Several equilibrium thermodynamic computer programs are available for modeling soil solution and solid phase chemistry by providing information on the thermodynamic possibility of certain reaction to occur. In addition to calculate the equilibrium speciation of chemical elements in the soil solution and precipitate/dissolution reactions, models such as GEOCHEM [77] and MINTEQA2

(USEPA) provide information on cation exchange reactions and metal ion adsorption.

These models are used to:

- 1) calculate the distribution of free metal ions and metal-ligand complexes in a soils solution,
- 2) predict the fate of metals added to soil by providing a list of which precipitation and adsorption reactions are likely to be controlling the solution concentration of metals, and
- 3) Provide a method for evaluating the effect that change one or more soil solution parameters, such as pH, redox, inorganic and organic ligand concentration, or metal concentration, has on the adsorption/precipitation behavior of the metal of interest.

These models are equilibrium models and as such do not consider the kinetics of the reactions. A significant effort is attributed to develop the predictive tool, which can describe the growth of biofilm forming microbes and their activities involved biosorption and bioaccumulation of Pb(II) on the simulated PRB.

The existing models of biobarrier can predict the remediation of considered contaminants. However, the simulations might not exactly predict the effect of bio-clogging on the permeable reactive biobarrier. Thus, the installation, operation and maintenance of biobarrier were estimated based on experience. Biobarrier can remediate and stabilise lead in a long term period, if the optimum condition is known.

It seems biobarrier can restore and stabilise the Pb(II), however the criteria for biobarrier design is little known [78-80]. The design of biobarrier is traditionally practiced. Hence, it cannot be ensured that the biobarrier is properly design and operate [67, 81]. A Mathematical model is developed to explain the mechanisms occurring in the biobarrier systems. The set of governing equations including the advective/dispersive flow of Pb(II) in the porous material, the biosorption/bioaccumulation of Pb(II) are employed to the developed model.

CHAPTER 3

A CONCEPTUAL MODEL FOR BIOBARRIER

In order to assess the stability of PRB, a mathematical model is developed. The unsaturated transport model is modified to determine the inflow-outflow of percolation wastewater. The growth of biofilm forming and their activities are involved in the model, the biosorption and bioaccumulation of Pb(II) on the synthesized biobarrier are included in the source/sink term.

3.1 Development of conceptual model

The major mechanisms of Pb(II) retardation in biomass are biosorption and bioaccumulation. The Pb(II) sorption and accumulation rely on the numbers of sorptive surface and the activities of acclimatised microbes, respectively. The numbers of active microbes can be defined as the thickness of biofilm. The high thickness of biofilm can bring the high capacity of Pb(II) retardation, but the biofilm can attribute the clogging zone that can reduce the pore velocity of biobarrier. The conceptual model for biobarrier is shown in Figure 3.1.

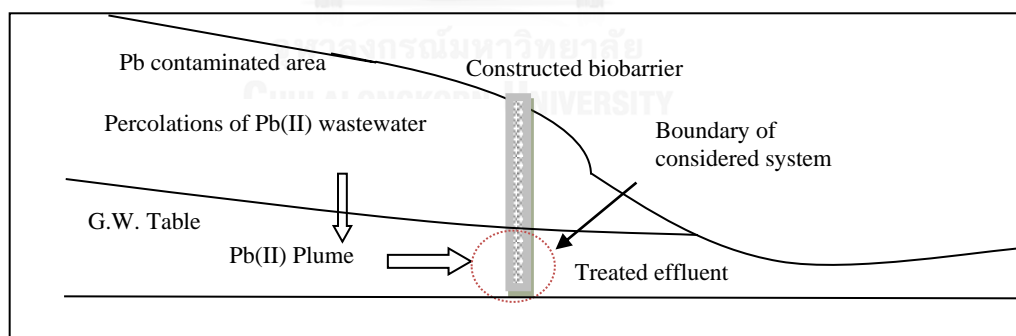


Figure 3.1 Conceptual model of biobarrier

The boundaries conditions, the constants for hydraulic properties model governed and reaction terms relating the microbial activities and Pb(II) retardation from the experiments are input to the UNSAT program [82].

In accordance with the mass balance concept, advection and dispersion terms are used to estimate the mass of contaminants that flow through a representative elementary volume of a porous medium. Biosorption and bioaccumulation reactions define the source/sink terms. This governing equation is in a form of a hyperbolic/parabolic partial differential equation (PDE) and consists of many idealised parameters such as D_z , q_z and R . Parameters D_z and q_z can be determined using Richards' equation. R can be expressed as a function according to the defined reactions.

3.2 Mass balance

Mass balance equation for Pb(II) in the aqueous phase in biobarrier can be expressed as

$$\frac{\partial C}{\partial t} = D \frac{\partial^2 C}{\partial z^2} - \frac{q}{n} \frac{\partial C}{\partial z} - R_{biosorption} - R_{bioaccumulation} \quad (3.1)$$

where C is the mass concentration of Pb(II) (M/L^3), D is diffusivity coefficient (M/L^2), q is Darcy's velocity, n is porosity and $R_{biosorption}$ and $R_{bioaccumulation}$ are the net rates of Pb(II) by biosorption and bioaccumulation reaction (M/L^3-T).

3.3 Transport part

Since the contaminated water flows through biobarrier, the behaviour of microbes can be divided into three stages in regard with microbial age. At an initial stage, the biofilm forming microbe is thin, the plume of contaminant can flow through the vacant pore inside a porous media. The movement of contaminant plume is mentioned as movement under a fully saturated porous media. At the second stage whenever biofilm becomes a thick layer of biomass, some pores are clogged. Water cannot pass throughout the porous media then the movement of contaminant plume can be considered to flow under variably saturated condition. The unsaturated flow, which is described by Richard's equation [83]. At the final stage, the porous media which are consisted of organic substances are collapsed and consolidated. The flow of contaminant plume will be controlled by the soil compact pores after consolidation. When the clogging zone is happened, the saturated flow can be estimated by Darcy's

Law [75]. In every case, the transient flow applied as the pore velocity will change over time due to the biological activities.

3.3.1 Saturated porous media

Darcy's Law is normally applied to estimate the pore velocity of fluid movement in a fully saturated porous media [84, 85]. It can be expressed as follows:

$$q = -K \frac{\partial \psi}{\partial z} \quad (3.2)$$

where q is Darcy's velocity (L/T), K is the fully saturation permeability (L/T), ψ is the hydraulic head (L) and x is the distance of flow path (L). Term $\frac{\partial \psi}{\partial z}$ is the hydraulic gradient (unitless).

3.3.2 Variably saturated porous media

Richard's equation is technically applied to evaluate the pore velocity of fluid movement in a variably saturated porous media [25].

$$q = -\frac{\partial}{\partial z} \left(K_z k_{rw} \left[\frac{\partial(\psi + z)}{\partial z} \right] \right) \quad (3.3)$$

where q is Darcy's velocity in vertical direction [L T⁻¹], k_{rw} is the relative hydraulic conductivity [unitless], K_z is the fully saturated hydraulic conductivity [L T⁻¹], S is the specific moisture capacity, x is the elevation head [L], t is the time interval [T] and ψ is the pressure head [L].

3.3.3 Consolidation of porous media

The movement of fluid through compressible porous media with a fully saturated condition can be described as follows [75]:

$$q = -\frac{\rho g}{S_s} \left[\frac{\partial}{\partial z} \left(\frac{K}{\mu} \frac{\partial \psi}{\partial z} \right) \right] \quad (3.4)$$

where ρ is fluid density (M/L^3), S_s is the specific storativity ($1/L$), g is the magnitude of gravitational acceleration (L/T^2) and μ is fluid viscosity ($M/L-T$)

3.4 Soil hydraulic properties equation

The flow of groundwater relates to volumetric water content in soil and changing pressure head in pore soil water. Thus, the equation describing the groundwater flow will present the relationship between pressure head with volumetric water content. The hydraulic property equation used in this research is derived by Van Genuchten (1980) [86].

Van Genuchten (1980) derived the hydraulic property equation based on the equation of Brooks and Coley (1964) [82]. The hydraulic property equation is presented as follows:

$$\theta = \theta_r + \frac{\theta_s - \theta_r}{(1 + (a|\psi|^p)^m)} \quad (3.5)$$

where a is the soil water retention function [L^{-1}], m and p are the empirical parameters yielded from the hydraulic properties curve [unitless], respectively.

3.5 Reaction part

The approximate mass of Pb(II) in the soil pore at the unsaturated zone is traditionally determined by the mass balance concept. The mass balance equation can be simplified as follows [82]:

According to the previous researches, the major mechanisms of Pb(II) retardation in biomass are biosorption and bioaccumulation. However, the rates of Pb(II) sorption and accumulation rely on the numbers of sorptive surface and acclimatised microbes, respectively. Both sorptive surface and numbers of active microbes can be defined as the thickness of biofilm as mentioned previously. Although, the higher the thickness of biofilm, the higher capacity of Pb(II) retardation; unfortunately, the higher potential of clogging will also occur which sequentially leads to the reduction of pore velocity through the biobarrier. The water table may rise up and the smearing zone of Pb(II) can be expanded over the model boundary.

3.5.1 Biosorption process

3.5.1.1 Langmuir isotherm

The important assumptions of Langmuir model are (1) the energy of adsorption is the same for all sites and is independent of degree of surface coverage, (2) adsorption occurs only on localised sites with no interaction between adjoining adsorbed molecules and (3) the maximum adsorption capacity (Q_{\max}) represents coverage on only single layer molecules. The Langmuir equation can be presented as:

$$C_s = \frac{X}{m} = \frac{abC_e}{1+bC_e} \quad (3.6)$$

$$\frac{\partial C_s}{\partial t} = \frac{k_L k_M \frac{\partial C_e}{\partial t}}{(1+k_M C_e)^2} \quad (3.7)$$

where C_s is the amount of Pb(II) adsorbed (M/M) at equilibrium; C_e is the concentration of Pb(II) at equilibrium (M/L^3), a is the theoretical saturation adsorption capacity of the monolayer (M/M) and b represents the Langmuir constant (L^3/M) which relates to the affinity of binding sites.

The degree of favourable adsorption can be expressed as follows:

$$R_L = \frac{1}{1+bC_0} \quad (3.8)$$

where C_0 is the initial concentration of Pb(II) (M/L^3). If $R_L > 1.0$, the isotherm is unsuitable; $R_L = 1.0$, the isotherm is linear; $0 < R_L < 1.0$, the isotherm is suitable; $R_L = 0$, the isotherm is irreversible.

3.5.1.2 Freundlich isotherm

Freundlich model was characterised by continuous adsorbing as the concentration of sorbate increases in the aqueous phase. A typical Freundlich isotherm plot shows that the mass of material sorbed is proportional to the aqueous phase concentration at low sorbate concentration and increases as the sorbate accumulates on

the sorbent surface. The Freundlich isotherm is quantified by as the following equations:

$$C_s = \frac{x}{m} = K_F C_e^{1/n} \quad (3.9)$$

$$\ln C_s = \left(\frac{1}{n}\right) \ln C_e + \ln K_F \quad (3.10)$$

$$\frac{\partial C_s}{\partial t} = k_F \left(\frac{1}{n}\right) C_e^{\left(\frac{1}{n}-1\right)} \quad (3.11)$$

where K_F is the Freundlich constant related to adsorption capacity of adsorbent and n is the Freundlich exponent related to adsorption intensity.

3.5.2 Bioaccumulation process

3.5.2.1 Modified Gompertz model

The modified Gompertz model is employed to fit the observations of time versus $\ln(C/C_0)$. The term C/C_0 refers to the reduction of substrate and Pb(II). The equations are presented as follows:

$$C = A \exp\left[-\exp\left(\frac{\mu_m e}{A} (\lambda - t) + 1\right)\right] \quad (3.12)$$

where μ_m is the specific substrate consumption rate, λ is the delay reaction time, t is time, A is asymptote $[\ln(C/C_0)]$ and e is Euler Number (2.718).

3.5.2.2 Monod kinetics equation

The Monod kinetics equation is often applied to express the growth-linked substrate utilisation of the living biomass in the batch Pb(II) biosorption experiment. The Pb(II) may involve the inhibition of substrate utilisation. The related equations are given as follows.

$$\mu = \frac{\mu_{\max} S}{K_S + S} I_{pb} \quad (3.13)$$

$$\frac{\partial C_S}{\partial t} = \left[\frac{\mu_b}{Y_b} \right] \left[\frac{C_S}{K_{sb} + C_S} \right] C_b^t k_m C_b^t \quad (3.14)$$

where S is the limiting substrate concentration which is determined as COD (mg/L), K_S is the half saturate concentration constant (mg COD/L), μ_{\max} is maximum specific growth rate (1/h) and I_{pb} is the empirical term for Pb(II) inhibition.



CHAPTER 4

MATERIALS AND THE EXPERIMENTAL SET-UP

4.1 Experimental framework

The aim of this research was to predict the retardation and migration of ionic lead through a synthesis biosorbent or biobarrier as PRB for the remediation of lead ions in groundwater. The experiments were separated into two parts as described below:

The first part is the preparation of the required materials, the procedure in setting up the column and the study mechanism of the constructed biobarrier in which the acclimatised biofilm can actively reduce the migration of lead by biosorption and bioaccumulation. These preparations are divided *into two phases*; the first phase is to test a non-active media and the second phase is to explain the active media that used a zeolite as an adsorbent in which microbes can adhere.

The second part is the development of a mathematical model for evaluating the retardation and migration of ionic lead through a constructed biobarrier by applying the numerical technique to produce a computational code using MATLAB technical language. Calibration and verification of the model were performed by using experimental result and its historical data.

The experimental framework is illustrated in Figure 4.1.

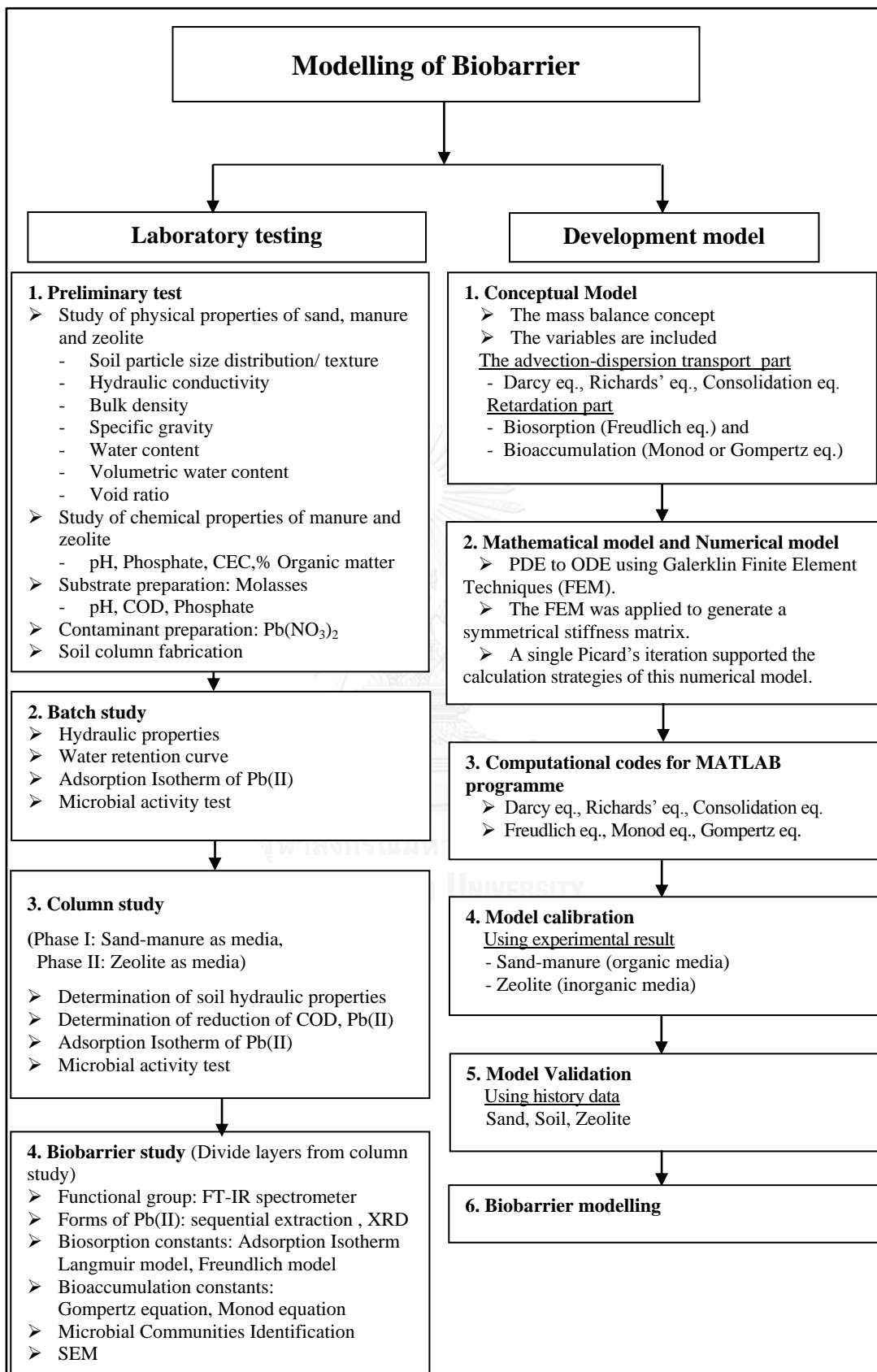


Figure 4.1 Experimental framework

4.2 Materials

4.2.1 Sand–manure sample preparation

Sand was used as a non-active media. The river sand was cleaned by deionised water and sieved to a medium grain size in between sieve No.50 (0.30 mm) and No.40 (0.425 mm). Then the animal manure (soil: cow dung of 2:1) with a diameter less than 2.00 mm was mixed with the cleaned sand at the ratio of 1:1 (w/w). The animal manure is applied as a carbon and nutrient sources for microbe and fine sand is used as a high permeability porous media. The Figure 4.2 shows the physical appearance of the materials.



Figure 4.2 Physical appearances of materials (a) sand; (b) manure; (c) sand-manure

4.2.2 Zeolite preparation

Clinoptilolite zeolite obtained from northern New South Wales in Australia was used as the active media in this study. The complex formula for clinoptilolite zeolite was $(\text{Na},\text{K},\text{Ca})_{2-3}\text{Al}_3(\text{Al},\text{Si})_2\text{Si}_{13}\text{O}_{36}\cdot 12(\text{H}_2\text{O})$. Its physical appearance is light pink powder or granulated chips. The zeolite was cleaned by DI water and sieved to particle sizes of 0.30-0.425 mm as shown in Figure 4.3.

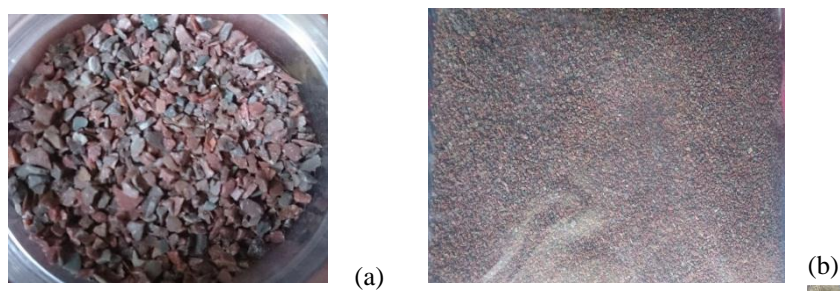


Figure 4.3 Physical appearances of (a) clean zeolite; (b) zeolite after sieved

4.2.3 Substrate preparation

4.2.3.1 Sand-manure column

The molasses solution with a concentration of 15 g COD/L at the pH range between 5.0 and 5.5 was fed to incubate the microbes in the sand-manure column at a rate of 500 cm³/d using a peristaltic pump. The quality and quantity of influent and effluent samples were daily determined.

4.2.3.2 Zeolite column

The molasses at concentration of 2.0 g COD/L with the pH range between 5.0 and 5.5 was fed to incubate the microbes at a rate of 100 cm³/d using a peristaltic pump. The quality and quantity of influent and effluent samples were daily determined.

4.2.4 Contaminant preparation

The chemical reagents used in this research were analytical grade. The synthetic wastewater was prepared by dissolving lead nitrate (Pb(NO₃)₂) in deionised water at the concentration of 0.2 mg Pb(II)/L. As the Pb content in original soil was high, the leaching of Pb could stimulate the high background concentration of Pb in leachate. This could interfere with the concentration of Pb(II) remaining in the effluent. Besides, the high concentration of Pb solution may inhibit the biological process.

4.2.5 Soil column fabrication

4.2.5.1 Sand-manure column

The mixture (soil: cow dung of 2:1) was packed into the column without compaction. The biomaterial bulk density was controlled at 0.529 g/cm³. The column had a diameter of 4.7 cm and an effective height of 16.0 cm.

4.2.5.2 Zeolite column

The natural zeolite (Clinoptilolite) was poured into a acrylic plastic column with the diameter of 6.5 cm and the effective height of 20 cm without compaction and the bulk density was 1.31 g/cm^3

Jet Fill tensiometer Model 2100F moisture probes were used to measure negative pore pressure. The probes were placed at the center of column, at the elevations of 5, 7.5, 10, 15 and 17.5 cm above the column base (datum) for detecting negative pore pressure which represented Pb(II) transport as illustrated in Figure 4.4



Figure 4.4 The experiment set up

4.3 Sand/Zeolite characterisation

Soil/zeolite properties were analysed physically and chemically. The parameters and analytical methods are given in Table 4.1.

Table 4.1 Parameters and analytical methods for testing of soil properties

Parameter	Analytical method	Reference
Physical properties		
Particle size distribution	Sieving in combination with	[87]
Soil classification	hydrometer method	[87]
Hydraulic conductivity	The textural triangle nomenclature	[87]
Bulk density	Standard test method for permeability	[87]
Soil water content	Sand replacement method using a sand cone pouring apparatus	[87]
Specific gravity	Oven drying method Soil particle density	[87]
Chemical properties		
Organic matter (%)	Walkley-Black procedure	[88]
Soil pH	Electrode pH meter method	[87]

4.4 Filtered water characterization

Lead can be detected in forms of total and soluble ions. In case of total Pb measurement, the contaminated soil was digested by microwave digestion and filtered with the membrane filter of 0.45 μm pore size (VertiClean™) prior to the determination of Pb. The content of lead in soluble form was analysed by Inductively Couple Plasma-Optical Emission Spectrometer (ICP-OES) (Method 200.7) following the US EPA guidelines. The effluent samples from every test were collected, filtered and analyzed in the same way as the influent. The value of pH of every effluent sample was measured using pH meter (model Sartorius PT-10).

4.5 Adsorption isotherm test

The test of Pb adsorption onto zeolite was conducted in the laboratory. A 100 mL of 4 mg/L of $\text{Pb}(\text{NO}_3)_2$ solution with the pH of 3.84 was mixed with 5 g of sorbent. The slurry was agitated in the incubator shaker, model LAB-Line 2528, with a speed of 250 rpm and temperature of 25 °C. The slurry samples were taken at 0, 20, 40, 60, 100, 120 and 1440 minute interval, the remaining soluble Pb and the final pH of the supernatants were analyzed in accordance with the Standard Methods [89], to estimate the equilibrium time for Pb adsorption. Then the Pb adsorption isotherm was investigated. One hundred mL of 10 mg/L of $\text{Pb}(\text{NO}_3)_2$ solution was mixed with various amounts of sorbent of 1, 2, 5, 10 and 20 g. The mixing procedure was same as those of the equilibrium time determination. The pH and concentration of Pb of the supernatants were examined.

4.6 Biosorption test

4.6.1 Sand-manure column

After 180 days, the matured biosorbent from the sand-manure column was separately collected for every 3.5 cm depth as the presence of microbial community might vary with depth. The functional groups of biopolymer in every layer of biosorbent were examined by FTIR spectrometer.

4.6.2 Zeolite column

Biosorption test was conducted by modifying the isotherm test with autoclaved biosorbent. The biosorbent samples were weighed at 1.0, 2.0, 5.0, 10.0 and 20.0 g and mixed with 2.5 mg Pb/L $\text{Pb}(\text{NO}_3)_2$ solution at pH 4. The mixtures were shaken at a speed of 250 rpm with a control temperature at 25°C, until achieving the equilibrium time. The effluent samples governed from every tests were filtered and analysed for Pb(II) ion concentration by an atomic adsorption spectroscopy (AAS) according to NIOSH guidelines. The bed of zeolite from the column was analysed for biopolymers using Fourier Transform Infrared (FT-IR) spectroscopy and the forms of Pb by X-ray diffraction (XRD) technique.

4.7 Bioaccumulation test

The bioaccumulation test was conducted using the samples of non-autoclaved biosorbent. The kinetic rate constants were analysed using biomathematical models, particularly modified Gompertz equation and the Monod equation. The biosorbent samples were weighed at 1.0 g. These samples were mixed with the solutions of $\text{Pb}(\text{NO}_3)_2$ at 2.5 and 4 mg/L at different pH levels of 4, 7 and 9. The mixtures were shaken at a speed of 250 rpm with a control temperature at 25 °C until achieving the equilibrium condition. The effluent samples from every tests were filtered and analysed for Pb(II) ion concentration by an atomic adsorption spectroscopy (AAS) according to NIOSH guidelines.

4.8 Development of synthetic biobarrier

4.8.1 Sand-manure column

The manure contains the organic carbon that can be supplied as a carbon source to microbes but it may not enough to serve all active microbes. The experimental setup and equipment are illustrated in Figure 4.5

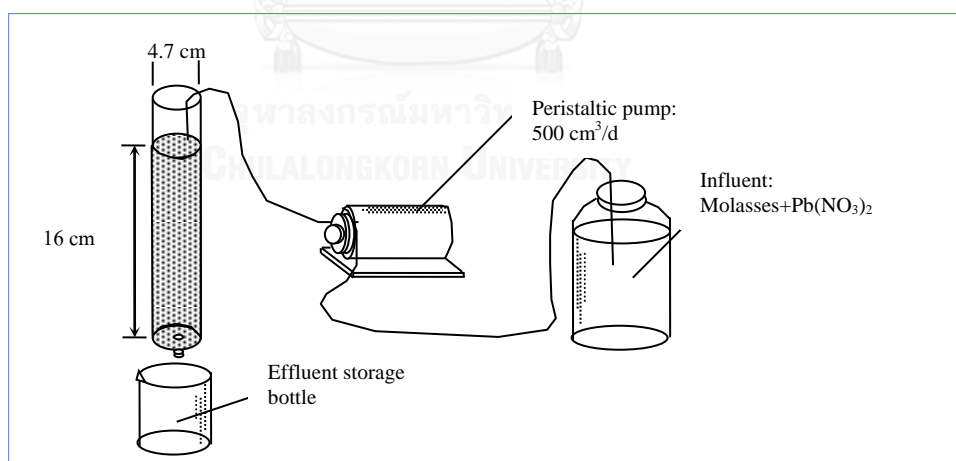


Figure 4.5 Experimental setup

The biofilm was acclimatised to Pb(II) by feeding with the acidic molasses solution spiked with 0.2 mg/L of $\text{Pb}(\text{NO}_3)_2$ for 101 days. The solution was fed at the same flow rate as at the incubation stage. The characteristics of influent and effluent

samples were daily analysed. The biofilm was acclimatised for another 79 days until the removal efficiencies of COD and Pb(II) were constant.

4.8.2 Zeolite column

The substrate with acclimatised seed was sprayed onto the surface of the packed zeolite column A-1. The feeding rate was controlled by a peristaltic pump at 100 mL/d. The quality and quantity of feeding influent and percolating effluent were daily determined in accordance with the Standard Methods [89]. The biofilm was obviously observed at the surface to 1.5 cm depth within 50 days after inoculation. The removal efficiencies of COD and Pb were 70 and 90%, respectively. The 0.2 mg/L Pb(NO₃)₂ solution was spread onto the surface of zeolite packed column A-2 at the feeding rate of 100 mL/d. The quality and quantity of influent and effluent were also determined as in the same manner as column A-1.

4.9 Microbial communities identification

4.9.1 DNA extraction and purification

DNA was extracted from the samples using the PowerSoil® DNA Isolation Kit (MoBio Laboratories, Inc., Carlsbad, CA, USA) according to the manufacturer's instructions. The DNA solution was stored at -20°C for further use in PCR amplification.

4.9.2 PCR amplification

The PCR was performed in 30 µL volumes containing 50 ng of template DNA, GoTaq® Green Master Mix (Promega, Mannheim, Germany), 20 pmol of each forward and reverse primer, and nuclease-free water to 30 µL. All PCR primers used in this study were listed in Table 4.2. The PCR amplification targeting bacterial 16S rDNA, primers 341F with a GC clamp and 520R were used. The PCR amplification condition was as follows:

- Initial denaturation step at 94 °C for 5 min
- Denaturation step at 94 °C for 1 min
- Annealing step at 55 °C for 1 min

- Extension step at 72 °C for 2 min
- Go to step 2-4 for 30 cycles
- Final extension at 72°C for 10 min

The PCR amplification targeting fungal, primers ITS1 with a GC clamp and ITS4 were used. The PCR amplification condition was as follows:

- Initial denaturation step at 94 °C for 5 min
- Denaturation step at 94 °C for 1 min
- Annealing step at 48 °C for 1 min
- Extension step at 72 °C for 2 min
- Go to step 2-4 for 30 cycles
- Final extension at 72 °C for 10 min

The PCR products were checked by electrophoresis in a 2% agarose gel in 1xTAE buffer through staining with ethidium bromide and visualized under UV light.

Table 4.2 Nucleotide sequences of primers used in this study

Primer name	Nucleotide sequences (5' - 3')	Reference
341F	CCTACGGGAGGCAGCAG	[90]
520R	ACCGCGGCTGCTGGC	
ITS1	TCCGTAGGTGAACCTGCGG	[91]
ITS4	TCCTCCGCTTATTGATATGC	
GC clamp	CGCCCGCCGCGCCCGCGCCCGTCCCG CCGCCCCCGCCCG	[92]

4.9.3 DGGE

DGGE was carried out using the DCode™ system (Bio-Rad Laboratories Inc., USA). PCR products were loaded onto 8% polyacrylamide gel with a 30% to 70% denaturant gradient (100% denaturant was defined as 7 M urea and 40% formamide). Electrophoresis was performed at a constant condition of 60°C and 130 V for 4.5 hours in 7 liters of 1x TAE buffer. After electrophoresis, the gel was stained with ethidium bromide for 15 minutes and visualized under UV light.

4.9.4 Sequencing of DGGE bands

4.9.4.1 Amplification of DNA and purification of PCR products

Bands excised from the DGGE gels were eluted in 30 μ l of distilled water over night at 4°C. Eluted DNA 1 μ l was used as the PCR template. The PCR products were checked by electrophoresis in a 2% agarose gel in 1xTAE buffer through staining with ethidium bromide and visualized under UV light. Then, the PCR products were purified by using Gel/PCR DNA Fragments Extraction Kit (Geneaid, Taipei, Taiwan) according to the manufacturer's instructions. Purified PCR products were stored at -20°C.

4.9.4.2 Cloning of PCR products

The purified PCR products were ligated through pGEM-T Easy Vector (Promega, USA) of which the reaction is described as below:

- 2X ligation buffer 5 μ l
- pGEM-T Easy Vector (50 ng) 1 μ l
- The purified PCR product (100 ng) 3 μ l
- T4 DNA Ligase (3 U) 1 μ l

The ligase reaction was incubated overnight at 4 °C. Then, the ligation mixture was transformed into the competent *E.coli* JM109 cell. Recombinant plasmid was transformed into competent cell by heat shock method [93]. Competent cell was thawed in ice. Three microliters of ligated recombinant plasmid was added to 100 μ l of competent cell, then mixed and incubated in ice for 20 minutes. Heat shocked the cell by putting into a heat box at 42°C for 45-50 seconds then put into the ice immediately for 2 minutes. Added 950 μ l of SOC broth and incubated at 37°C for at least 1 hour. Then, the transformed solution was spread on the LB agar containing 100 μ g/ml of ampicillin, 100 μ g/ml of X-gal, and 100 μ g/ml of IPTG. The plate was incubated at 37 °C for 16 – 24 hours. The white colonies were picked to check the

insert fragment. The white colonies were grown in the LB broth containing 100 µg/ml ampicillin at 37 °C overnight.

4.9.4.3 Plasmid extraction

The plasmid was extracted by using Presto™ Mini Plasmid Kit (Geneaid, Taipei, Taiwan) according to the manufacturer's instructions. Plasmid solution was stored at -20°C until being used.

4.9.4.4 Digestion of recombinant plasmid by restriction enzyme

Extracted plasmid was digested with *EcoRI* restriction enzyme to confirm the presence of inserted fragment. The restriction digestion condition was described as below:

- Plasmid (pGEM-T Easy Vector) 1 µl
- 10X Buffer 1 µl
- EcoRI* enzyme (0.5 U) 1 µl
- Steriled water 7 µl

The digest reaction was incubated overnight at 37 °C. The insert fragment was examined by running in 2% agarose gel electrophoresis.

4.9.4.5 Nucleotide base sequencing

Three clones of each band were sent for nucleotide base sequencing at 1st Base Co. Ltd., Malaysia. The sequence results were analyzed using BLASTn program to identify the bacterial species.

4.10 Pb species detection

The sequential extraction technique [94] was used to examine the various forms of Pb(II) adhered onto cell wall of living microbes due to bioaccumulation. This method could determine the fraction of lead by extraction with different reagents as shown in Table 4.3.

Table 4.3 The reagents for five fractions of sequential extraction method

Fraction	Reagents
1. Exchangeable	1 M $\text{MgCl}_2 \cdot 6\text{H}_2\text{O}$ @pH 7
2. Bound to Carbonates	1 M $\text{CH}_3\text{COONa} \cdot 3\text{H}_2\text{O}$ @pH 5
3. Bound to Iron and Manganese Oxides	0.04 M $\text{NH}_2\text{OH} \cdot \text{HCl}$
4. Bound to Organic Matter	0.02 M HNO_3 , 30% H_2O_2 @pH 2 and 3.2 M $\text{CH}_3\text{COONH}_4$
5. Residual	Residue from (4) was digested by microwave.

The following chemical extraction methods were retained for further study; the quantities indicated below refer to 1-g sediment sample (dry weight of the original sample used for the initial extraction). The first step started with water soluble fraction, 1 g of sample was extracted with 15 mL of deionised water for 2 hours in a 50 mL polypropylene centrifuge tube, with continuous agitation on the wrist action shaker. Then, the following 5 steps as listed below were carried out:

(i) *Exchangeable*: The sediment was extracted at room temperature for 1 h with 8 mL of either magnesium chloride solution (1 M MgCl , pH 7.0) or sodium acetate solution (1 M NaOAc , pH 8.2) with continuous agitation.

(ii) *Bound to Carbonates*: The residue from (i) was leached at room temperature with 8 mL of 1 M NaOAc adjusted to pH 5.0 with acetic acid. Extract with continuous agitation on the wrist shaker for 5 h.

(iii) *Bound to Fe-Mn Oxides*: The residue from (ii) was extracted with 20 mL of 0.04 M $\text{NH}_2\text{OH} \cdot \text{HCl}$ in 25% (v/v) HOAc . The latter experiments were performed at 96 ± 3 °C with occasional agitation and 6 h for complete dissolution of the free iron oxides was evaluated.

(iv) *Bound to Organic Matter*: To the residue from (iii), 3 mL of 0.02 M HNO_3 and 5 mL of 30% H_2O_2 adjusted to pH 2 with HNO_3 were added, and the mixture was heated to 85 ± 2 °C for 2 h with occasional agitation. A second 3-mL aliquot of 30% H_2O_2 (pH 2 with HNO_3) was then added and the sample was then heated again to 85 ± 2 °C for 3 h with intermittent agitation. After cooling, 5 mL of

3.2 M NH_4OAc in 20% (v/v) HNO_3 was added and the sample was diluted to 20 mL and agitated continuously for 30 min. The addition of NH_4OAc is designed to prevent adsorption of extracted metals onto the oxidized sediment.

(v) *Residual*: The residue from (iv) was digested by microwave.

Between each successive extraction, solid-liquid separation was achieved by centrifuging at 2750 rpm for 30 min. The supernatant was decanted and filtered through a 0.2 μm nylon syringe filter, five drops of 1:10 HNO_3 was added to the sample to maintain the pH below 2.



CHAPTER 5

EXPERIMENTAL OBSERVATION

5.1 Sand-manure biobarrier

5.1.1 Properties of manure and substrate solution

The average values of triplicate sampling are present in Table 5.1. The laboratory experiment showed that the manure itself contained the organic substances and nutrients, which can be supplied to the microbes. The pH of manure was slightly alkaline. The manure can be the habitat of natural living microbes [95]. The ratio of COD:TKN:soluble P ratio of manure was 295:6.5:1. The ratio of these substrates was higher than the recommended ratio for biological treatment under aerobic condition of C:N:P ratio 250:5:1 [96]. However, the manure may partially contain the non-available C and N substrates. To be ensured that the microbes can obtain enough consumable substances C and N, the molasses was fed to inoculate the living microbes. The ratio of COD: TKN: soluble P of molasses is 160: 2: 1. Nevertheless the C: N: P of molasses is lower than the recommended ratio [96], the fractions of available C, N and P of molasses was highly and promptly to be consumed by microbes. Therefore, the solution of molasses was employed to the system in order to enhance the assimilation process of microbes.

Table 5.1 Properties of manure and molasses

Parameters	Manure	Molasses
COD (g kg ⁻¹)	678	606
TKN (g kg ⁻¹)	14.9	7.9
Soluble P (g kg ⁻¹)	2.3	3.9
pH*	8.00	4.33
Organic Matter, OM (%)	39.3	N/A

*solid to water ratio of 1:5 was applied to manure sample, but the conventional pH measurement was used for molasses solution. N/A is non-available.

5.1.2 Biofilm formation

Under natural condition, the mixed microbial species present at the contaminated site should be able to tolerate Pb(II). The physical appearance of biofilm is shown in Figure 5.1 The biofilm producing seeds were from manure or cow dung. The natural microbial seeds were incubated with molasses to increase the biomass of Pb(II)-tolerance microbes prior to acclimatisation with Pb(NO₃)₂. A thick biofilm was observed within 111 d after feeding the synthetic acidic substrate with Pb(II) solution at a hydraulic loading rate of 0.291 m³ m⁻² d⁻¹ (500 mL d⁻¹). However, a thick layer of dark coloured biofilm was presented on the top layer of 0-1 cm depth only. The clogging and ponding had been observed so that the loading rate was reduced to 0.174 m³ m⁻² d⁻¹ (300 mL d⁻¹). The removal efficiencies of COD and Pb(II) were constant at 30% and 60%, respectively. The biomedias were then removed from the column to determine their properties.



Figure 5.1 Physical appearance of biofilm on the top layer of biosorbent (0-7 cm depth).

The FTIR spectra can reflect the functional groups of biopolymer observed in the thick film layer on biosorbent, the results are illustrated in Figure 5.2. The possible functional group at every assigned wave number are summarised in Table 5.2 [97]. Table 5.3 provides the summary of the presence of functional groups of the

biopolymer in each layer along the biosorbent. The functional groups of alkyl, hydroxyl or amino substituent and C=O stretching in carboxyl and amide group were observed in the entire column as same as the raw biomaterial. These functional groups were presented the background of the raw biomaterial, which were hydrophobic biosorbent containing the long chain of exchangeable anionic species. The functional group C=O stretching in carboxyl and amide group were developed after biofilm forming. These functional groups indicated that the biofilm could either bind or sorb the Pb(II) onto the peptide linkages of biofilm. The functional group C=O stretching in carboxyl and amide group was peaked at the top layer (0-3.5 cm depth), indicating the high numbers of peptide linkages that were originated from the biomass.

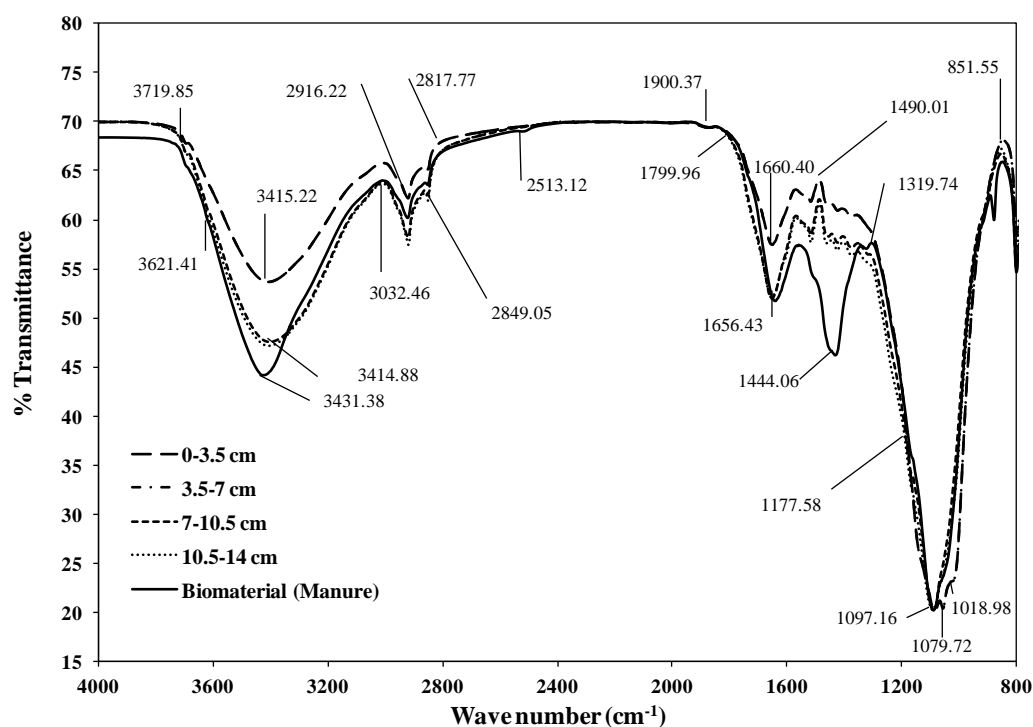


Figure 5.2 FT-IR spectra of biosorbent and biomaterial.

Table 5.2 Possible functional group at assigned wave number

Possible assignments	Wavenumber (cm ⁻¹)
H-bonded OH groups (polysaccharides) and NH ₂ stretching (proteins)	3600-3200
Aliphatic C-H stretching (fatty acids)	2960-2850
C=O carbonyl stretching, -CN stretching (amide I) group of protein peptide bond	1660-1650
C=N stretching (amide II)	1542
Phenolic -OH and C=O carboxylate stretching	1455-1423
C-H bending, CH ₃ stretching, COO symmetric stretching (amino acid side chains, fatty acids)	1396-1389
C-O-C and -OH stretching of polysaccharides	1207
P-O-C, P-O-H stretching (phospholipids, ribose phosphate chain pyrophosphate)	970-1022

Table 5.3 Functional group of biopolymer appeared in artificial biosorbent

Sample (depth below the surface)	Functional group of biopolymer			
	Hydroxyl or amino compound (3500-3200)*	Alkyl Group (C-H stretching) (3000-2850)*	C=O Stretching in carboxyl and amide group (1650-1550)*	Alkyl group- Hydroxyl or possibly amino substituent (1375-1300)*
Biosorbent				
0-3.5 cm (inlet)	Yes	Yes	Yes	Yes
3.5-7 cm	Yes	Yes	Yes	Yes
7-10.5 cm	Yes	Yes	Yes	Yes
10.5-14 cm (outlet)	Yes	Yes	Yes	Yes
Biomaterial (manure)	Yes	Yes	No	Yes

*the wavenumbers (cm⁻¹) of FTIR spectra

5.1.3 Bioaccumulation test

The accumulation of sorbed Pb(II) in the non-autoclaved sample (A1-biosorbent) was determined at the top layers (0-3.5 cm depth) of biosorbent as the dense community of biofilm was obtained in this region. The data were fitted with the modified Gompertz model (Figure 5.3). The pH of Pb(II) solution could possibly inhibit the activities of living cell; therefore, the substrate with Pb(II) solutions at pH of 4.0, 7.0 and 9.0 were tested. The bioaccumulation of Pb(II) onto A1-biosorbent occurred quickly, as the lag time was very short. Under the pH levels of 4.0, 7.0 and 9.0, the rate constants of the sorption were 0.046, 0.050, 0.052 mg sorbed Pb(II) h⁻¹, respectively. The maximum accumulated Pb(II) on biosorbent under the pH at 4.0, 7.0 and 9.0, are 14.0, 16.0 and 16.6 mg Pb g⁻¹ organic matter (OM), respectively. This suggests that under the alkaline condition (pH = 9.0), the biofilm could still well accumulate the Pb(II). On the other hand, the acidic condition (pH = 4.0) could inhibit the accumulation of Pb(II) in the biofilm. This effect was due to the fact that pH might influence bioactivity or affect Pb(II) dissolution/precipitation. Since the forms of Pb(II) species may change with pH and some species can deposit better than others.

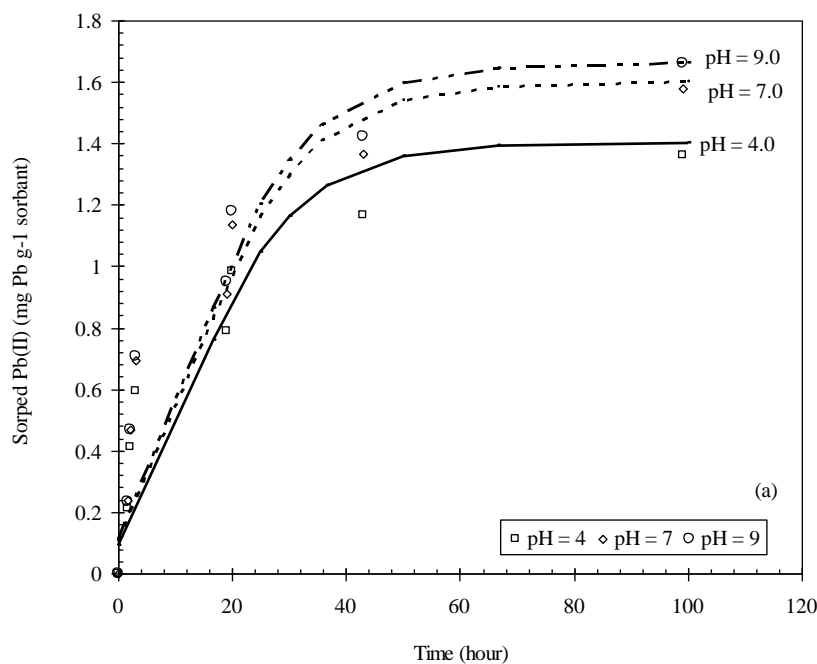


Figure 5.3 Biosorbent is fitted with modified Gompertz model

In the case of acclimatised microbial seed, the inhibition of Pb(II) on bioactivity may influence to the biosystem. The bioaccumulation process of Pb(II) under the acidic pH was further studied in the macroscopic scale. The Monod model was employed to determine the linkage between substrate utilisation rate and microbial growth. The graphical plot of Monod model is illustrated in Figure 5.4. The constants for Monod model are summarised in Table 5.4. Since the Pb(II) was accounted as the co-substrate or trace element, which could be biologically utilised by the acclimatised microbes, as indicated by higher μ_{\max} value of the biosystem fed by the pure substrate solution. The pure solution with $[S_0] \ll K_s$ refers that the plenty amount of substrates are served to microbes. There is no substrate competitive condition in the biosystem when it is supplied with Pb(II) mixed substrate solution. In other words, the Pb(II) ions could stimulate the substrate utilisation of biofilm as they are trace element.

Table 5.4 Constants for Monod equation

Substrate	K_s (g COD L ⁻¹)	μ_{\max} (h ⁻¹)	R^2
Molasses	40	333	0.949
Molasses + Pb(II)	57	500	0.855

Table 5.5 Parameters of adsorption isotherm on manure and biosorbent

Sample	1/n	K_F	R^2
A2-Biosorbent (autoclaved)	0.10	0.09	0.921
Biomaterial (manure)	1.04	0.62	0.917

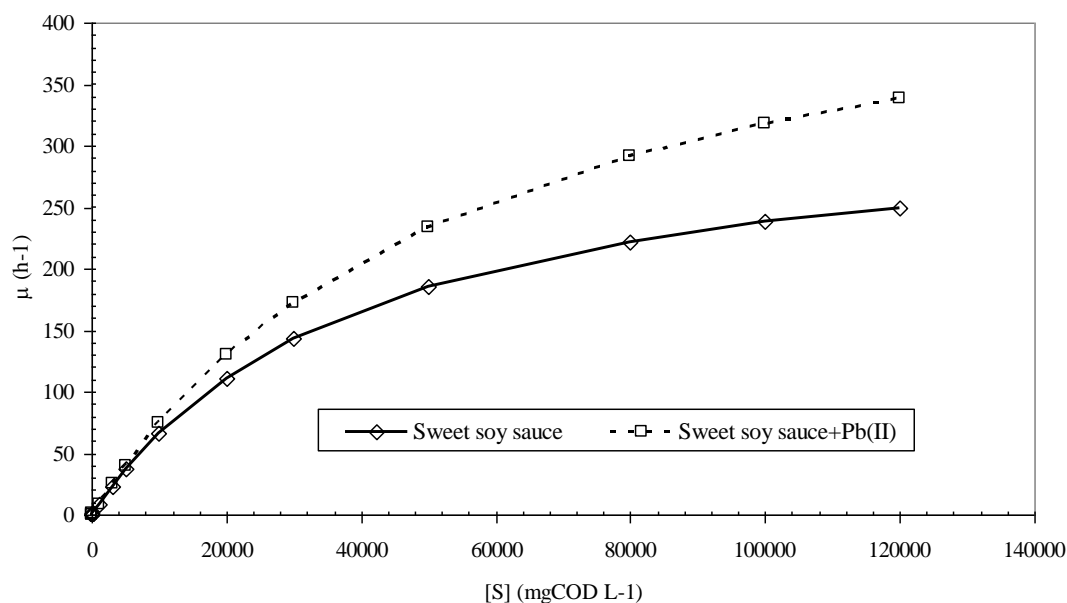


Figure 5.4 Specific substrate utilisation rate fitted by Monod model.

5.1.4 Biosorption test

The pH of $\text{Pb}(\text{NO}_3)_2$ synthetic wastewater was controlled at 4, with only ionic Pb(II) species were present. The reaction between Pb(II) and biosorbent could reach the equilibrium condition within 100 min. The data of isotherm test were well fitted with Freundlich isotherm model. The Freundlich model constants were summarised in Table 5.5. The final pH of bioslurry samples was 7.6 which indicated that the manure had the pH buffering system, which could self-adjust and maintain the pH of biosystem at the neutral range. In associate with the diagram for Pb(II) species at various pH levels (Figure 5.3b), the Pb(II) species were stored in the manure by forming the precipitants of $\text{Pb}(\text{CO}_3)$ [98]. The manure had a low affinity and capacity for Pb(II) adsorption as the low values of $1/n$ and K_F were yielded. The adsorption isotherm results confirmed that the Pb(II) could be adsorbed onto A2-biosorbent. The higher values of $1/n$ and K_F pointed out that the biosorbent could provide the higher affinity and capacity for Pb(II) biosorption. Since the value of $1/n$ is close to 1, the A2-biosorbent could sorb Pb(II) and form a mono layer of sorbed Pb(II) onto the surface. The A2-biosorbent represented the homogeneity surface, which could

effectively biosorb Pb(II) species. The maximum biosorption capacity was 6.2 mg Pb g⁻¹ OM at the top portion of biosorbent.

The sorbed form of Pb(II) on the biosorbent was determined by the sequential extraction process. The results are given in Figure 5.5. After leaching with Pb(NO₃)₂ solution, the low amount of Pb remained in the biomaterial and the Pb species were mostly trapped onto OM. In the matured biosorbent, a higher amount of sorbed Pb was kept in the biosorbent than the initial biomaterial. The Pb was predominately fixed on the OM at the top layer, expecting the biofilm played a significant role in Pb(II) sorption [99]. The high amount of residual Pb was present in the entire column and the levels of residual Pb were constant in every layer. The residual Pb(II) refers to the inert Pb(II), which was sorbed by the organic constituents containing in the substrate solution. The amounts of Pb bound-to-Fe & Mn were stagnant along the column, assuming Pb(II) species were sorbed onto the oxides of Fe and Mn originated from substrate solution too. Little amount of Pb bound to carbonate was detected in the biosorbent. The Pb bound to carbonate could not maintain in the acidic pH condition, so this sorbed Pb might dissolve and liberate from the biosystem, or form the complex of Pb(CO₃)-OM.

Consequently, the amounts of total sorbed Pb were decreased along the depth of biosorbent, indicating the absence of active living biomass. The soluble and exchangeable Pb(II) species were of major concern, as they could easily escape from the thin biofilm. The lower amount of free Pb(II) could be observed at the lower portion of biosorbent. The finding suggested that the dead biomass could slightly retard the migrations of soluble and exchangeable Pb(II). This confirmed that even the dead biomass, the harmful Pb(II) species in the forms of exchangeable and soluble could be stored as same as the living biomass in the fresh biosorbent.

The major mechanisms for Pb(II) restoration in this active biosorbent were bioaccumulation and biosorption. A 56% of Pb(II) was kept on living cell by bioaccumulation and another 44% of Pb(II) was sorbed onto dead cell by biosorption. In the active zone of biosorbent, the biopolymers played an important role in both bioaccumulation and biosorption. Besides, the synthetic biosorbent was acidic resistant, it could be applied to restore free Pb(II) from the acidic Pb contaminated wastewater.

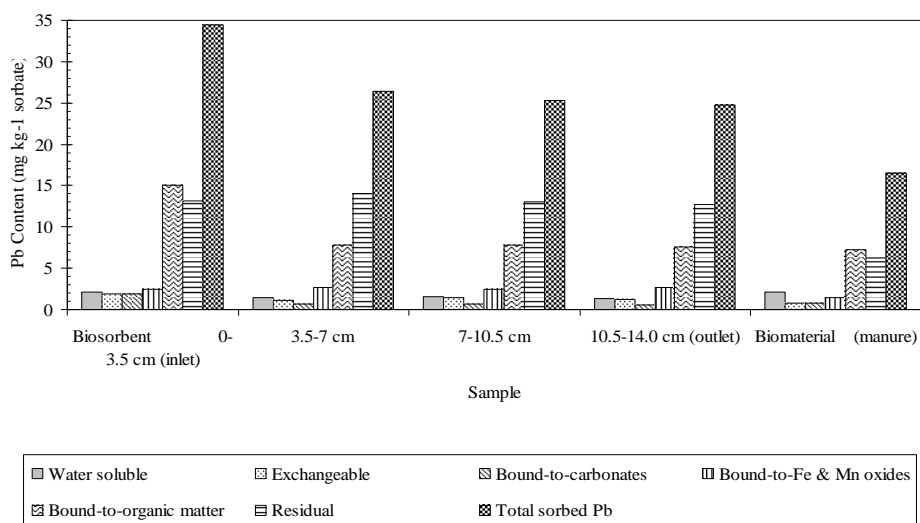


Figure 5.5 The sequential extraction of sand-manure biobarrier

The sequential extraction are also applied for many purposes, mainly to examine the forms of sorbed species [100]. Sequential extraction is an analytical process that chemically leaches metals out of soil, sediment and sludge samples. The purpose of sequential “selective” extraction is to mimic the release of the selective metals into solution under various environmental conditions. In defining the desired partitioning of trace metals, concern was taken to choose fractions likely to be affected by various environmental conditions; the following five fractions were selected.

Fraction 1 Exchangeable: The sediments or constituents (clays, hydrated oxides of iron and manganese, humic acids) have demonstrated the adsorption of trace metals; changes in water ionic composition (e.g., in estuarine waters) are likely to affect sorption-desorption processes.

Fraction 2 Bound to Carbonates: The significant trace metal concentrations can be associated with sediment carbonates; this fraction would be susceptible to changes of pH.

Fraction 3 Bound to Iron and Manganese Oxides: Iron and manganese oxides exist as nodules, concretions, cement between particles, or simply as a coating on particles; these oxides are excellent scavengers for trace metals and are thermodynamically unstable under anoxic conditions.

Fraction 4 Bound to Organic Matters: Trace metals may be bound to various forms of organic matter: living organisms, detritus, coatings on mineral particles, etc. The complexation and peptisation properties of natural organic matter (notably humic and fulvic acids) are well recognised, as is the phenomenon of bioaccumulation in certain living organisms. Under oxidising conditions in natural waters, organic matter can be degraded, leading to a release of soluble trace metals.

Fraction 5 Residual: Once the first four fractions have been removed, the residual solids should contain mainly primary and secondary minerals, which may hold trace metals within their crystal structure. These metals are not expected to be released in solution over a reasonable time span under the conditions normally encountered in nature.

5.1.5 Mechanism between Pb(II) and microbial community

Analyses of microbial community by DNA extraction and purification, PCR amplification, DGGE, and sequencing of DGGE bands were also performed in this study. Three clones of each band were sent for sequencing at 1st Base Co. Ltd., Malaysia. The sequence results were analyzed using BLASTn program to identify the bacterial species as shown in Figure 5.6.

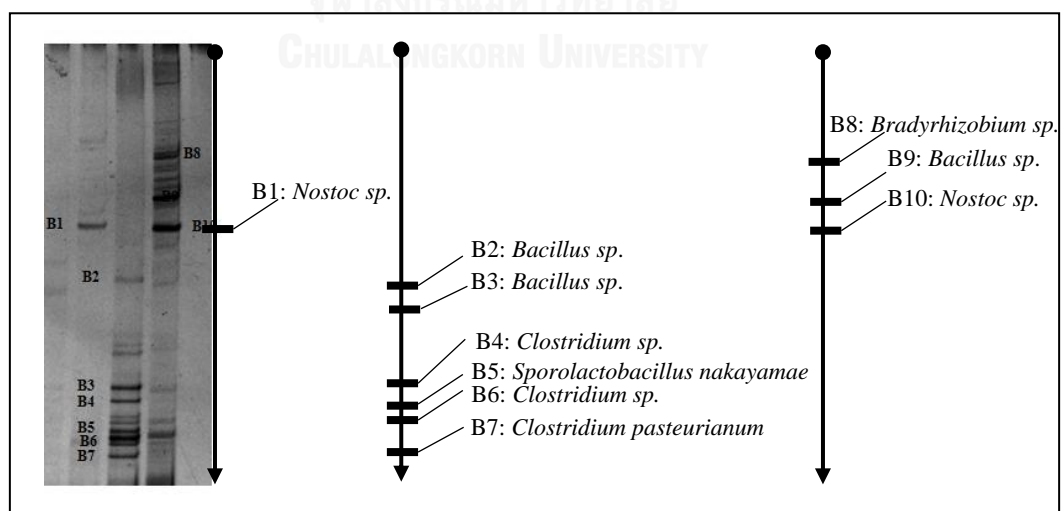


Figure 5.6 Bands for sequencing to identify the species of microbial

Table 5.6 Microbial communities profile determined with PCR-DGGE of partial 16S rRNA genes fragments in sand-manure biobarrier.

DNA band	Bacterial strains	Accession number	% similarity
B2	<i>Bacillus sp.</i>	GU932940	94
B3	<i>Bacillus sp.</i>	KC422653	100
B4	<i>Clostridium sp.</i>	AY925093	99
B5	<i>Sporolactobacillus nakayamae</i>	JQ897433	100
B6	<i>Clostridium sp.</i>	AY082483	99
B7	<i>Clostridium pasteurianum</i>	EF656617	98

The microbial strains isolated from matured sand-manure biobarrier determined with PCR-DGGE of partial 16S rRNA genes fragments showed predominant species which are *Bacillus sp.*, *Sporolactobacillus nakayamae*, *Clostridium sp.*, and *Clostridium pasteurianum* shown in Figure 5.6 and Table 5.6. These species have been previously found by many studies to be able to retain several metal ions and could grow in an anaerobic environment. Govarthan et al. (2013) reported that *Bacillus sp.* KK1 had mineralized the active Pb ions to inactive Pb or biomineralization of lead in mine tailings. Francis et al. (2015) found out that *Clostridium sp.* can precipitated soluble Tc(VII) to Tc(IV) in contaminated soils at nuclear and norm Sites. The reduced Tc was associated with the cell biomass, as well as being associated with organic metabolic products in solution. *Clostridium sp.* can solubilize and precipitate uranium in a sludge and sediment sample [101, 102]. Members of the genus *Sporolactobacillus* have been defined as catalase-negative, spore-forming, homofermentative, lactic acid-producing organisms that belong to the family *Lactobacillaceae*. Six species in the genus *Sporolactobacillus* have been reported, including *S. inulinus*, *S. kofuensis*, *S. lactosus*, *S. laevolacticus*, *S. nakayamae*, and *S. terrae* [103]. Chang et al. (2008) used molasses substrate to study biohydrogen production from an anaerobic continuous-flow fermentation system, *Sporolactobacillus nakayamae* and *Clostridium sp.* shown in the system. The results from RNA based analysis of hydrogenase gene and 16S rRNA gene suggested that *Clostridium* was existed in the fermentative hydrogen-producing system and might be the dominant hydrogen-producing. [104]

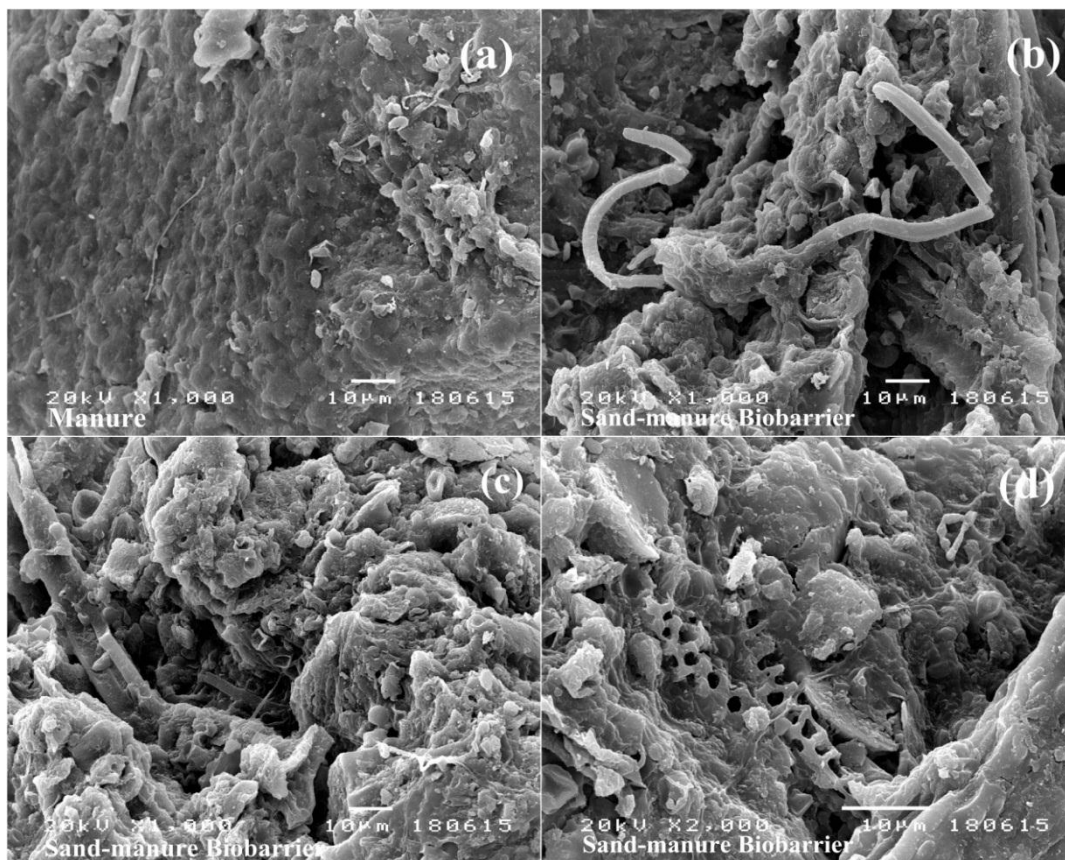


Figure 5.7 Scanning electron microscopy (SEM) images of (a) Sand-manure (b,c,d) Sand-manure Biobarrier

Scanning electron microscopy (SEM), JEOL, JSM-5410 LV found some of filamentous and thin film that can stabilize Pb(II) shown in Figure 5.7. Ben et al. revealed that *Bacillus sp. PZ-1* can sorption to Pb(II) involved surface adsorption, ion exchange and micro-precipitate [105].

5.2 Zeolite Biobarrier

5.2.1 Inoculum and biobarrier properties

The efficiencies of COD removal during incubating, acclimatising and attaching on barrier are illustrated in Figure 5.6(a). The molasses substrate solution with 2.0 g COD/L was fed to SBR bioreactor during the first 40 days, the microbes used molasses as substrate. The COD removal efficiency was very high with an average of 90%. The number of microbes was quickly increased from 50.6 to 56.6 g VSS/L. After that, the 0.2 mg/L of $\text{Pb}(\text{NO}_3)_2$ solution was added to the substrate solution to acclimatise this microbial seed. The microbes could quickly adapt to $\text{Pb}(\text{NO}_3)_2$ containing substrate within 40 days. The averaged COD removal efficiency dropped to 50%, only Pb resistant microbes could survive. The Pb resistant microbes were derived from the natural microbial species via substrate selection. These microbes could take up organic carbon from molasses and tolerate the ionic Pb.

However, the numbers of microbes were reduced significantly to 42.7 g VSS/L. The suspended cells were gradually poured into zeolite column to build the biomat. Basically, the microbes prefer to attach on the media rather than suspense in the solution. The thin film of microbes was emerged within a week at the surface of column A-1. The COD removal efficiency was still remained at 50%. The numbers of microbes at the biofilm continuously increased and the thickness of the biomat of 10 cm (half of media length) was achieved within 50 days. The COD removal slightly increased to 70%. The Pb(II) removal efficiencies during acclimatilising and attaching on media were presented in Figure 5.6(b). The Pb(II) could be removed by suspended-growth microbes with 50% efficiency during the acclimatisation. The Pb(II) removal efficiency was elevated to 70-80% by the attached growth microbial communities on zeolite media. As the number of Pb resistant microbes was high, the Pb(II) could be stored by the living cells via metabolic and non-metabolic processes.

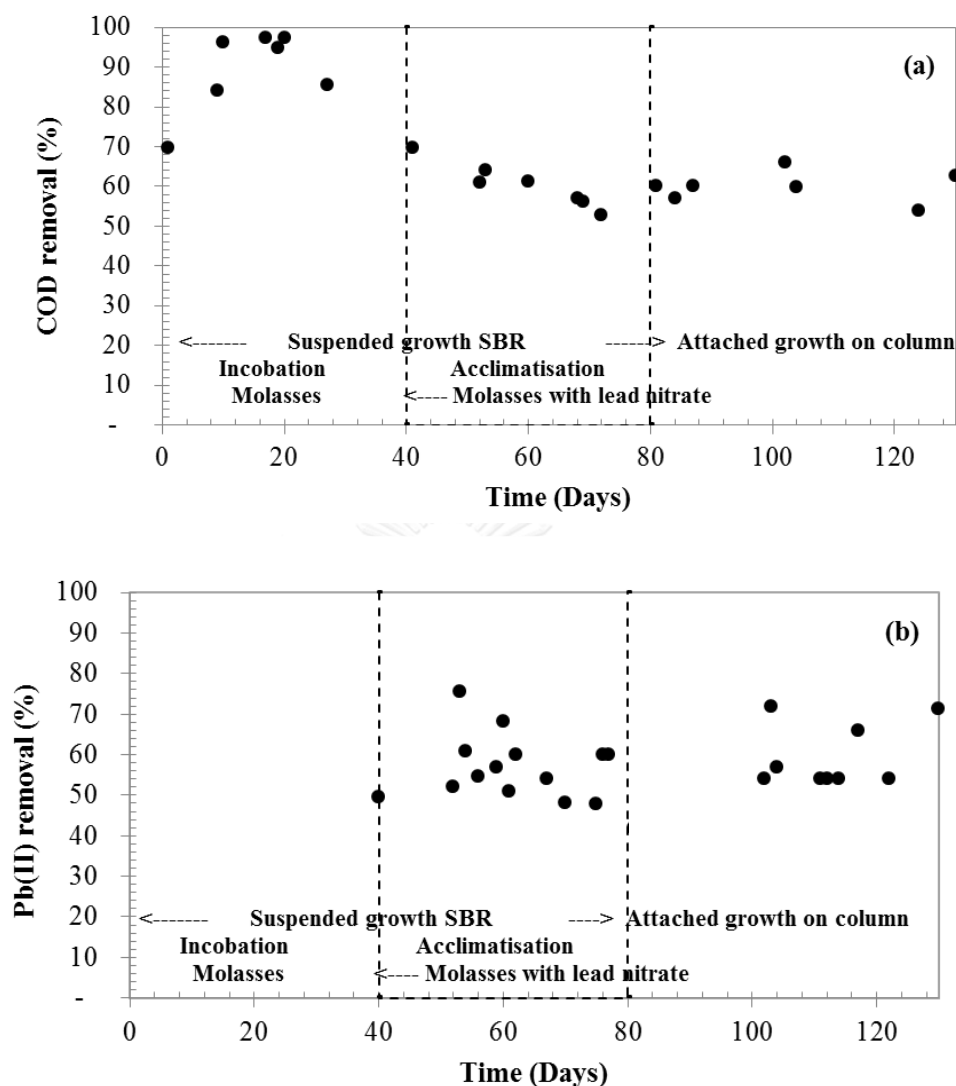


Figure 5.8 Removal efficiencies of (a) COD and (b) Pb(II) in suspended growth SBR and attached growth on column A-1

A laboratory scale biobarrier column A-1 was maintained for another 272 days by feeding with mixed substrate solution of molasses and $\text{Pb}(\text{NO}_3)_2$. A fresh zeolite was packed into column A-2, the 0.2 $\text{Pb}(\text{NO}_3)_2$ solution was fed through the media to determine the sorption capacity of zeolite. The removal efficiency of COD of column A-1 seemed to be constant at 70% for the whole testing period of 272 days. The removal efficiencies of Pb(II) of columns A-1 and A-2 were averaged at 85 and 96%, respectively. After 250 days, the zeolite in column A-2 was breakthrough. The Pb(II)

could not be further adsorbed, as the adsorptive surface of the zeolite was saturated with Pb(II). On the other hand, the biobarrier in column A-1 have not yet reach the breakthrough. The results are presented in Figure 5.7 By comparison, Pb(II) was stored in A-1 column longer than A-2 column, the infinite capacity of Pb(II) restoration was relied on microbial activities, as they could immobilise and retarde the Pb(II) [106].

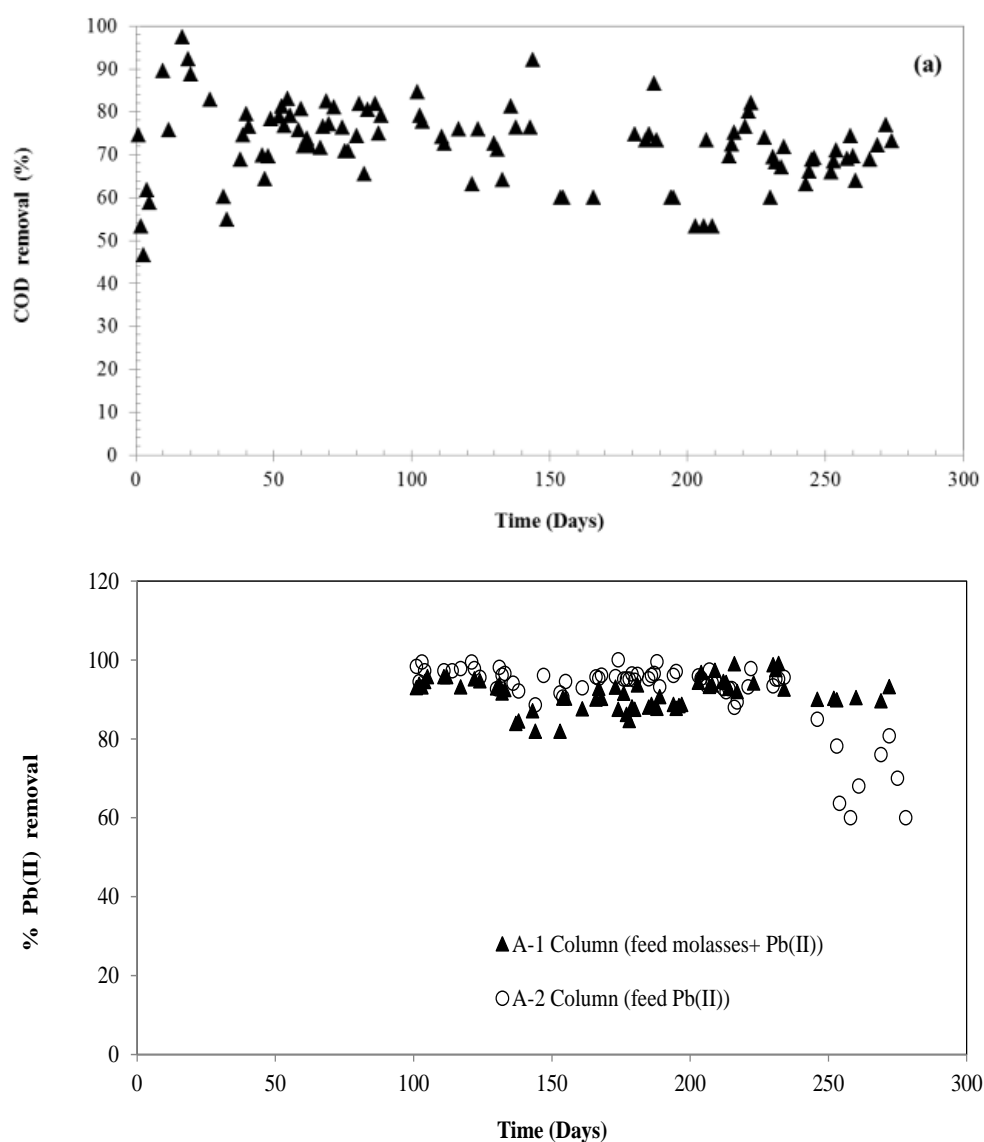


Figure 5.9 Removal efficiencies of (a) COD and (b) Pb(II) in biobarrier (column A-1) and fresh zeolite (column A-2)

5.2.2 Adsorption of Pb onto zeolite

The breakthrough curve was constructed for both columns A-1 and A-2. However; to be better understand the adsorption behavior in the column, the unknown maximum adsorption capacity (q_0) must be defined by a batch test of adsorption isotherm. The samples of biobarrier and fresh zeolite were taken and tested for equilibrium time. The equilibrium time of Pb(II) adsorption was 120 minutes. The data governed from adsorption isotherm test were sequentially plotted using Langmuir and Freundlich isotherm models. Freundlich model was better fitted to the observation data. This revealed that Pb(II) could interact with the active site only and physisorption is predominantly. The data obtained from isotherm study are presented in Table 5.7. The Thomas model was used to explain the observation data in order to predict the breakthrough curves of Pb(II) of columns A-1 and A-2. The constants of Thomas model are presented in Table 5.8. This confirms that bioaccumulation and biosorption in biobarrier can enlarge the capacity of Pb(II) adsorption on sorbent.

Table 5.7 Adsorption constant rate of Pb(II) batch adsorption on sorbent

Sample	1/n	K_F	R^2
Biobarrier	0.662	0.0169	0.985
Zeolite	1.402	0.0009	0.913

Table 5.8 Adsorption constant rate of Pb(II) column adsorption on sorbent

Sample	q_0 (mg Pb/g)	k_{th} (mL/mg-min)	R^2
Biobarrier (Column A-1)	70.12	0.00015	0.917
Zeolite (Column A-2)	54.24	0.00038	0.921

5.2.3 Biosorption and bioaccumulation of Pb onto biobarrier

FTIR spectra of the zeolite and biobarrier are presented in Figure 5.10. Biobarrier in column A-1 has enriched with biopolymers, the major functional groups were Si-OH, O-H, aliphatic C-H (fatty acids), C=O, cationic metals, C=O, N=O, Si-

CH₃, Si-O-Si, Si-O-Al, Si-O-Si, C-N, Metal-H, PO₄³⁻ and N-C-N,-OH (polysaccharides) and -NH₂ (proteins), aliphatic C-H (fatty acids), PO₄³⁻, P-O-C and P-O-H (phospholipids and ribose phosphate chain pyrophosphate). For the zeolite in A-2 column, most of the same functional groups were identified excluding of aliphatic C-H (fatty acid).

As a result, the zeolite and the synthetic Pb(NO₃)₂ have no organic carbon compounds. Ahemad and Kibret [107] reported that the major mechanisms of biosorption and bioaccumulation were physical sequestration, exclusion, complexation and detoxification. In fact, binding of heavy metals to extracellular materials can immobilise the metal and prevent its intake into bacterial cell. For instance, many metals bind the anionic functional groups (e.g., sulfhydryl, carboxyl, hydroxyl, sulfonate, amine and amide groups) present on cell surfaces. Likewise, bacterial extracellular polymers, such as polysaccharides, proteins and humic substances, also competently bind heavy metals via biosorption. On the surface of immobilised bacteria, the complex formation and ionic interactions between the metal cation and functional groups are yielded [22]. The biobarrier can enhance the adsorptive sites.

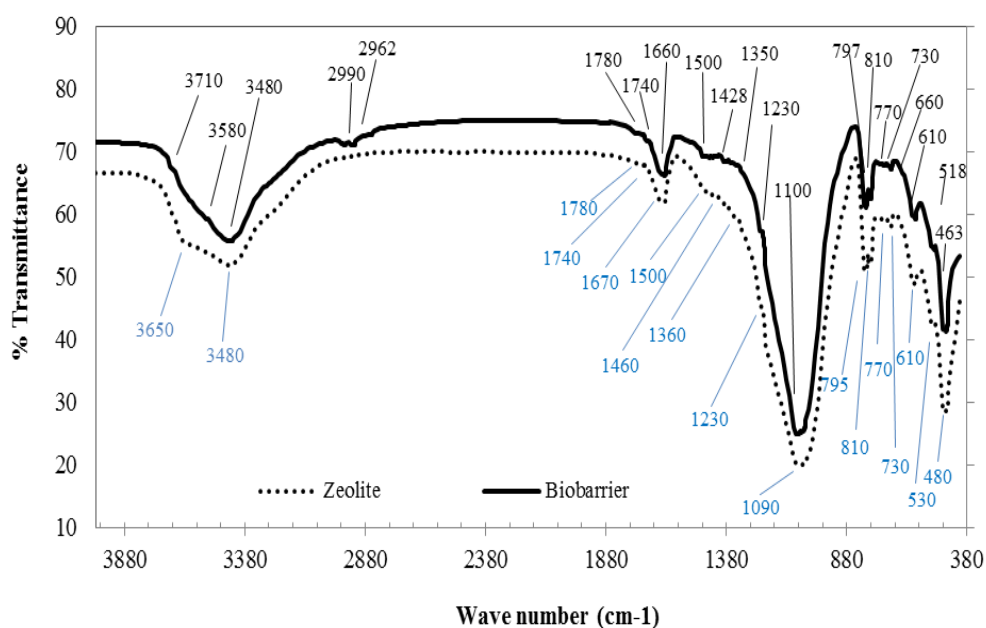


Figure 5.10 FTIR results of zeolite and biobarrier

For the better understanding of the surface deposition of Pb(II) onto zeolite and biobarrier, the X-ray diffraction (XRD) technique was introduced to identify the forms of Pb in the biobarrier (A-1 column). The thick film at top of column (0-5 cm below surface) showed several peaks which corresponding to the positions of wuartz (SiO_2), heulandite-Na ($\text{Na}_{1.56}\text{H}_{2.34}\text{Al}_{1.32}(\text{Al}_{7.86}\text{Si}_{28.14}\text{O}_{72})(\text{H}_2\text{O})$) and lead phosphate ($\text{Pb}_2\text{P}_2\text{O}_7$). At the thick film layer of 15-10 cm below surface (middle of column), the results showed the peak of quartz alpha - SiO_2 - hexagonal, clinoptilolite ($\text{Na}_{1.32}\text{K}_{1.28}\text{Ca}_{1.72}\text{Mg}_{0.52}(\text{Al}_{6.77}\text{Si}_{29.23}\text{O}_{72})(\text{H}_2\text{O})$), mordenite - $(\text{Na}_2, \text{Ca}, \text{K}_2)\text{Al}_2\text{Si}_{10}\text{O}_{24} \cdot 7\text{H}_2\text{O}$, minium, syn Pb_3O_4 , massicot – PbO . The biofilm at the upper layer could bind Pb with phosphate but the biofilm at lower layer could be less active as most of Pb was bound to oxides. The peak positions at zeolite sorbent at column A-2 were quartz alpha (SiO_2), clinoplilolite ($\text{Na}_{1.32}\text{K}_{1.28}\text{Ca}_{1.72}\text{Mg}_{0.52}(\text{Al}_{6.77}\text{Si}_{29.23}\text{O}_{72})(\text{H}_2\text{O})$), mordenite ($(\text{Na}_2, \text{Ca}, \text{K}_2)\text{Al}_2\text{Si}_{10}\text{O}_{24.7}\text{H}_2\text{O}$). These results reveal that biofilm could not react with oxides of metal on zeolite. Zeolite had active soluble metals and oxides, which could stimulate the Pb sorption onto biobarrier. The results are given in Figure 5.11, 5.12, 5.13.

(a)

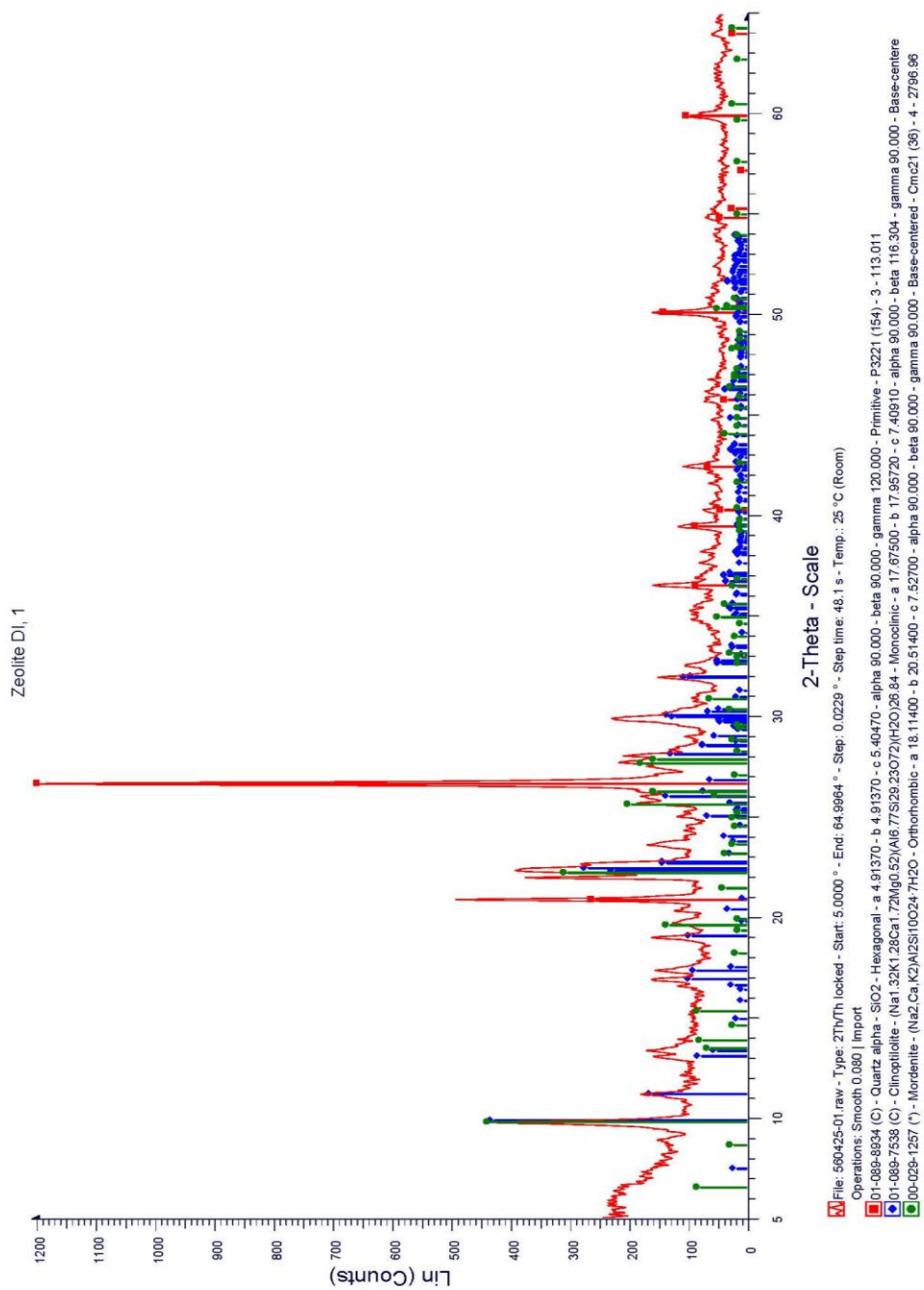


Figure 5.11 XRD peaks in (a) zeolite

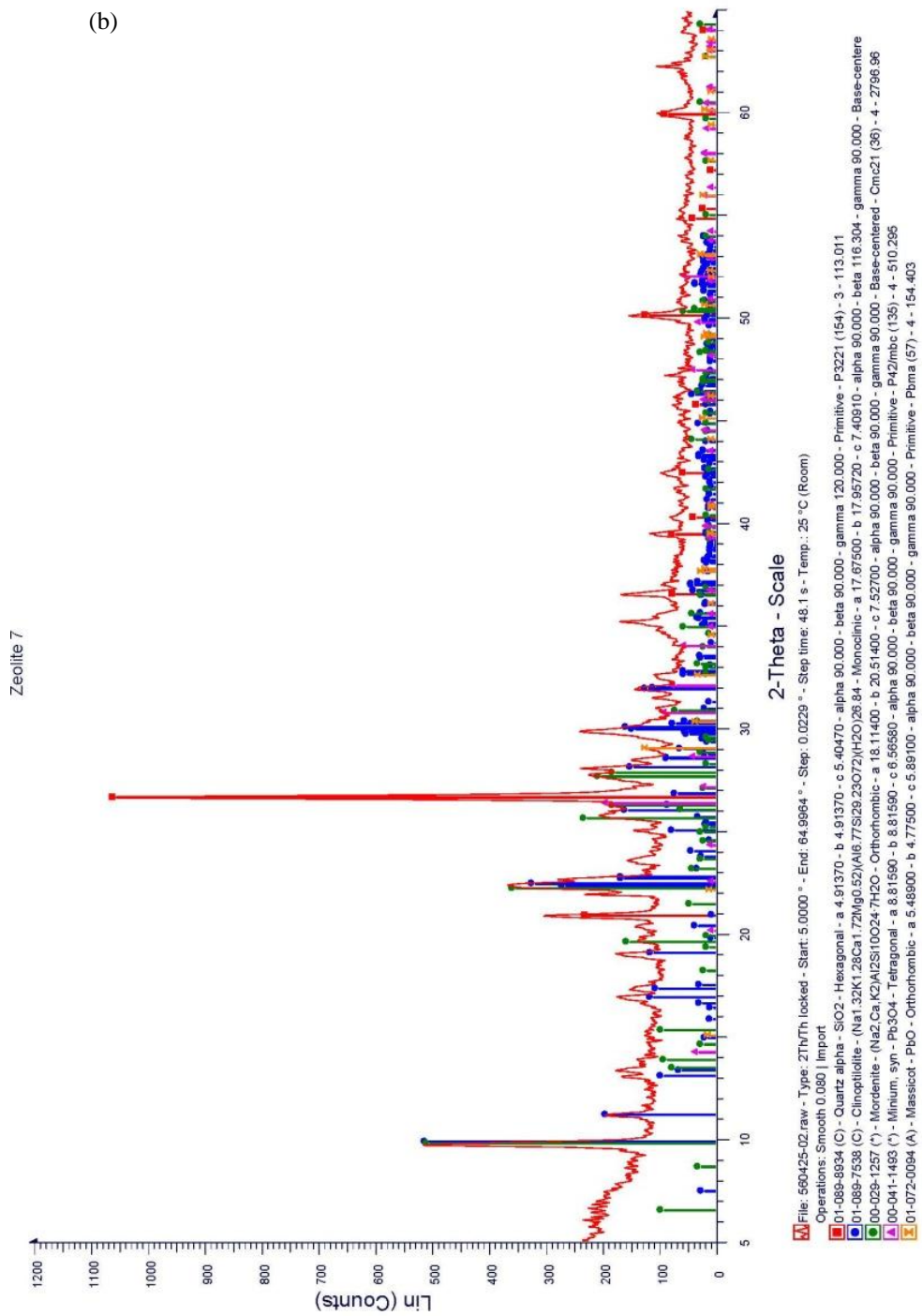


Figure 5.12 XRD peaks in biofilm layer at middle of biobarrier

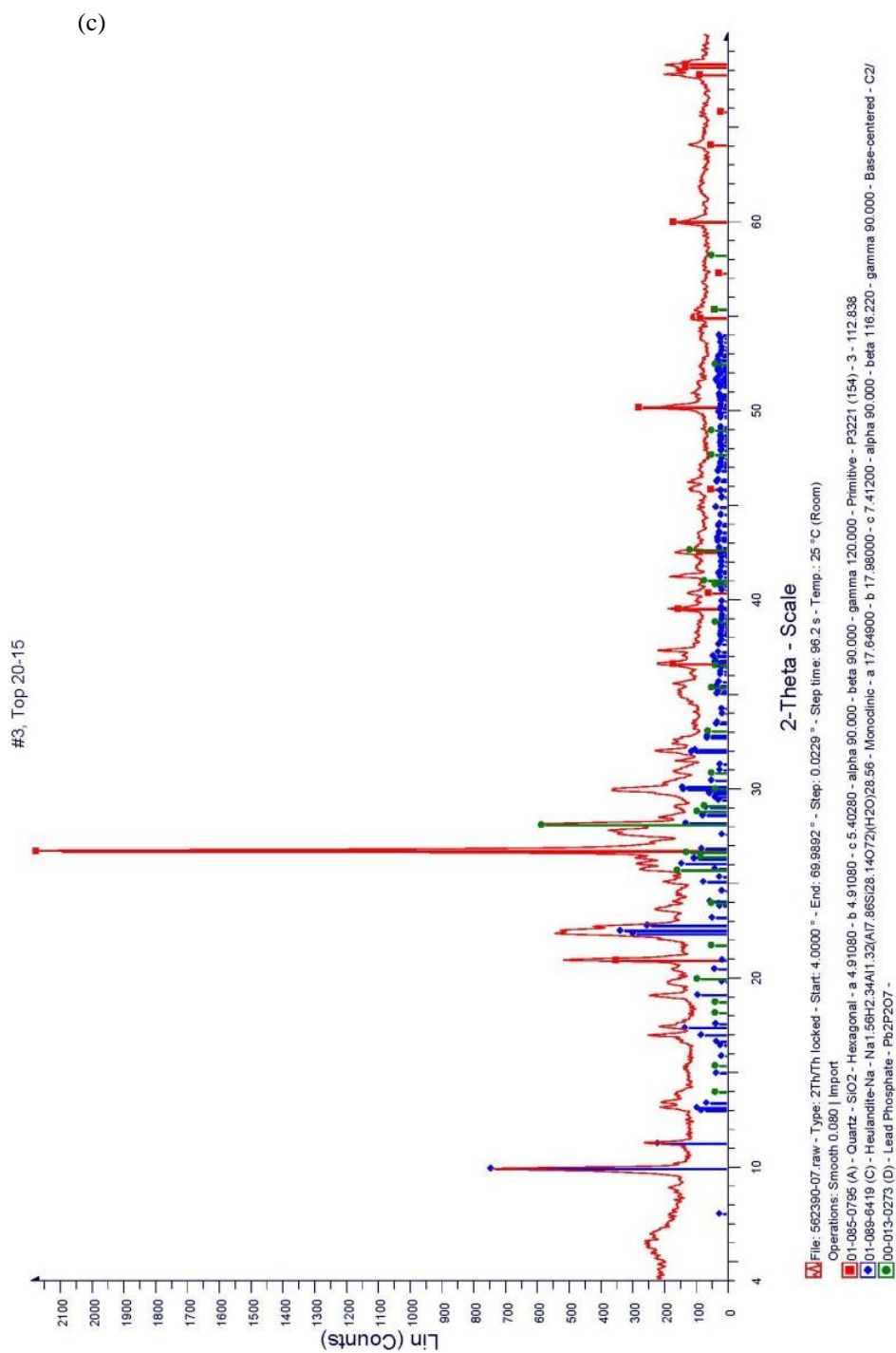


Figure 5.13 XRD peaks in (c) upper biofilm layer of zeolite biobarrier

The sorbed form of Pb(II) on the biosorbent was determined by the sequential extraction process. The results are given in Tables 5.9 and 5.10 and Figure 5.14.

Table 5.9 Chemical forms of Pb in biomaterial based zeolite, zeolite column fed Pb(II) and Biosorbent based zeolite

Chemical form (%)	Feeding		
	Biomaterial based zeolite	Pb(II) only	Biosorbent based zeolite
	mg/kg	mg/kg	mg/kg
Water soluble fraction	0.495	0.42	0.405
Exchangeable	0.32	1.256	0.752
Bound-to-carbonates	0.08	0.32	4.16
Bound-to-Fe & Mn oxides	0.42	1.28	0.48
Bound-to-organic matter	2.772	26.28	12.492
residual	4.976	26.76	26.58
Total sorbed Pb	9.063	56.32	44.871

Table 5.10 Chemical forms of Pb in biomaterial based zeolite, zeolite column fed Pb(II) and Biosorbent based zeolite

Chemical form (%)	Biomaterial based zeolite	Feeding Pb(II)	
		only	Biosorbent based zeolite
Water soluble fraction	5.46	0.75	0.90
Exchangeable	3.53	2.23	1.68
Bound-to-carbonates	0.88	0.57	9.27
Bound-to-Fe & Mn oxides	4.63	2.27	1.07
Bound-to-organic matter	30.59	46.66	27.84
Residual	54.90	47.52	59.24

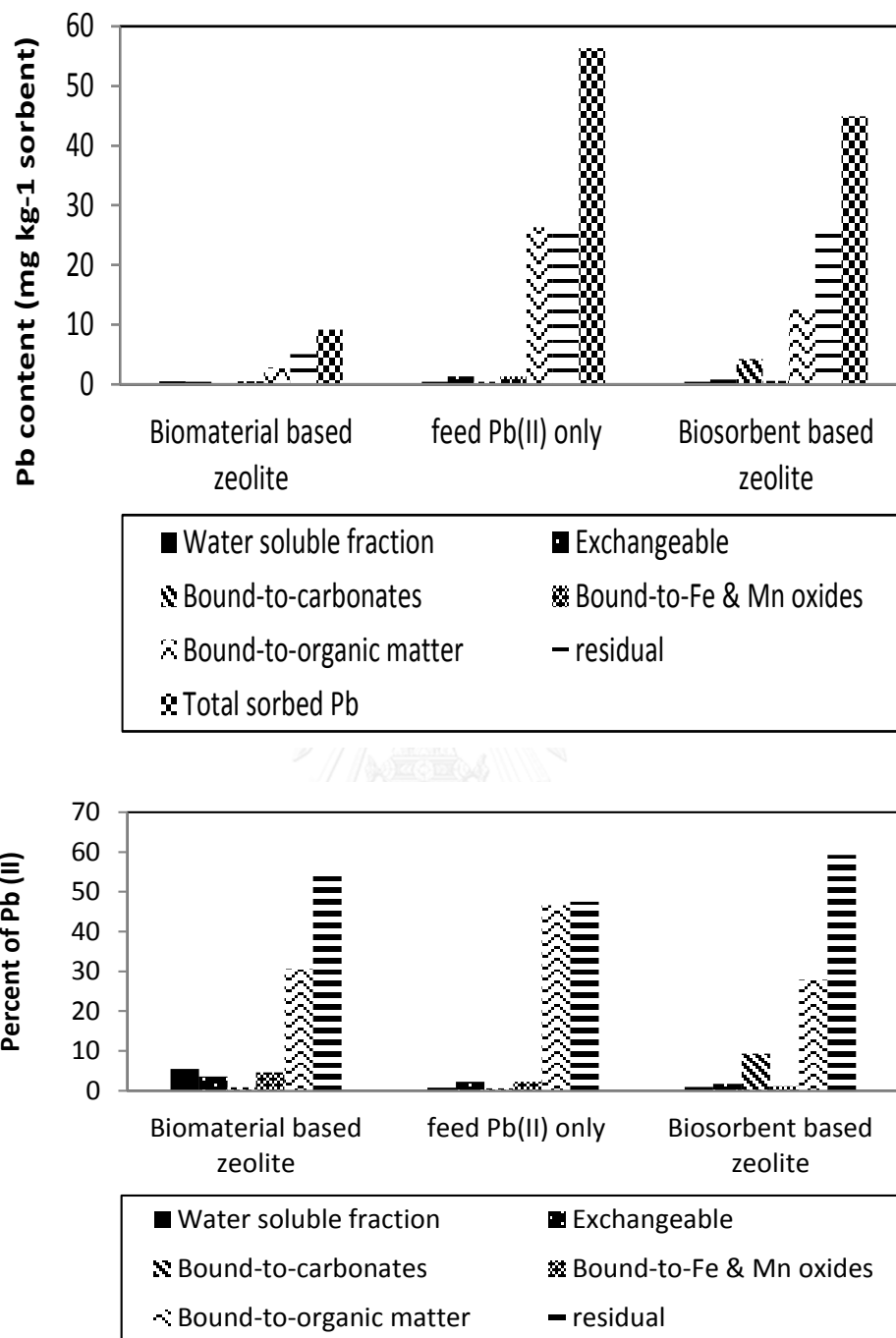


Figure 5.14 Sequential extraction of zeolite biobarrier.

The Monod's constants shown that molasses as substrates and molasses with Pb(II) as substrate were not different shown in Table 5.11.

Table 5.11 Constants for Monod equation of biobarrier

Substrate	K_s (g COD L ⁻¹)	μ_{max} (h ⁻¹)	R^2
Molasses	4.93	14.77	0.9480
Molasses + Pb(II)	4.95	15.57	0.9636

5.2.4 Mechanism between Pb(II) and microbial community

Analysis of archaeal community by DNA extraction and purification, PCR amplification, DGGE, and sequencing of DGGE bands were conducted and the data given in Table 5.12. The strains isolated from matured biobarrier were *Bacillus sp.*, *Nostoc sp.*, and *Bradyrhizobium sp.* Gupta and Rastogi [108] also found that *Nostoc sp.*, *Bradyrhizobium sp.*, and *Bacillus sp.* could remove Pb(II) from aqueous solutions in a batch system under varying range of pH (2.99–7.04), contact time (5–300 min), biosorbent dose (0.1–0.8 g/L), and initial metal ion concentrations (100 and 200 mg/L). Reichman [109] suggested that *Bradyrhizobium japonicum* strain CB1809 recently identified as a plant growth-promoting rhizobacteria in high arsenic substrate had potential to grow in arsenic contaminated sites and possibly other sites contaminated with other heavy metals. Bai et al. [110] also found that *Bacillus subtilis* DBM could form complex compounds with cell surface functional groups or precipitated on the cell surface, and 38.5% was intracellularly accumulated. Complexation of Pb(II) with carboxyl, hydroxyl, carbonyl, amido, and phosphate groups, $Pb_5(PO_4)_3OH$, $Pb_5(PO_4)_3Cl$ and $Pb_{10}(PO_4)_6(OH)_2$ were found on the cell surface during the biosorption process. This ensured that the microbial communities on biobarrier were actively, they could resist Pb. The stored Pb(II) was on biopolymers generating via microbial activity and free ions and oxides, Pb could be both biosorped and chemisorped. The Pb resistant species can perform a bioaccumulation. Pb(II) can be transformed to immobilised Pb, without disturbing microbial activities.

Table 5.12 Microbial communities profile determined with PCR-DGGE of partial 16S rRNA genes fragments in zeolite biobarrier

DNA band	Bacterial strains	Accession number	% similarity
B1	<i>Nostoc</i> sp.	DQ265952	86
B8	<i>Bradyrhizobium</i> sp.	JX284238	99
B9	<i>Bacillus</i> sp.	JQ740569	100
B10	<i>Nostoc</i> sp.	DQ265952	86

Scanning electron microscopy (SEM), JEOL, JSM-5410 LV. Found some of round and rod shape and thin film in zeolite biobarrier. The microbial identified *Bacillus* sp. normally in rod shape shown in Figure 5.15.

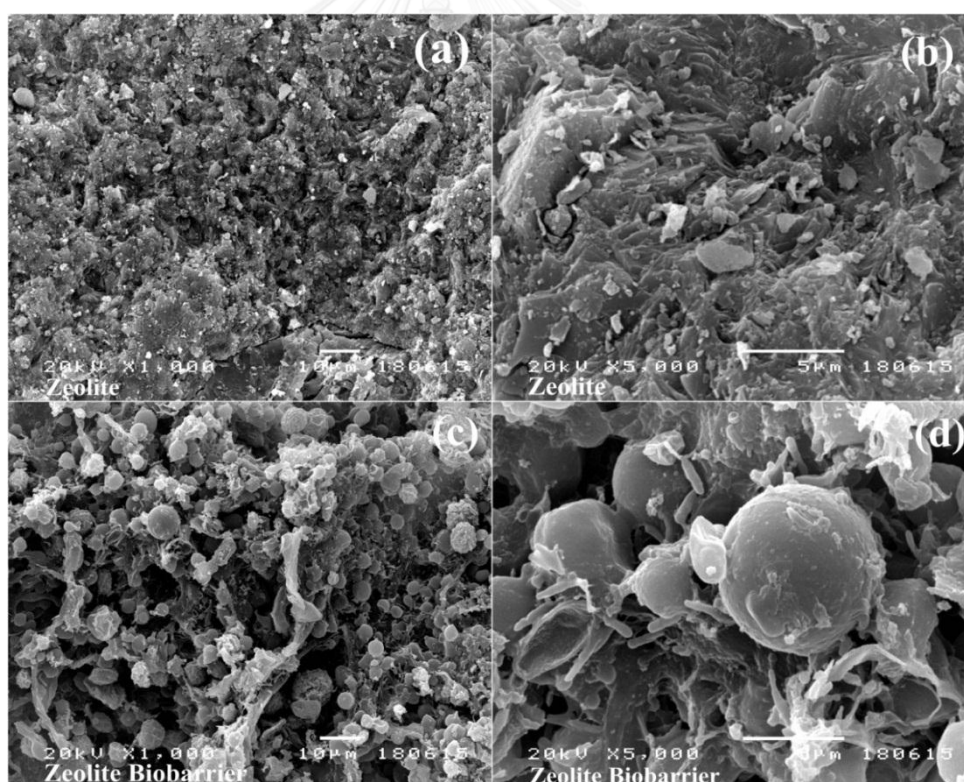


Figure 5.15 Scanning electron microscopy (SEM) images of (a,b) Zeolite
(c,d) Zeolite Biobarrier

CHAPTER 6

MODELLING OF DEVELOPED BIOBARRIER

6.1 Hydraulic properties curve

The flow of groundwater could consider the volumetric water content in soil convert pressure head in pore soil water. This equation presented the relationship between pressure head and volumetric water content. The hydraulic properties curves used in this research is derived by van Genuchten's model [86].

Van Genuchten derived the hydraulic properties equations based on the equation of Brooks and Coley. The hydraulic properties equations are presented as follows.

$$\theta = \theta_r + \frac{\theta_s - \theta_r}{(1 + (a|\psi|^p)^m)} \quad (6.1)$$

where a is the soil water retention function [L^{-1}], m and p are the empirical parameters yielded from the hydraulic properties curve [unitless], respectively.

The relative hydraulic permeability can be defined as follows.

$$k_{rw} = \frac{[1 - (a|\psi|)^{p-1} [1 + (a|\psi|)^p]^{-m}]^2}{[1 + (a|\psi|)^p]^{m/2}} \quad (6.2)$$

The constant values for the coefficients presented in van Genuchten equations were given in Table 6.1[111]. The coefficients were sorted by soil textures in accordance with USDA textural classes [112]

Table 6.1 Constant empirical coefficients for van Genuchten equations

Soil Type	Saturated Moisture Content, θ_s	Residual Moisture Content, θ_r	a (cm ⁻¹)	p
Clay*	0.38	0.068	0.008	1.09
Clay loam	0.41	0.095	0.019	1.31
Loam	0.43	0.078	0.036	1.56
Loam sand	0.41	0.057	0.124	2.28
Silt	0.46	0.034	0.106	1.37
Silt loam	0.45	0.067	0.020	1.41
Silty clay	0.36	0.070	0.005	1.09
Silty clay loam	0.43	0.089	0.010	1.23
Sand	0.43	0.045	0.145	2.68
Sandy clay	0.38	0.100	0.027	1.23
Sandy clay loam	0.39	0.100	0.059	1.48
Sandy loam	0.41	0.065	0.075	1.89

Note: *Agricultural soil, less than 60% clay.

The hydraulic properties curve was prepared to convert the pressure head to volumetric water content is given in Figure 6.1. The constants for hydraulic properties curve was obtained by van Genuchten's model are summarised in Table 6.2.

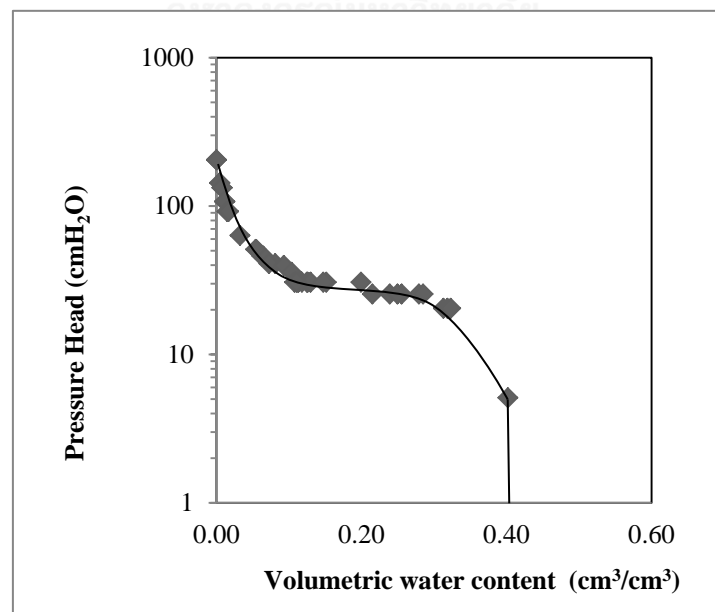


Figure 6.1 Water retention curve on zeolite sample

Table 6.2 Constants for hydraulic properties

Parameters	Sample	
	Reference value sand	Calculation Zeolite
θ_s	0.460	0.402
θ_r	0.034	0.026
a	0.106	0.148
p	1.370	1.057
m	0.403	0.054
Kzz(cm/hour)	-	0.27

The infiltration water could rapidly absorb at initial stage. As soon as the pore was full with water, the cumulative water could move downwards under gravitational force. Hence, the hydraulic properties curve for sample had shown in the shaped of inverted s-curve. The uniform flow was observed in the layer of zeolite due to the uniformity of sand particles.

6.2 Zeolite column test

6.2.1 Gravitational infiltration system

The simulation of advection transport in a gravitational system was undertaken using Richards' equation and van Genuchten(VG) . The input parameters are given in Table 6.3

Table 6.3 Inputs for Pb(II) movement pass through zeolite column

Parameter	Values
Domain	20 cm thick zeolite layer
Total considered period	1, 2, 4, 8, 12,24, 48, 60 and 72 hours
Number of time step	120
Hydraulic properties model	van Genuchten (constants are in Table 6.2)
Boundaries condition	Refer to the pressure head reading

In this experiment, the water percolated very slowly. The observation of the wetting fronts were presented in Figure 6.2, 6.3. The wetting fronts reached the distance of 17.5, 15, 7.5 and 5 cm within period of 1, 2, 24 and 48 hours, respectively.

The simulation results for distributions of pressure head in column tests were well agreed with the observation. The averaged Darcy's velocity on the column at period of 1, 2, 4, 8, 12, 24, 48, 60 and 72 hours were -4×10^{-5} , -5×10^{-5} , -6×10^{-5} , -7.55×10^{-5} , -8.06×10^{-5} , -8.3×10^{-5} , -7.5×10^{-5} , -7.02×10^{-5} and -6.56×10^{-5} cm/h, respectively. Darcy's velocity were lower than the saturation hydraulic conductivity (0.27 cm/h). This indicates the movement of water through the zeolite column was still in a transient flow condition.

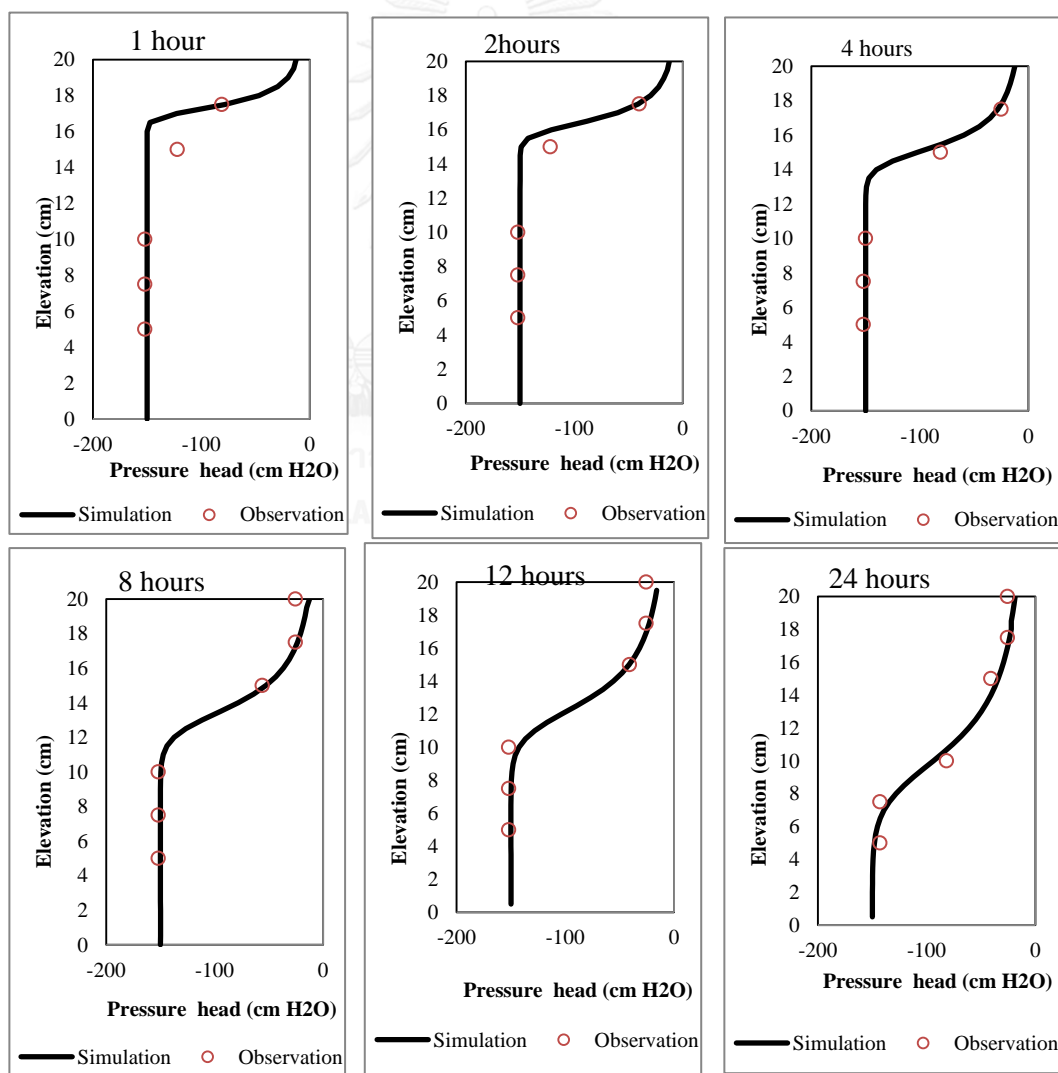


Figure 6.2 Pressure Head (cmH₂O) of zeolite column at 1, 2, 4, 8 12 and 24 hours

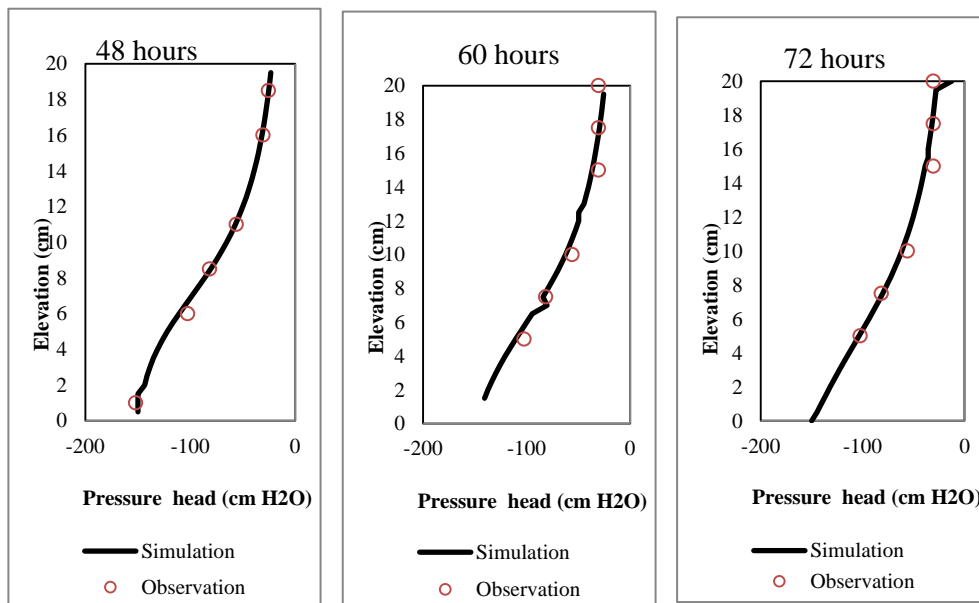


Figure 6.3 Pressure Head (cmH₂O) of zeolite column at 48, 60 and 72 hours

The simulation of moisture water content profile are given in Figure 6.4. The moisture content observed were 0.34-0.38. The wetting front was observed at the distance of 17.5, 15,10, 7.5 and 2.5 cm within 1, 2, 8, 24 and 60 hours, respectively. Pressure head and moisture content profiles generated the same estimates travel time.

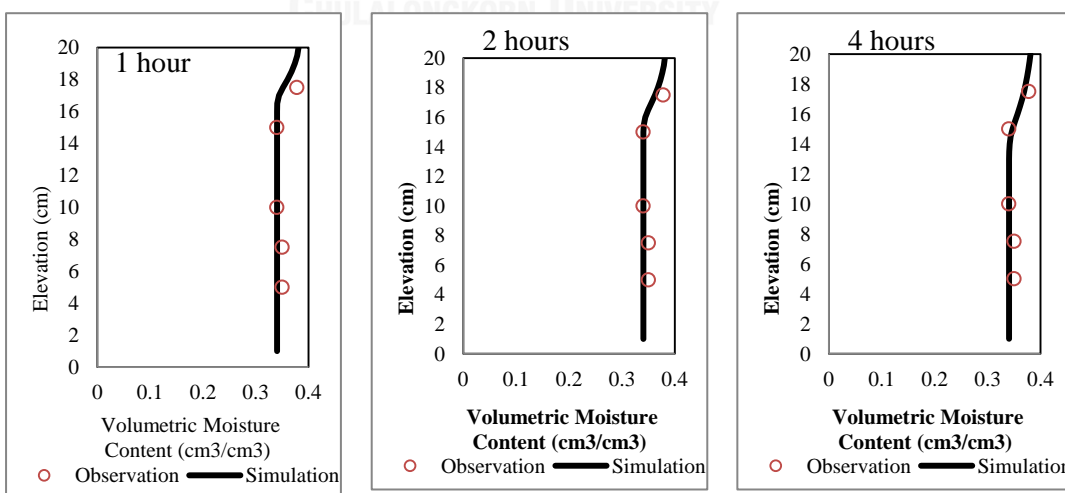


Figure 6.4 Volumetric water content (θ) of zeolite column at 1, 2, and 4 hours

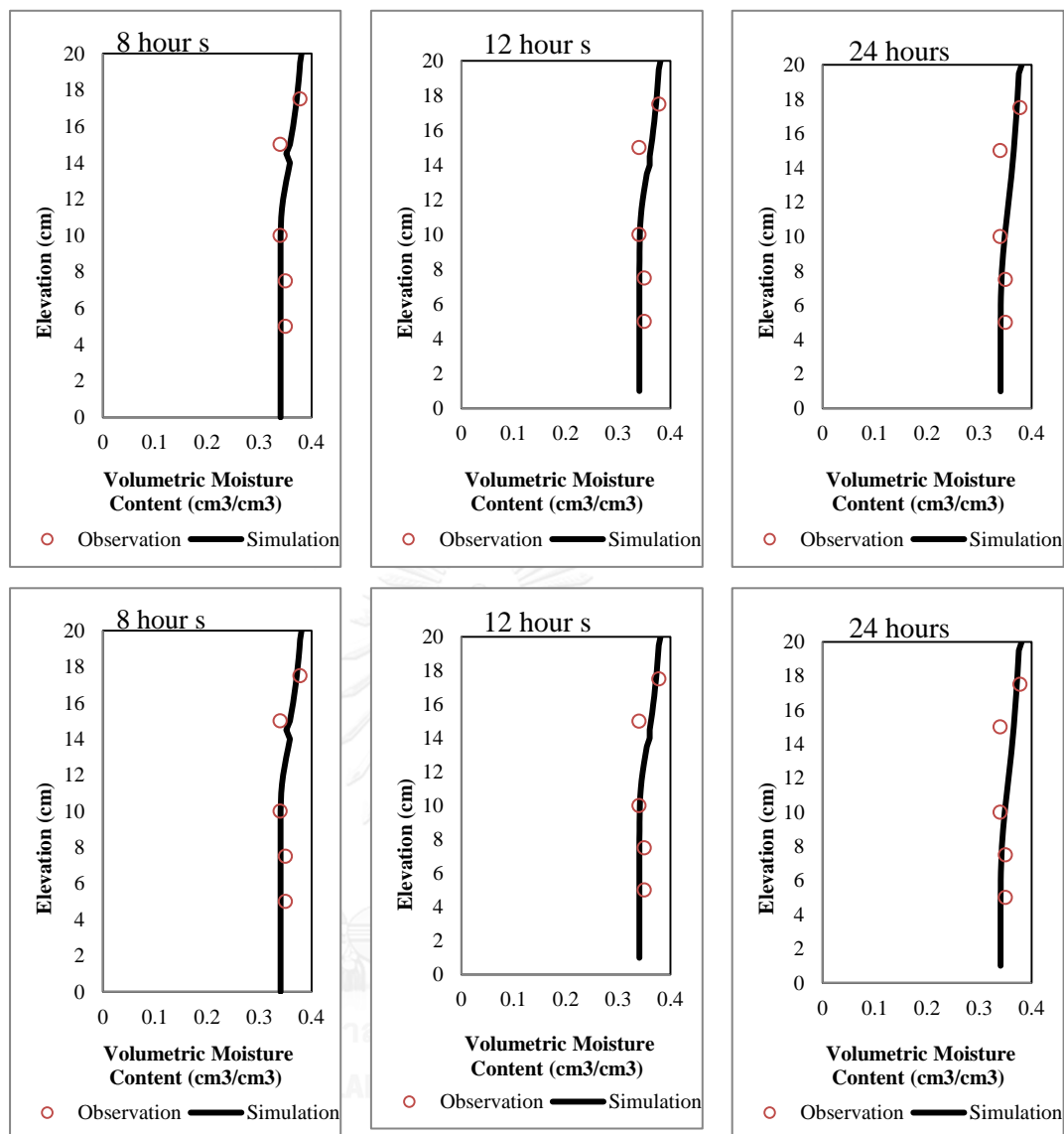


Figure 6.5 Volumetric water content (θ) of zeolite column at 8,12, 24, 48, 60 and 72 hours

Figure 6.6 presented the pressure head distribution over time. The simulations matched well the observations. The travel time of water through 20 cm deep zeolite layer was better estimated by the pressure head profiles. Simulations obtained using Richards' and van Genuchten equations generated the estimated travel times of 72 hours. The whole column fully after 20 days of continuous feeding. The travel time was very long. The zeolite had a high porosity and its water storage capacity to the porosity was also high. The maximum storage capacity was 0.3809. This value was

close to the porosity of zeolite (0.3859). The maximum pressure head was -27.9 cmH₂O. This pressure head was closer to the capillary pressure of -26.4 cmH₂O [82]

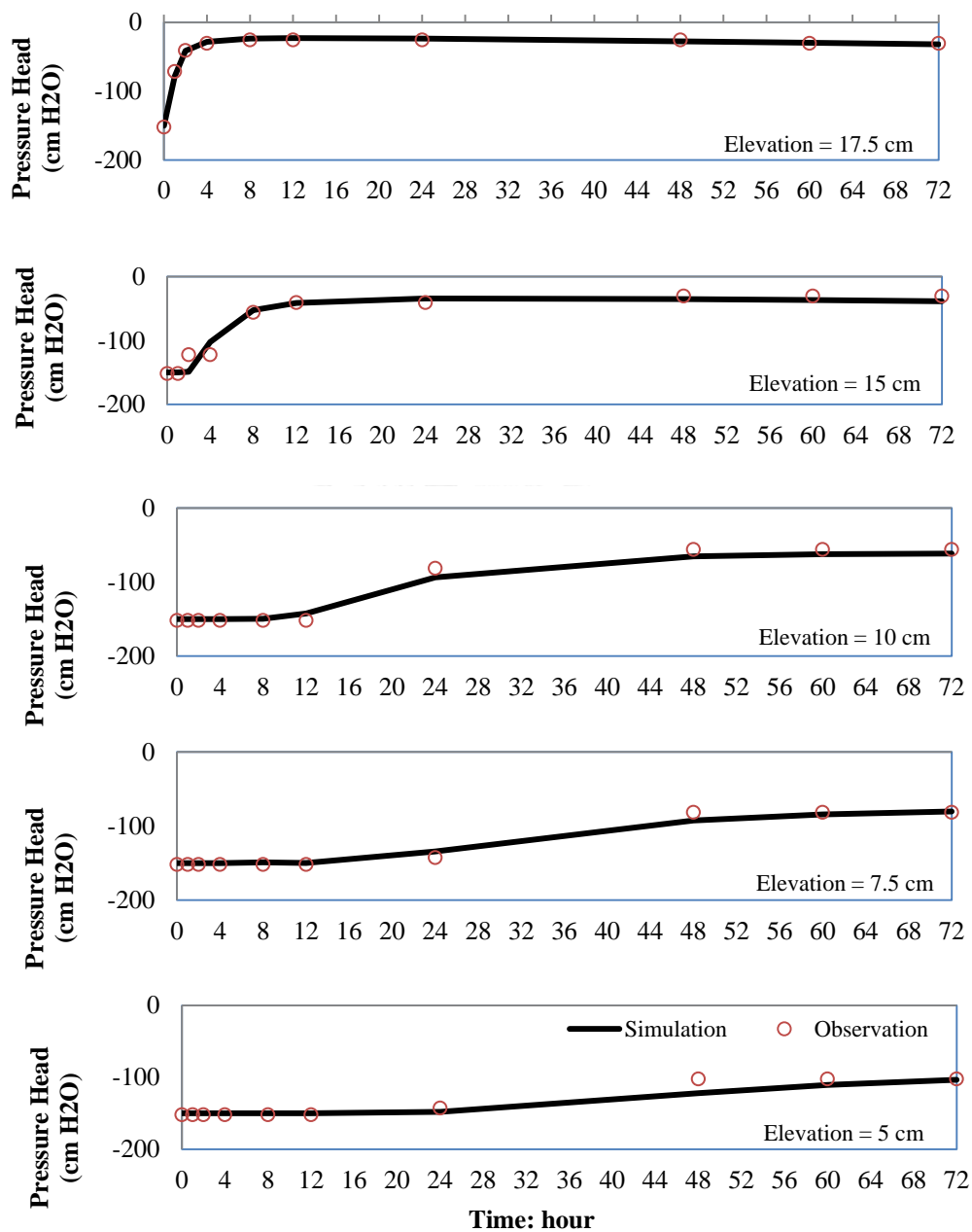


Figure 6.6 Simulation of time series of elevated pressure head in zeolite column using Richards' and van Genuchten equations (datum at the column test)

6.2.2 Gravitational infiltration and capillary force system

The input parameters for simulations of pressure head and moisture content in the system of gravitational infiltration and capillary force system are given in Table 6.4

Table 6.4 Inputs for Pb(II) movement pass through zeolite column

Parameter	Values
Domain	20 cm thick zeolite layer
Total considered period	48 hour
Number of time step	120
Hydraulic properties model	Van Genuchten (constants are in Table 6.2)
Boundaries condition	Refer to pressure head reading

The simulation results for distributions of pressure head in column tests well agree with the observation are given in Figure 6.5. The averaged Darcy's velocity on the column at 1, 2, 4, 8, 12, 24, 48, 60 and 72 hours were -5.95×10^{-3} , -5.17×10^{-3} , -8.07×10^{-3} , -3.85×10^{-3} , -3.52×10^{-3} , -3.47×10^{-3} , -2.63×10^{-3} , -2.52×10^{-3} and -2.43×10^{-3} cm/h, respectively. Darcy's velocities increased non-linearly over time. were lower than the saturation hydraulic conductivity (0.27 cm/h). This indicates the movement of water through the zeolite column was still in a transient flow condition

The simulation of moisture water content profile are given in Figure 6.7. The moisture content observed were 0.37-0.39. The lowest moisture content was constant at 0.37 and it was observed at 18 cm. The wetting front was observed at the distance of 17.5, 15, 10, 7.5 and 2.5 cm within 1, 2, 8, 24 and 60 hours, respectively. Pressure head and moisture content profiles generated the same estimates travel time.

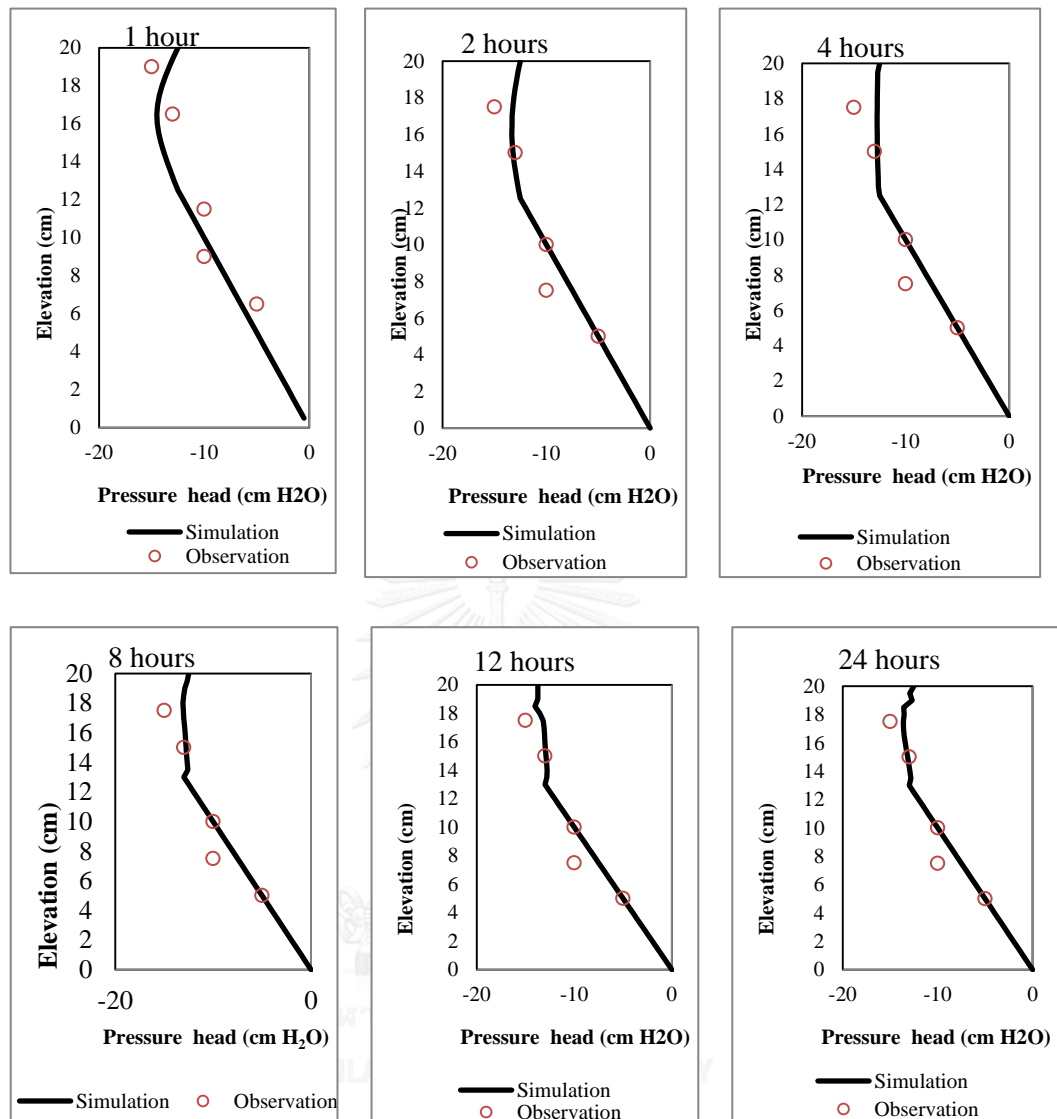


Figure 6.7 Pressure Head (cmH₂O) versus time

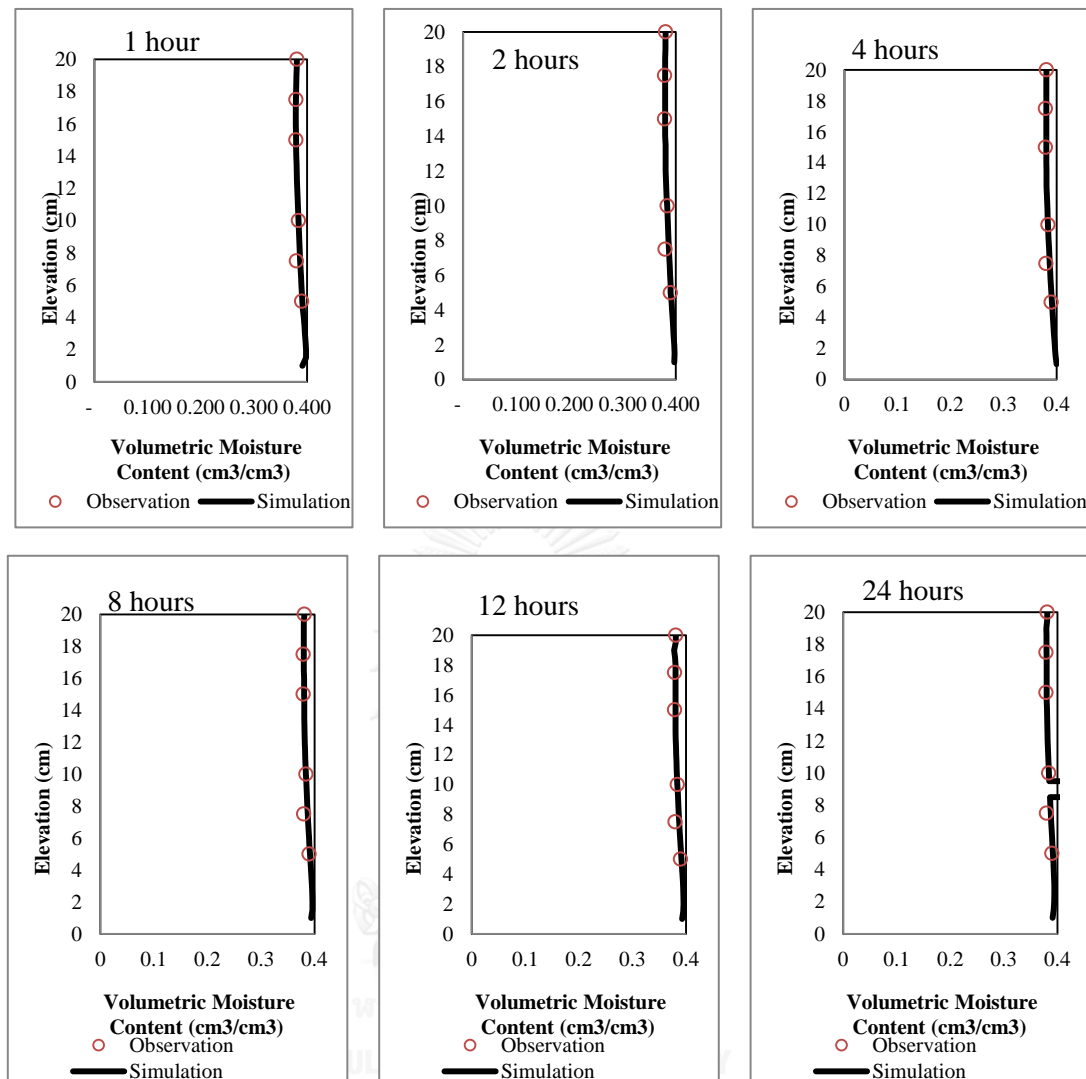


Figure 6.8 Volumetric water content (θ) of zeolite column

6.2.3 Dispersion transport in the laboratory scale zeolite column

The travel times of Pb(II) obtained from both simulations equaled the travel time of water. The average diffusion-dispersion coefficients D_z are given in Table 6.5. The dispersion coefficients governed by substituting Darcy's velocity obtained from Richards' and VG equations in case of gravitational infiltration system and gravitational infiltration and capillary force system, were in the range of $4.88 \times 10^{-4} - 5.27 \times 10^{-4}$ and $3.7 \times 10^{-2} - 1.13 \times 10^{-2} \text{ cm}^2/\text{h}$, respectively. The difference might result from the different estimated pore velocities. However, the D_z value obtained was in the possible range that was

proposed by Pickens and Grisak (1981) of $0.037 \text{ cm}^2/\text{h}$ (or $1.02 \times 10^{-5} \text{ cm}^2/\text{s}$). The D_z was a time varying and non-linear function, and it relied upon Darcy's and pore velocities (Wierenga 1995). The value of D_z suggests that molecular diffusion was 12-25% of total dispersion, and the mechanical dispersion played a significant role in the dispersion transport.

Table 6.5 Average diffusion-dispersion coefficients for zeolite column

Time (hours)	Average diffusion-dispersion coefficient; D_z (cm^2/h)	
	Gravitational infiltration system	Gravitational infiltration and capillary force system
1	0.000488	0.0084
2	0.000504	0.0074
4	0.000522	0.0113
8	0.000539	0.0056
12	0.000547	0.0052
24	0.000550	0.0045
48	0.000540	0.0040
60	0.000530	0.0038
72	0.000527	0.0037

6.3 Quality of filtered effluent from zeolite column

The quality of filtered effluent was improved after passing through the zeolite column. The boundaries conditions and the constants for hydraulic properties model governed from the previous tests are input to the UNSAT program. The simulation of contaminants transport through considered areas in this study and their details are given as follows. Inputs parameters for Pb(II) movement pass through zeolite column: transport part and retardation

Table 6.6 Inputs parameters for Pb(II) movement pass through zeolite column

Parameter	Values
Boundaries condition	
Number of Element	40
Length of Element	0.5
The observation nodes	Column depth 20 cm
The number of time step	250
The begin of considered time period	0
The end of considered time period	6000 hr
Soil bulk density; rho-B	1.286
Gravitational infiltration	
The hydraulic pressure head at the top	-12.5 cmH ₂ O
The hydraulic pressure head at the bottom	-152 cmH ₂ O
The hydraulic pressure head at initial	-152 cmH ₂ O
Van Genuchten	
The saturated hydraulic conductivity	0.27 cm ² /hr
The saturated moisture content	0.402
The residual moisture content	0.026
The empirical p	1.057
The empirical a	0.148

Table 6.7 Inputs parameters for Pb(II) movement pass through zeolite column (continued)

Parameter	Values
Contaminant	
Pb(II)	
The concentration of Pb(II) at the column surface	0.2 mg/L(2×10^{-4} g/L)
The concentration of Pb(II) at the column base	0.018 mg/L (1.8×10^{-5} g/L)
The molecular diffusion coefficient; D_{mol}	0.00108 cm ² /h [113]
The fraction of molecular diffusion; F_f	0.4
The transverse dispersivity; α_T (L)	0.53 cm
Freundlich Adsorption rate; K_d	0.74
Organic compound	
The substrate saturation constant; K_{SO}	4.952
Biological kinetic rate; μ_m	15.57

The concentration of Pb(II) profile in the biobarrier was reduced as a result of adsorption and microbial activity. The simulations corresponded well to the observations are present in Figure 6.9. The highest Pb(II) removal was observed at the top 10 cm of column. The concentration Pb(II) was reduced in this layer. The Pb(II) remaining in the effluent was very low, with a concentration of 0.018 mg/L. The overall Pb(II) removal efficiency was 90% of Pb(II) applied.

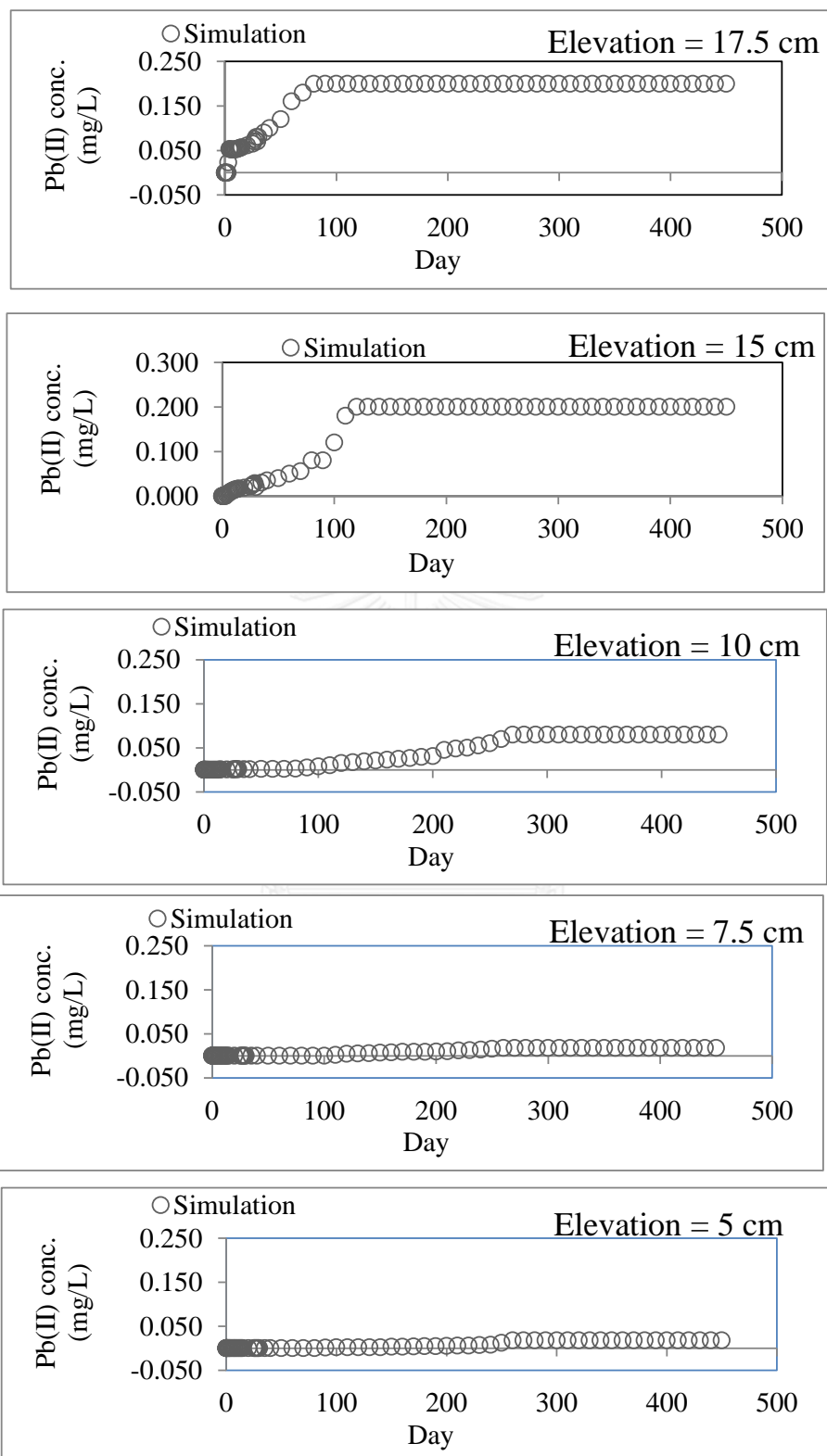


Figure 6.9 Pb(II) concentration profiles in zeolite biobarrier

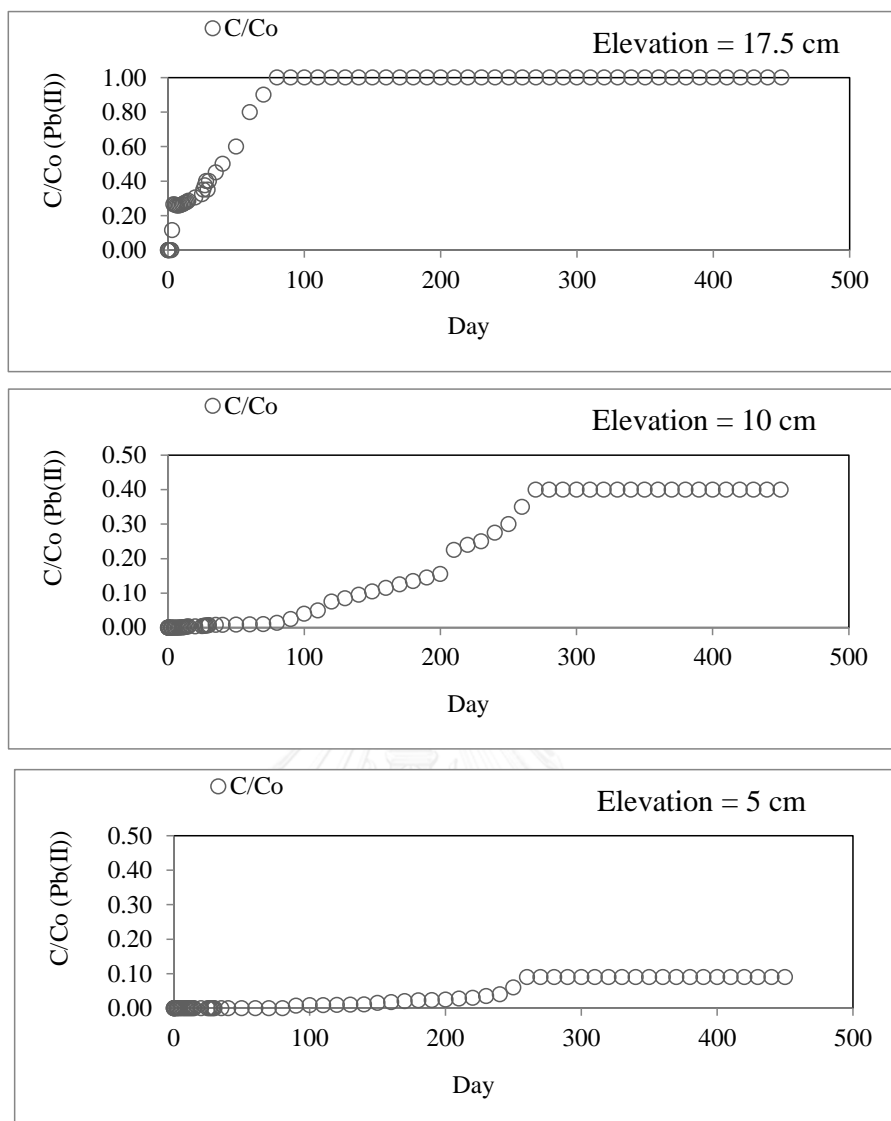


Figure 6.9 Pb(II) concentration profiles in zeolite biobarrier (cont')

The UNSAT program respond to the observations of pressure head distribution, volumetric water content distribution as well as Pb(II) concentration profile in biobarrier. The program had presented the constants, such as Darcy's velocity, averaged volumetric moisture content and Pb(II) dispersion coefficient, which were useful to magnitude the migration of Pb(II) in biobarrier. These constants are provided in Table 6.8. High dispersion and low velocity condition could provide a benefit to Pb(II) retardation in biobarrier.

Table 6.8 Constants for Pb(II) movement in zeolite biobarrier

Parameter	Constant values
Darcy's velocity (cm/h)	-0.00389
Averaged volumetric moisture content (cm ³ /cm ³)	0.1893
Pb(II) dispersion coefficient (cm ² /h)	0.00985

The design implication for defining efficiency of constructed PRB. The modeling as a tool for media selection is best use in a column experiment based on analyses at different locations within the column.



6.4 Application of contaminant transport model

Transport of Pb(II) movement in sand-manure column

The UNSAT model was validated with the transport of Pb(II) movement through the gravitational infiltration sand-manure column. The input parameters shown in Table 6.9.

Table 6.9 Inputs parameters for Pb(II) movement pass through sand-manure barrier

Parameter	Values
Boundaries condition	
Number of Element	32
Length of Element	0.5
The observation nodes	Column depth 12 cm
The number of time step	250
The begin of considered time period	0
The end of considered time period	0 to 1920 hrs
Soil bulk density; rho-B	0.529 g/cm ³
Gravitational infiltration	
The hydraulic pressure head at the top	-12.5 cmH ₂ O
The hydraulic pressure head at the bottom	-152 cmH ₂ O
The hydraulic pressure head at initial	-152 cmH ₂ O
Van Genuchten	
The saturated hydraulic conductivity	0.18 cm ² /hr
The saturated moisture content	0.441
The residual moisture content	0.014
The empirical p	1.480
The empirical a	0.312

The concentration of Pb(II) profile in the sand-manure biobarrier was reduced as a result of adsorption and microbial activity. The simulations corresponded well to the observations are present in Figure 6.10. The highest Pb(II) removal was observed at the

top at 16-10 cm of column. The concentration Pb(II) was reduced in this two layers. The Pb(II) remaining in the effluent was very low, with a concentration of 0.048 mg/L. The overall Pb(II) removal efficiency was 85% of Pb(II) applied.

Table 6.10 Inputs parameters for Pb(II) movement pass through sand-manure barrier (continued)

Parameter	Values
Contaminant	
Pb(II)	
The concentration of Pb(II) at the column surface	0.21 mg/L (2.1×10^{-4} g/L)
The concentration of Pb(II) at the column base	0.048 mg/L (4.8×10^{-5} g/L)
The molecular diffusion coefficient; D_{mol}	0.00108 cm ² /h [113]
The fraction of molecular diffusion; F_f	0.4
The transverse dispersivity; α_T (L)	0.53 cm
Freundlich Adsorption rate; K_d	0.62
Organic compound	
The substrate saturation constant; K_{SO}	57
Biological kinetic rate; μ_m	500

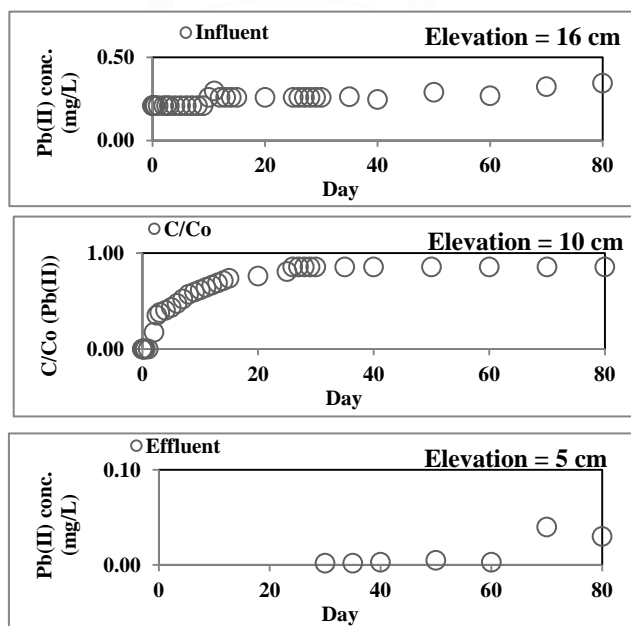


Figure 6.10 Pb(II) concentration profiles in sand-manure biobarrier

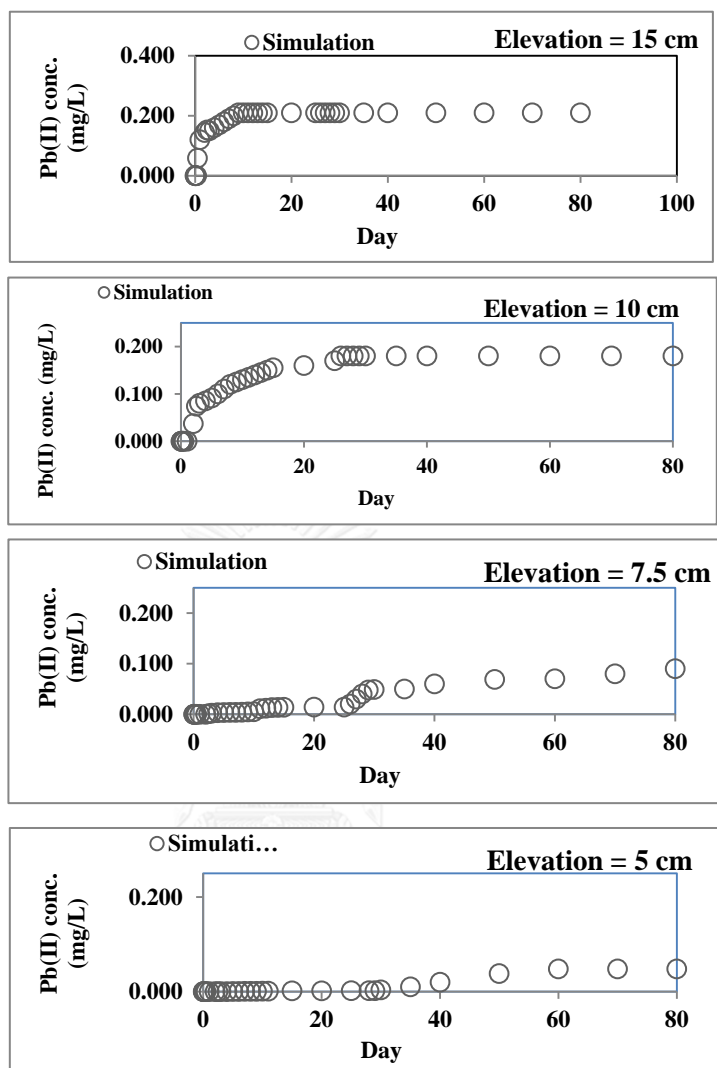


Figure 6.10 Pb(II) concentration profiles in sand-manure biobarrier (cont')

The simulation had presented the constants of Darcy's velocity, averaged volumetric moisture content and Pb(II) dispersion coefficient are -0.00034 cm/h, 0.2032 cm³/cm³, and 0.001346 cm²/h, respectively. The Pb(II) dispersion coefficient is higher than zeolite column. High dispersion and low velocity condition could provide a benefit to Pb(II) retardation in sand-manure biobarrier.

CHAPTER 7

CONCLUSION AND RECOMMENDATION

7.1 General approaches

This research aims to develop a mathematical model on lead remediation for finding the criteria and optimum conditions of biobarrier by using MATLAB program. This theses investigate the efficiency of laboratory scale biobarrier in immobilising soluble Pb(II). The sand-manure is utilised as an organic media while zeolite utilize as an active media for Pb acclimatised microbial seed.

The major mechanisms for Pb(II) restoration in this active sand-manure biosorbent are bioaccumulation and biosorption. The 56% of Pb(II) was kept on living cell by bioaccumulation and another 44% of Pb(II) was sorbed onto dead cell by biosorption. In the active zone of biosorbent, the biopolymers played an important role in both bioaccumulation and biosorption as the synthetic biosorbent was an acidic resistant, it could be applied to restore and free Pb(II) from the acidic Pb contaminated wastewater. The microbial strains which were isolated from matured sand-manure biobarrier determined with PCR-DGGE of partial 16S rRNA genes fragments showed the predominant species are *Bacillus* sp., *Sporolactobacillus nakayamae*, *Clostridium* sp., and *Clostridium pasteurianum*.

Laboratory results confirmed that the zeolite biobarrier can retard Pb(II). The zeolite itself has a maximum Pb(II)sorption capacity of 54.24 g Pb(II)/kg, while the maximum sorptive capacity of fabricated biobarrier is increased to 70.12 g Pb(II)/kg. X-ray diffraction (XRD) technique is introduced to identify the forms of Pb in the biobarrier. The precipitants of lead phosphate ($\text{Pb}_2\text{P}_2\text{O}_7$) are observed on the surface of biobarrier. Fourier Transform Infrared (FT-IR) spectroscopy can reflect that the same functional groups of biopolymer on zeolite and biobarrier are governed, they are H-bonded OH groups (polysaccharides) and NH_2 stretching (proteins), Aliphatic C-H stretching (fatty acids), PO_4^{3-} and P-O-C, P-O-H stretching (phospholipids and ribose phosphate chain pyrophosphate). The microbial strains which were isolated from matured zeolite biobarrier, namely *Bacillus* sp., *Nostoc* sp., and *Bradyrhizobium* sp. They are the Pb resistant microbes, which stay in root of

plants. These can promote the immobilisation of Pb via metabolic and non-metabolic processes. The Pb(II) resistant microbe can partially retard Pb(II) via biosorption and bioaccumulation.

7.2 Specific approaches

The computational code used in the advective-dispersive transport (Richards' equation) was applied to the data obtained from the laboratory scale soil columns. Simulation results for the hydraulic pressure head and moisture content in zeolite columns matched the observed data well. The concentration of Pb(II) profile in biobarrier was reduced as a result of adsorption and microbial activity. Highest Pb(II) removal was observed at the top 10 cm column and the concentration of Pb(II) was reduced in this layer. Pb(II) remained in the effluent was very low, with a concentration of 0.018 mg/L and overall Pb(II) removal efficiency was 93% of Pb(II) applied. The UNSAT's model could satisfactorily estimate the contaminant concentration and retardation zone. Simulation had presented the constants of Darcy's velocity, averaged volumetric moisture content and Pb(II) dispersion coefficient are -0.00389 cm/h, 0.1893 cm³/cm³, and 0.00985 cm²/h, respectively.

The case studies of sand-manure column were used for verification processes. The simulation that presented the constants of Darcy's velocity, averaged volumetric moisture content and Pb(II) dispersion coefficient are -0.00034 cm/h, 0.2032 cm³/cm³, and 0.001346 cm²/h, respectively. The Pb(II) dispersion coefficient is higher than zeolite column. High dispersion and low velocity condition could provide a benefit to Pb(II) retardation in biobarrier.

The developed model could effectively predict the profiles of pressure head and moisture content observed by infiltration-redistribution systems. The model as a tool for media selection used in a column experiment is based on analyses at different locations within the column. This indicates that the developed model is an effective alternative tool for predicting the development of biobarrier as it design implication for defining efficiency of constructed permeable reactive biobarrier.

7.3 Recommendations for future research

Based on the results calculate can recommended how width of biobarrier can retard Pb(II) amount in area issue. The estimate of design parameter suggested that inoculation could significantly value of biomass support medium.

1. The predictive data could further applied for other media.
2. Based on the results calculate we can recommended how width of biobarrier can retard Pb(II) in area issue.
3. The estimate of design parameter suggested that inoculation microbial.



REFERENCES

1. Park, J.H., et al., *Role of organic amendments on enhanced bioremediation of heavy metal(loid) contaminated soils*. Journal of Hazardous Materials, 2011. 185(2-3): p. 549-574.
2. Pusapakdepop, J., et al., *Health risk assessment of villagers who live near a lead mining area: a case study of Klity village, Kanchanaburi Province, Thailand*. The Southeast Asian Journal of Tropical Medicine Public Health, 2007 38(1): p. 168-177.
3. Sikkema, J.K., et al., *Mercury regulation, fate, transport, transformation, and abatement within cement manufacturing facilities: Review*. Science of The Total Environment, 2011. 409(20): p. 4167-4178.
4. Panagiotis, M., *Application of natural zeolites in environmental remediation: A short review*. Microporous and Mesoporous Materials, 2011. 144(1-3): p. 15-18.
5. Hashim, M.A., et al., *Remediation technologies for heavy metal contaminated groundwater*. Journal of Environmental Management, 2011. 92(10): p. 2355-2388.
6. Sud, D., G. Mahajan, and M.P. Kaur, *Agricultural waste material as potential adsorbent for sequestering heavy metal ions from aqueous solutions - A review*. Bioresource Technology, 2008. 99(14): p. 6017-6027.
7. Huang, T., J. Xu, and D. Cai, *Efficiency of active barriers attaching biofilm as sediment capping to eliminate the internal nitrogen in eutrophic lake and canal*. Journal of Environmental Sciences, 2011. 23(5): p. 738-743.
8. Diels, L., et al., *Heavy metals bioremediation of soil*. Molecular Biotechnology, 1999. 12(2): p. 149-158.
9. Liu, Y.-G., et al., *Heavy Metal Accumulation in Plants on Mn Mine Tailings*. Pedosphere, 2006. 16(1): p. 131-136.
10. Kim, J.-W., H. Choi, and Y.A. Pachepsky, *Biofilm morphology as related to the porous media clogging*. Water Research, 2010. 44(4): p. 1193-1201.
11. Li, M.-Y., et al., *Evaluation of Biological Characteristics of Bacteria Contributing to Biofilm Formation*. Pedosphere, 2009. 19(5): p. 554-561.
12. Adriano, D.C., *Trace Elements in Terrestrial Environments*. 2001: Springer, Berlin, Heidelberg.
13. Kunhikrishnan, A., et al., *Chapter Five - The Influence of Wastewater Irrigation on the Transformation and Bioavailability of Heavy Metal(Loid)s in Soil*, in *Advances in Agronomy*, L.S. Donald, Editor. 2012, Academic Press. p. 215-297.
14. McLean, J.E. and B.E. Bledsoe, *Ground Water Issue; Behavior of Metals in Soils*. 1992. p. 25.
15. Mattigod, S.V., G. Sposito, and A. L. Page, *Factors affecting the solubilities of trace metals in soils*. In D. E. Baker (Ed.). *Chemistry in the soil environment*. ASA Special Publication No 40. 1981, Madison, WI.: American Society of Agronomy.
16. Paul, M., *Chapter 6 - Lead Concentrations in Environmental Media Relevant to Human Lead Exposures*, in *Trace Metals and other Contaminants in the Environment*. 2011, Elsevier. p. 117-213.
17. PCD, *Annual Report M.o.N.R.a.E*. Pollution Control Department, Thailand, Editor. 2009.

18. HumanRightWatch, *Toxic Water, Tainted Justice, Thailand's Delays in Cleaning Up Klity Creek*. 2014.
19. Ahemad, M., *Remediation of metalliferous soils through the heavy metal resistant plant growth promoting bacteria: Paradigms and prospects*. Arabian Journal of Chemistry, 2014(0).
20. Wang, X., et al., *Biosorption of Cu(II) and Pb(II) from aqueous solutions by dried activated sludge*. Minerals Engineering, 2006. 19(9): p. 968-971.
21. Sobolev, D. and M.F. Begonia, *Effects of heavy metal contamination upon soil microbes: lead-induced changes in general and denitrifying microbial communities as evidenced by molecular markers*. Int J Environ Res Public Health, 2008. 5(5): p. 450-6.
22. Manasi, V. Rajesh, and N. Rajesh, *Adsorption isotherms, kinetics and thermodynamic studies towards understanding the interaction between a microbe immobilized polysaccharide matrix and lead*. Chemical Engineering Journal, 2014. 248(0): p. 342-351.
23. Tabak, H., et al., *Developments in Bioremediation of Soils and Sediments Polluted with Metals and Radionuclides – 1. Microbial Processes and Mechanisms Affecting Bioremediation of Metal Contamination and Influencing Metal Toxicity and Transport*. Reviews in Environmental Science and Bio/Technology, 2005. 4(3): p. 115-156.
24. Chapman, J.C.E.b.D., *Water Quality Assessments - A Guide to Use of Biota, Sediments and Water in Environmental Monitoring - Second Edition*. Chapter 9* - Groundwater 1992, 1996.
25. Bunsri, T., M. Sivakumar, and D. Hagare, *Simulation of Water and Contaminant Transport Through Vadose Zone - Redistribution System, in Hydraulic Conductivity - Issues, Determination and Applications*, P.L. Elango, Editor. 2011, InTech. p. 395-418.
26. Osman, K., *Soil Pollution*, in *Soil Degradation, Conservation and Remediation*. 2014, Springer Netherlands. p. 149-226.
27. Phillips, D.H., *Permeable reactive barriers: A sustainable technology for cleaning contaminated groundwater in developing countries*. Desalination, 2009. 248(1-3): p. 352-359.
28. Thiruvengkatachari, R., S. Vigneswaran, and R. Naidu, *Permeable reactive barrier for groundwater remediation*. Journal of Industrial and Engineering Chemistry, 2008. 14(2): p. 145-156.
29. Obiri-Nyarko, F., S.J. Grajales-Mesa, and G. Malina, *An overview of permeable reactive barriers for in situ sustainable groundwater remediation*. Chemosphere, 2014. 111(0): p. 243-259.
30. Duarte Zaragoza, V.M., R. Carrillo, and C.M. Gutierrez Castorena, *Lead sorption-desorption from organic residues*. Environmental Technology, 2011. 32(4): p. 353-361.
31. Akar, T. and S. Tunali, *Biosorption characteristics of Aspergillus flavus biomass for removal of Pb(II) and Cu(II) ions from an aqueous solution*. Bioresource Technology, 2006. 97(15): p. 1780-1787.
32. Sag, Y., B. Tatar, and T. Kutsal, *Biosorption of Pb(II) and Cu(II) by activated sludge in batch and continuous-flow stirred reactors*. Bioresource Technology, 2003. 87(1): p. 27-33.

33. Alimohamadi, M., G. Abolhamd, and A. Keshtkar, *Pb(II) and Cu(II) biosorption on Rhizopus arrhizus modeling mono- and multi-component systems*. Minerals Engineering, 2005. 18(13-14): p. 1325-1330.
34. Tokcaer, E. and U. Yetis, *Pb(II) biosorption using anaerobically digested sludge*. Journal of Hazardous Materials, 2006. 137(3): p. 1674-1680.
35. Gundogdu, A., et al., *Biosorption of Pb(II) ions from aqueous solution by pine bark (Pinus brutia Ten.)*. Chemical Engineering Journal, 2009. 153(1-3): p. 62-69.
36. Yurtsever, M. and I.A. Sengil, *Biosorption of Pb(II) ions by modified quebracho tannin resin*. Journal of Hazardous Materials, 2009. 163(1): p. 58-64.
37. Ouellet-Plamondon, C., R. Lynch, and A. Al-Tabbaa, *Metal Retention Experiments for the Design of Soil-Mix Technology Permeable Reactive Barriers*. CLEAN – Soil, Air, Water, 2011. 39(9): p. 844-852.
38. Słaba, M. and J. Długoński, *Efficient Zn²⁺ and Pb²⁺ uptake by filamentous fungus Paecilomyces marquandii with engagement of metal hydrocarbonates precipitation*. International Biodeterioration & Biodegradation, 2011. 65(7): p. 954-960.
39. Zeyrek, M., et al., *An Ion Chromatography Method for the Determination of Major Anions In Geothermal Water Samples*. Geostandards and Geoanalytical Research, 2010. 34(1): p. 67-77.
40. Velmurugan, N., et al., *Isolation, identification, Pb(II) biosorption isotherms and kinetics of a lead adsorbing Penicillium sp. MRF-1 from South Korean mine soil*. Journal of Environmental Sciences, 2010. 22(7): p. 1049-1056.
41. Chojnacka, K., *Biosorption and bioaccumulation – the prospects for practical applications*. Environment International, 2010. 36(3): p. 299-307.
42. Lee, Y.-C., et al., *Bench-scale ex situ diesel removal process using a biobarrier and surfactant flushing*. Journal of Industrial and Engineering Chemistry, 2012. 18(3): p. 882-887.
43. Teerakun, M., et al., *Coupling of zero valent iron and biobarriers for remediation of trichloroethylene in groundwater*. Journal of Environmental Sciences, 2011. 23(4): p. 560-567.
44. Tica, D., M. Udovic, and D. Lestan, *Immobilization of potentially toxic metals using different soil amendments*. Chemosphere, 2011. 85(4): p. 577-583.
45. Boni, M.R. and S. Scaffoni, *The potential of compost-based biobarriers for Cr(VI) removal from contaminated groundwater: Column test*. Journal of Hazardous Materials, 2009. 166(2-3): p. 1087-1095.
46. Zhang, M., *Adsorption study of Pb(II), Cu(II) and Zn(II) from simulated acid mine drainage using dairy manure compost*. Chemical Engineering Journal, 2011. 172(1): p. 361-368.
47. Su, C. and R.W. Puls, *Removal of added nitrate in the single, binary, and ternary systems of cotton burr compost, zerovalent iron, and sediment: Implications for groundwater nitrate remediation using permeable reactive barriers*. Chemosphere, 2007. 67(8): p. 1653-1662.
48. Hernandez-Soriano, M.C. and J.C. Jimenez-Lopez, *Effects of soil water content and organic matter addition on the speciation and bioavailability of heavy metals*. Science of The Total Environment, 2012. 423(0): p. 55-61.

49. Lee, Y.-C., et al., *Biodegradation of diesel by mixed bacteria immobilized onto a hybrid support of peat moss and additives: A batch experiment*. Journal of Hazardous Materials, 2010. 183(1–3): p. 940-944.
50. Parat, C., et al., *Long-term effects of metal-containing farmyard manure and sewage sludge on soil organic matter in a fluvisol*. Soil Biology and Biochemistry, 2005. 37(4): p. 673-679.
51. Guo, Q. and D.W. Blowes, *Biogeochemistry of two types of permeable reactive barriers, organic carbon and iron-bearing organic carbon for mine drainage treatment: Column experiments*. Journal of Contaminant Hydrology, 2009. 107(3–4): p. 128-139.
52. Delkash, M., B. Ebrazi Bakhshayesh, and H. Kazemian, *Using zeolitic adsorbents to cleanup special wastewater streams: A review*. Microporous and Mesoporous Materials, 2015. 214(0): p. 224-241.
53. Oliva, J., et al., *Biogenic hydroxyapatite (Apatite II™) dissolution kinetics and metal removal from acid mine drainage*. Journal of Hazardous Materials, 2012. 213–214(0): p. 7-18.
54. Jang, A. and P.L. Bishop, *Remediation potential of mulch for removing lead*. Environmental Technology, 2011. 33(6): p. 623-630.
55. Conca, J.L. and J. Wright, *An Apatite II permeable reactive barrier to remediate groundwater containing Zn, Pb and Cd*. Applied Geochemistry, 2006. 21(8): p. 1288-1300.
56. Ebigbo, A., et al., *Modelling biofilm growth in the presence of carbon dioxide and water flow in the subsurface*. Advances in Water Resources, 2010. 33(7): p. 762-781.
57. Seo, Y. and P.L. Bishop, *The monitoring of biofilm formation in a mulch biowall barrier and its effect on performance*. Chemosphere, 2008. 70(3): p. 480-488.
58. Kim, G., S. Lee, and Y. Kim, *Subsurface biobarrier formation by microorganism injection for contaminant plume control*. Journal of Bioscience and Bioengineering, 2006. 101(2): p. 142-148.
59. Hashimoto, Y., et al., *EXAFS speciation and phytoavailability of Pb in a contaminated soil amended with compost and gypsum*. Science of The Total Environment, 2011. 409(5): p. 1001-1007.
60. Farrell, M., et al., *Migration of heavy metals in soil as influenced by compost amendments*. Environmental Pollution, 2010. 158(1): p. 55-64.
61. Gibert, O., et al., *In-situ remediation of acid mine drainage using a permeable reactive barrier in Aznalcóllar (Sw Spain)*. Journal of Hazardous Materials, 2011. 191(1-3): p. 287-295.
62. Sasaki, K., et al., *Effect of saw dust on borate removal from groundwater in bench-scale simulation of permeable reactive barriers including magnesium oxide*. Journal of Hazardous Materials, 2011. 185(2-3): p. 1440-1447.
63. Ludwig, R.D., et al., *A Permeable Reactive Barrier for Treatment of Heavy Metals*. Ground Water, 2002. 40(1): p. 59-66.
64. Benner, S.G., D.W. Blowes, and C.J. Ptacek, *A Full-Scale Porous Reactive Wall for Prevention of Acid Mine Drainage*. Ground Water Monitoring & Remediation, 1997. 17(4): p. 99-107.

65. Di Natale, F., et al., *Groundwater protection from cadmium contamination by permeable reactive barriers*. Journal of Hazardous Materials, 2008. 160(2-3): p. 428-434.
66. Blowes, D.W., et al., *Treatment of inorganic contaminants using permeable reactive barriers*. Journal of Contaminant Hydrology, 2000. 45(1-2): p. 123-137.
67. Bartzas, G. and K. Komnitsas, *Solid phase studies and geochemical modelling of low-cost permeable reactive barriers*. Journal of Hazardous Materials, 2010. 183(1-3): p. 301-308.
68. Moraci, N. and P.S. Calabrò, *Heavy metals removal and hydraulic performance in zero-valent iron/pumice permeable reactive barriers*. Journal of Environmental Management, 2010. 91(11): p. 2336-2341.
69. Han, Y.-S., et al., *FeS-coated sand for removal of arsenic(III) under anaerobic conditions in permeable reactive barriers*. Water Research, 2011. 45(2): p. 593-604.
70. Simon, F.-G., et al., *Behaviour of uranium in hydroxyapatite-bearing permeable reactive barriers: investigation using ^{237}U as a radioindicator*. Science of The Total Environment, 2004. 326(1-3): p. 249-256.
71. Abdel Rahman, R.O., et al., *Preliminary investigation of zinc transport through zeolite-X barrier: Linear isotherm assumption*. Chemical Engineering Journal, 2012. 185–186(0): p. 61-70.
72. Park, J.-B., et al., *Lab scale experiments for permeable reactive barriers against contaminated groundwater with ammonium and heavy metals using clinoptilolite (01-29B)*. Journal of Hazardous Materials, 2002. 95(1-2): p. 65-79.
73. Woinarski, A.Z., G.W. Stevens, and I. Snape, *A Natural Zeolite Permeable Reactive Barrier to Treat Heavy-Metal Contaminated Waters in Antarctica: Kinetic and Fixed-bed Studies*. Process Safety and Environmental Protection, 2006. 84(2): p. 109-116.
74. Bunsri, T., M. Sivakumar, and D. Hagare, *Numerical modelling of tracer transport in unsaturated porous media*. Journal of Applied Fluid Mechanics, 2008. 1(1): p. 62-70.
75. Barry, D.A., et al., *Analytical approximations for flow in compressible, saturated, one-dimensional porous media*. Advances in Water Resources, 2007. 30(4): p. 927-936.
76. Santillan-Medrano, J. and J.J. Jurinak, *The chemistry of lead and cadmium in soils: solid phase formation*. Soil Science Society of America, Proceedings, 1975. 29: p. 851-856.
77. Mattigod, S.V.a.G.S., *Chemical modeling in aqueous systems*. Chemical modeling of trace metals equilibrium in contaminated soil solutions using the computer program GEOCHEM. Vol. In E. A. Jenne (ed.). Chemical modeling in aqueous systems. ACS No.93. 1979, Washington, D.C.: American Chemical Society.
78. Ahmad, F., S.P. Schnitker, and C.J. Newell, *Remediation of RDX- and HMX-contaminated groundwater using organic mulch permeable reactive barriers*. Journal of Contaminant Hydrology, 2007. 90(1-2): p. 1-20.
79. Baker, L.R., P.M. White, and G.M. Pierzynski, *Changes in microbial properties after manure, lime, and bentonite application to a heavy metal-contaminated mine waste*. Applied Soil Ecology, 2011. 48(1): p. 1-10.

80. Scheckel, K.G. and J.A. Ryan, *In vitro formation of pyromorphite via reaction of Pb sources with soft-drink phosphoric acid*. Science of The Total Environment, 2003. 302(1-3): p. 253-265.
81. Bea, S.A., et al., *Geochemical and environmental controls on the genesis of soluble efflorescent salts in Coastal Mine Tailings Deposits: A discussion based on reactive transport modeling*. Journal of Contaminant Hydrology, 2010. 111(1-4): p. 65-82.
82. Bunsri, T., *CONTAMINANT TRANSPORT PROCESSES IN ONSITE WASTE DISPOSAL SYSTEMS*, in *SCHOOL OF CIVIL, MINING AND ENVIRONMENTAL ENGINEERING*. 2006, University of Wollongong: Wollongong.
83. Chen-Charpentier, B.M., D.T. Dimitrov, and H.V. Kojouharov, *Numerical simulation of multi-species biofilms in porous media for different kinetics*. Mathematics and Computers in Simulation, 2009. 79(6): p. 1846-1861.
84. Chen, B.M. and H.V. Kojouharov, *Non-standard Numerical Methods Applied to Subsurface Biobarrier Formation Models in Porous Media*. Bulletin of Mathematical Biology, 1999. 61(4): p. 779-798.
85. Chen-Charpentier, B.M. and H.V. Kojouharov, *Numerical simulation of biofilm-forming bacteria and other microbes in porous media*, in *Developments in Water Science*, R.J.S.W.G.G. S. Majid Hassanizadeh and F.P. George, Editors. 2002, Elsevier. p. 819-826.
86. Van Genuchten, M.T., *A closed-form equation for predicting the hydraulic conductivity of unsaturated soils*. Soil science society of America journal, 1980. 44(5): p. 892-898.
87. (ASTM), A.S.f.T.a.M.I., *Annual book of ASTM Standards*, Pennsylvania: ASTM international., 1997. 04.08.
88. Schnitzer, M., *Methods of Analysis, Past 2. Chemical and Microbiology Properties-Agronomy Monograph no.9, 2nd ed., Madison, WI, USA, pp. 581-594.* . , 1982.
89. American Public Health Association, A., *Standard methods for the examination of water and wastewater, 20th ed. Washington, DC: APHA.* . 1998.
90. Muyzer, G., E.C. de Waal, and A.G. Uitterlinden, *Profiling of complex microbial populations by denaturing gradient gel electrophoresis analysis of polymerase chain reaction-amplified genes coding for 16S rRNA*. Applied and Environmental Microbiology, 1993. 59(3): p. 695-700.
91. White, T., et al., *Amplification and direct sequencing of fungal ribosomal RNA genes for phylogenetics*, in *PCR Protocols: A Guide to Methods and Applications*, M. Innis, et al., Editors. 1990, Academic Press. p. 315-322.
92. Kim, S.H., et al., *Isolation and characterization of a Drosophila homologue of mitogen-activated protein kinase phosphatase-3 which has a high substrate specificity towards extracellular-signal-regulated kinase*. The Biochemical Journal, 2002. 361(1): p. 143-151.
93. Sambrook, J.R., D. , *Molecular Cloning: a Laboratory Manual*. 3rd edn. Cold Spring Harbor, NY: Cold Spring Harbor Laboratory., 2001.
94. Tessier, A., P.G.C. Campbell, and M. Bisson, *Sequential extraction procedure for the speciation of particulate trace metals*. Analytical Chemistry, 1979. 51(7): p. 844-851.

95. Doan, T.T., et al., *Influence of buffalo manure, compost, vermicompost and biochar amendments on bacterial and viral communities in soil and adjacent aquatic systems*. Applied Soil Ecology, 2014. 73(0): p. 78-86.
96. Metcalf & Eddy., T., G., Burton, F. L. 1., & Stensel, H. D. , *Wastewater engineering: Treatment and reuse (4th ed.)*. Boston: McGraw-Hill. 2003.
97. Khankruer D, M.S., Chinnarasri C, Bunsri T. , *Application of biomathematical model for Pb(II) biosorption and bioaccumulation*. Sustainable Environmental Research Journal, 2012. 22(6): p. 379-386.
98. Giraldo, L. and J.C. Moreno-Piraján, *Pb²⁺ adsorption from aqueous solutions on activated carbons obtained from lignocellulosic residues*. Brazilian Journal of Chemical Engineering, 2008. 25: p. 143-151.
99. Chiang, K.Y., H.J. Huang and C.N. Chang, , *Enhancement of heavy metal stabilization by different amendments during sewage sludge composting process*. Sustainable Environment Research Journal, 2007. 17(4): p. 249-256
100. Jing, C., X. Meng, and G.P. Korfiatis, *Lead leachability in stabilized/solidified soil samples evaluated with different leaching tests*. Journal of Hazardous Materials, 2004. 114(1-3): p. 101-110.
101. Govarathanan, M., et al., *Significance of autochthonous Bacillus sp. KK1 on biomineralization of lead in mine tailings*. Chemosphere, 2013. 90(8): p. 2267-2272.
102. Francis, A.J. and Y.V. Nancharaiah, 9 - *In situ and ex situ bioremediation of radionuclide-contaminated soils at nuclear and norm sites*, in *Environmental Remediation and Restoration of Contaminated Nuclear and Norm Sites*, L.v. Velzen, Editor. 2015, Woodhead Publishing. p. 185-236.
103. Huang, K., et al., *Genome Sequence of Sporolactobacillus terrae DSM 11697, the Type Strain of the Species*. Genome Announcements, 2014. 2(3).
104. Chang, J.-J., et al., *Molecular monitoring of microbes in a continuous hydrogen-producing system with different hydraulic retention time*. International Journal of Hydrogen Energy, 2008. 33(5): p. 1579-1585.
105. Ren, G., et al., *Characteristics of Bacillus sp. PZ-1 and its biosorption to Pb(II)*. Ecotoxicology and Environmental Safety, 2015. 117(0): p. 141-148.
106. Bolan, N., et al., *Remediation of heavy metal(loid)s contaminated soils – To mobilize or to immobilize?* Journal of Hazardous Materials, 2014. 266(0): p. 141-166.
107. Ahemad, M. and M. Kibret, *Mechanisms and applications of plant growth promoting rhizobacteria: Current perspective*. Journal of King Saud University - Science, 2014. 26(1): p. 1-20.
108. Gupta, V.K. and A. Rastogi, *Biosorption of lead(II) from aqueous solutions by non-living algal biomass Oedogonium sp. and Nostoc sp.—A comparative study*. Colloids and Surfaces B: Biointerfaces, 2008. 64(2): p. 170-178.
109. Reichman, S.M., *Probing the plant growth-promoting and heavy metal tolerance characteristics of Bradyrhizobium japonicum CB1809*. European Journal of Soil Biology, 2014. 63(0): p. 7-13.
110. Bai, J., et al., *Biosorption mechanisms involved in immobilization of soil Pb by Bacillus subtilis DBM in a multi-metal-contaminated soil*. Journal of Environmental Sciences, 2014. 26(10): p. 2056-2064.
111. Carsel, R.F.a.P., R. S. , *Developing joint probability distributions of soil-water retention characteristics*. Water Resources Research, 1988. 24(5): p. 755-769.

112. (USGS), U.S.G.S., *Groundwater resources for the future-Atlantic Coastal Zone, Fact Sheet 085-00, Reston, VA. . 2000.*
113. Obiri-Nyarko, F., et al., *Geochemical modelling for predicting the long-term performance of zeolite-PRB to treat lead contaminated groundwater.* Journal of Contaminant Hydrology, 2015. 177–178(0): p. 76-84.



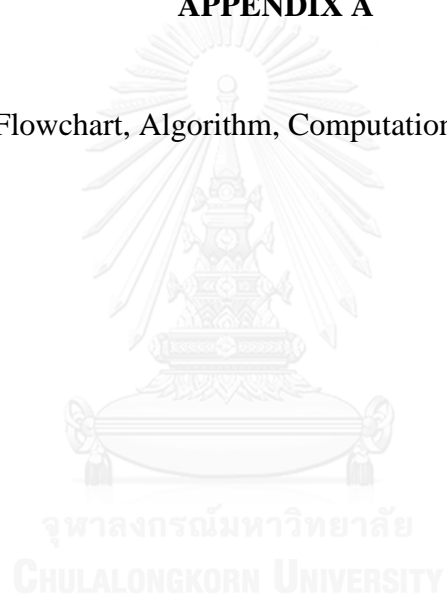
APPENDIX



จุฬาลงกรณ์มหาวิทยาลัย
CHULALONGKORN UNIVERSITY

APPENDIX A

Flowchart, Algorithm, Computational codes

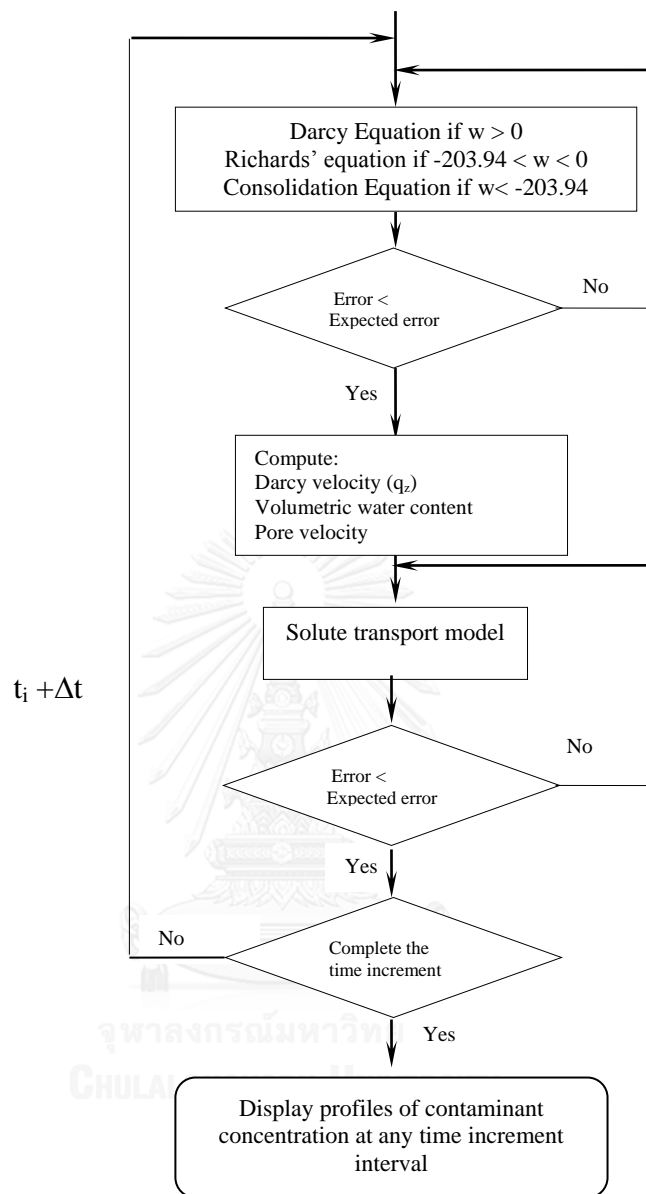


A.1 Flow Chart

The flow chart of the model solution process

The flow chart of the model solution process is provided in Figure A.1. Firstly, Richards' equation was solved. The approximated solution of pressure head (ψ_j), moisture content (θ), Darcy's velocity (q_z) and pore velocity (v) were obtained. Secondly, these solutions were substituted into the advection and dispersion terms presented in the contaminant transport model. The concentration profiles and the reduction zone were evaluated. Finally, the simulation results were reported.





FigureA.1 Schematic flowchart of the solution for the model developed

A.2 Algorithm

A.2.1 Algorithm for transport model

1. Input the geometry of the considered area (x) and the number of nodes in the considered area, to compute the nodal space (Δx).
2. Compute and store element properties such as the elemental depth, nodal coordinate, nodal connective.
3. Select the hydraulic properties equations: VG function. Input the coefficients for hydraulic properties. Compute relative permeability (k_{rw}), and specific moisture capacity (M_C).
4. Input the initial and boundary conditions.
5. Compute and store the weighting function (N_i) and its derivative (dN_i/dx) for each node of the element.
6. Compute and store the shape function (N_j) and its derivative (dN_j/dx) for each node of the element.
7. Compute the element matrix and vectors $[A_{ij}]$, $[B_{ij}]$ and $\{E_i\}$.
 - If " $w_{top} > 0$ " compute Darcy equation
 - if " $w_{top} > -203.94$ " compute consolidation equation
 - if " $-203.94 > w_{top} > 0$ " compute Richards' equation
8. Assemble the element matrix to the global matrix $[A_{ij}]^e$, $[B_{ij}]^e$ and $\{E_i\}^e$.
9. Store the global matrix $[A_{ij}]^e$, $[B_{ij}]^e$ and $\{E_i\}^e$ for the component on scratch files.
10. Compute the initial nodal pressure head (ψ_0) according to the capillary pressure head (ψ_c).
11. Input the initial time (t_0), the final time (t_f) and the number of time step, as well as compute the time increment (Δt).
12. Set the starting node " $j = 0$ " and starting time " $t = 0$ " as well as set iteration count.
 - "count = 0".
13. **While** " $t < t_f$ " do Steps 14 to 26.
14. **For** " $j = 1$ " to the " n^{th} " node, do Steps 15 to 26.
15. Compute term $B = \frac{1}{\Delta t} \sum_{i=1}^{nnode} [B_{ij}] \{\psi\}^t$

16. Set up the allowance maximum error (E_{max})
 17. **For** “ $j=1$ ” to the “ n ” node, do Steps 18 to 26 for each component.
 18. Retrieve the global matrices $[A_{ij}]^e$, $[B_{ij}]^e$ and $\{E_i\}^e$ from the scratch files.
 19. Update the term “ B ” according to the boundary conditions during $[t, t+\Delta t]$.
 20. **If** “ $j=1$ ” go to Step 22
 21. **Elseif** “ $j=n$ ” go to Step 22
 22. $\{\psi\}^{t+\Delta t} = \{\psi_0\}$
 23. **Else**, solve the nodal pressure head $\{\psi\}^{t+\Delta t}$ according to

$$\left(\frac{1}{2} [A_{ij}]^k + \frac{1}{\Delta t} [B_{ij}]^k \right) (\{\psi\}^{t+\Delta t} - \{\psi\}^t) = \{E_i\} - [A_{ij}]^k \{\psi\}^t$$
 24. Compute the error; $\text{Error} = \|\{\psi\}^{t+\Delta t} - \{\psi\}^t\|$
 25. **If** “ $\text{Error} \geq E_{max}$ ” hold $\{\psi\}^t = \{\psi\}^{t+\Delta t}$ and then go to Step 14
 26. **Else**, compute the iteration count according to

$$\text{count} = \text{count} + 1$$

$$t = t + 1$$
 and then, go to Step 13.
 27. Compute the nodal Darcy flux (q_z)
 28. Display the results
- End.

A.2.2 Algorithm for contaminant transport model

1. Recall the input coefficient from Richards’ equation and calculate Darcy’s velocity (q_z) and pore velocity (v). Add the required inputs for contaminant reaction including adsorption rate (K_d), soil bulk density (ρ_B), The substrate saturation constant (K_s), and monod’s kinetic rate (μ_m)
2. Input the initial and boundary conditions.

3. Recall the weighting function (N_i) and its derivative (dN_i/dz) as well as the shape function (N_j) and its derivative (dN_j/dz) for each node of the element from Richards' equation.
4. Compute the element matrix and vectors for the solute transport equation $[P_{ij}]$, $[Q_{ij}]$, $[R_{ij}]$ and $\{S_i\}$.
5. Assemble the element matrices to the global matrix $[P_{ij}]^e$, $[Q_{ij}]^e$, $[R_{ij}]^e$ and $\{S_i\}^e$.
6. Store the global matrix $[P_{ij}]^e$, $[Q_{ij}]^e$, $[R_{ij}]^e$ and $\{S_i\}^e$ for the component on scratch files.
7. Input the initial nodal concentration (C_i).
8. Input the initial time (t_0), the final time (t_f) and the number of time step, as well as compute the time increment (Δt).
9. Set the starting node " $j = 0$ " and starting time " $t = 0$ ", as well as set the iteration "count = 0".
10. **While** " $t < t_f$ " do Step 11 to 22.
11. **For** " $j=1$ " to the " n^{th} " node, do Steps 12 to 22
12. Compute term
$$P = \frac{1}{\Delta t} \sum_{i=1}^{nnode} \left([P_{ij}] + [R_{ij}] \right) \{C\}^t$$
13. Set up the allowance maximum error (E_{max})
14. **For** " $j=1$ " to the " n^{th} " node, do Steps 15 to 22 for each component.
15. Retrieve the global matrix $[P_{ij}]^e$, $[Q_{ij}]^e$, $[R_{ij}]^e$ and $\{S_i\}^e$ from the scratch files.
16. Update the term P according to the boundary conditions $[t, t+\Delta t]$.
17. **If** " $j=1$ " node go to Step 18
18. $\{C\}^{t+\Delta t} = \{C_i\}$
19. **Else**, solve the nodal concentration $\{C\}^{t+\Delta t}$ according to

$$\left(\frac{1}{2} \left([P_{ij}] + [R_{ij}] \right) + \frac{1}{\Delta t} [Q_{ij}] \right) \left(\{C\}^{t+\Delta t} - \{C\}^t \right) = \{S_i\} - \left([P_{ij}] + [R_{ij}] \right) \{C\}^t$$
20. Compute the error; $\text{Error} = \left\| \{C\}^{t+\Delta t} - \{C\}^t \right\|$
21. **If** "**Error** $\geq E_{max}$ " hold $\{C\}^t = \{C\}^{t+\Delta t}$ and then go to Step 13
22. **Else**, compute the iteration count according to

$$\text{count} = \text{count} + 1$$

$$t = t + 1$$

- and then, go to Step 10.
23. Display the input and output solution for the water movement model and/or the solute transport model.
 24. Display the results
- End.

References

- Bunsri, T. Contaminant Transport Processes in Onsite Waste Disposal Systems.
Doctor of Philosophy SCHOOL OF CIVIL, MINING AND
ENVIRONMENTAL ENGINEERING University of Wollongong, 2006.



A.3 Input parameters

Table A.3.1 Input parameters for modelling of biobarrier

Input parameters description	Formulation symbol	Codes
Required parameters for grid characteristics The number of degree of freedoms per nodes The total number of elements in the system A nodal connectivity of each element The number of nodes per element The total degree of freedom in the system The degree of freedom in each element The element depth	- - - - - - -	ndof nelem nnode nnel sdof edof deltl
Required parameters for time step interval The Number of time interval The starting time interval The ending time interval The length of time interval	- - - -	nt ti tf dt
Required parameters for initial and boundary conditions The hydraulic pressure head at the column surface The hydraulic pressure head at the column base The initial hydraulic pressure head at any nodes Pb(II) The concentration at the column surface The concentration at the column base The initial concentration at any nodes Organic-C The org-C concentration at the column surface The org-C concentration at the column base The initial org-C concentration at any nodes	$\psi(0,t)$ $\psi(z,t)$ $\psi(z,0)$ $C(0,t)$ $C(z,t)$ $C(z,0)$ $C(0,t)$ $C(z,t)$ $C(z,0)$	wtop wbot wint Ctop Cbot Cint Ctop Cbot Cint
Required parameters for the hydraulic properties equation The saturation moisture content The residual moisture content The saturated hydraulic conductivity The van Genuchten model: The coefficient p The coefficient a	θ_s θ_r K _{zz} p a	zetas zetar K _{zz} n ap
Required parameters for dispersion determination Pb(II) The molecular diffusion coefficient The fraction of molecular diffusion The transverse dispersivity Organic-C The molecular diffusion coefficient The fraction of molecular diffusion The transverse dispersivity	D* F α_T D* F α_T	Dmm Mfact or alpha_ T Dmm

		Mfact or alpha_ T
--	--	----------------------------

Table A.3.1 (cont.) Input parameters for modelling of biobarrier for remediation at lead contaminated sites

Input parameters description	Formulation symbol	Codes
<i>Required kinetics parameters for solute transport model</i>		
Soil bulk density	ρ_B	rhoB
Pb(II) adsorption rate	K_d	Kd
Microbial growth-decay rate constants	K_C	Kg
Biological kinetic rate	u_m	um
<i>The obtained input from hydraulic properties model</i>		
The nodal moisture content	$\theta(z,t)$	zsol
The relative permeability coefficient	k_{rw}	krww
The specific moisture content capacity	M_C	smcw
<i>The obtained input from water movement model</i>		
The nodal Darcy's velocity	$q_z(z,t)$	qsol
The pore velocity of each elements	(z,t)	nuesol

Note: The symbol presented units in the computational codes were including of:

L is length unit that was possible in unit of mm, cm and m, the recommended length unit was cm.

M is mass unit that was possible in unit of mg, g and kg, the recommended mass unit was g.

T is time unit that was possible in unit of s, min, hour and day, the recommended time unit was day.

A.4 Computational codes

```

function SOLUTE_LEAD
%
% *****
% function description:
% To calculate the nodal pressure head at any time interval in 1-
dimension
%
% Richard's equation
%  $M \cdot D(w, t) / Dt = K \cdot krw \cdot D\{ [D(w, zz) / Dz] + 1 \} / Dz$ 
%
% To evaluate the concentration profile of the considered contaminant
at
% any time interval.
%
% Advective dispersive equation
%  $D(Dz \cdot D(C, z), z) - D(qz \cdot C, z) = D(zeta \cdot kapta \cdot C, t) + (lamda \cdot zeta \cdot kapta \cdot C)$ 
%
% This main program is coded for supporting all contaminant transport
in
% on-site waste disposal system in 1-Dimension.
%
%% Variable declaration
%
% ~~~~~
% Part: 1 Matrices for the element integration
% ~~~~~
% a = element matrix for time-independent term (w,z)
% [aa] = system of a
% b = element matrix for time-dependent term (w,t)
% [bb] = system of b
% bi = element vector for shape function
% [bbi] = system vector for bi
% qi = effective element vector with containing Darcian velocity
% [qqi] = effective system vector qi
% ~~~~~
% Part: 2 Element distribution
% ~~~~~
% gcoord = coordinate values of each node
% nodes = nodal connectivity of each element
% index = a vector containing system of the degree of freedom (dof)
% associated with each element
% bcdof = a vector containing dofs associated with boundary
conditions
% bcval = a vector containing boundary condition values associated
with
% the dofs in bcdof
% nnel = The number of nodes per element
% ndof = The number of degree of freedoms per node
% nele = The total number of elements in the system
% deltl, leng = The length of element (L)
% ~~~~~
% Part: 3 Water movement boundary conditions
% ~~~~~
% wtop= The pressure head (L) at the upper boundary
% wbot= The pressure head (L) at the lower boundary

```

```

% wint=      The initial pressure head (L) at any nodes
% ~~~~~~
% Part: 4 Time integration
% ~~~~~~
% nt = The Number of time interval (o)
% dt = The length of time interval (T)
% tf= The final time (T)
% ti= The initial time (T)
% ~~~~~~
% Part: 5 Parameters for hydraulic properties models
% ~~~~~~
% Kzz(w)= The saturated hydraulic conductivity in w-based form(L/T)
% krw(w)= The relative permeability in w-based form (o/o)
% smc = The specific moisture capacity (1/L)
% zetas = The saturated moisture content (o/o)
% zetar = The residual moisture content(o/o)
% n,m,ap= The emperical coefficients for van Genutchten Model
% A,a, b,r= The emperical coefficients for Haverkamp Model
% ~~~~~~
% Part: 6 Solute transport boundary conditions
% ~~~~~~
% Ctop = The concentration at the upper boundary (M/L^3)
% Cbot = The concentration at the lower boundary (M/L^3)
% Cint = The initial concentration at any nodes (M/L^3)
% ~~~~~~
% Part: 7 Dispersion coefficients
% ~~~~~~
% Dmol = The moleclar diffusion coefficient (L^2/T)
% Dmec = The mechanical dispersion coefficient(L^2/T)
% alpha_T=The transverse dispersivity (o)
% nue = Soil pore-water velocity (L/T)
% mfactor= The fraction of Dmol in pure water over Dmol in soil
% ~~~~~~
% Part: 8 Kinetics parameters for the retardation reactions
% ~~~~~~
% lamda = The decay rate constant (1/T)
% Kd = The partitioning distribution coefficients (L^3/M)
% rho_B= Soil bulk density; (M/L^3)
% kapta= The retardation coefficient
%
% =====
format long e;
% =====
% 1. ELEMENT DISTRIBUTION
%
% To separate the considered system in many small elements, again
connect
% these elements to form the system.
% =====
% Nodal coordinate
% =====
% ##### Step-1: The Element Distribution
#####
clc
fprintf('~~~~~\n');
fprintf(' 1-DIMENSIONAL UNSATURATED WATER MOVEMENT&SOLUTE TRANSPORT
MODELS \n');
fprintf('~~~~~\n');

```

```

fprintf('                STEP-1: THE ELEMENT DISTRIBUTION          \n');
fprintf('                                                                \n');
fprintf('To separate the considered system in many small
elements,\n');
fprintf('and then connect these elements to form the system. \n');
fprintf('                                                                \n');
fprintf('Enter the values for the grid characteristic parameters:
\n');
fprintf('                                                                \n');
nelem=input('Number of Element; nelem          : '); %
deltl=input('Length of Element; delta-l (L)   : '); %
nobs=input('The observation nodes; nobs      : ');%
ndof=1;
nnode=nelem+1;
nnel=2;
sdof=nnode*ndof;
edof=nnel*ndof;
for ii=1:1:nnode;
    gcoord(ii,1)=(nnode-ii)*deltl;
end
for jj=1:1:nelem;
    mcoord(jj,1)=((2*(nnode-jj))-1)*(deltl/2);
end
[zdepth]=zeros(sdof,1);
[zdepth]=[zdepth]+gcoord;
% =====
% Nodal connectivity
% =====
for jj=1:1:nelem;
    nodes(jj,1)=jj;
    nodes(jj,2)=jj+1;
end
%
% =====
% Boundary of the system
% =====
bcdof(1)=1;
bcdof(2)=nnode;
bcval(1)=0.0;
bcval(2)=0.0;
% =====
% 2.TIME ITERATION STEP
%
% To identify the initial and final time for the considered system.
% =====
% ##### Step-2: Define the Time Step Interval
% #####
clc
fprintf('~~~~~\n');
fprintf(' 1-DIMENSIONAL UNSATURATED WATER MOVEMENT&SOLUTE TRANSPORT
MODELS \n');
fprintf('~~~~~\n');
fprintf('  STEP-2: DEFINE THE TIME STEP INTERVAL          \n');
fprintf('                                                                \n');
fprintf('To identify the initial and final time for the considered
system. \n');
fprintf('                                                                \n');
fprintf('Enter the values for time step interval parameters: \n');

```

```

fprintf('
nt=input('The number of time step; nt
ti=input('The begin of considered time period; t-int (T):
tf=input('The end of considered time period; t-final (T):
dt=(tf-ti)/nt;
%
=====
% 3.INITIAL AND BOUNDARY CONDITIONS FOR WATER MOVEMENT
%
% To identify the initial and boundary conditions for the considered
system.
% =====
% initial condition
% =====
% ##### Step-3:Define the Initial&Boundary Condition
#####
clc
fprintf('~~~~~\n');
fprintf(' 1-DIMENSIONAL UNSATURATED WATER MOVEMENT&SOLUTE TRANSPORT
MODELS \n');
fprintf('~~~~~\n');
fprintf('STEP-3: DEFINE INITIAL&BOUNDARY CONDITIONS FOR WATER
MOVEMENT MODEL \n');
fprintf('
\n');
fprintf('To identify the initial and boundary conditions for the
considered \n');
fprintf('system. \n');
fprintf('
\n');
fprintf('SELECT INFILTRATION BOUNDARY CONDITION-from the display
menu: \n');
clc
option=menu('INFILTRATION COLUMN OPERATION
MODES:', 'Gravitational&Capillary Forces', 'Only Gravitational Force');
wi=zeros(sdof,1);
if option==1;
% ##### for capillary pressure head
#####
fprintf('~~~~~\n');
fprintf(' 1-DIMENSIONAL UNSATURATED WATER MOVEMENT&SOLUTE
TRANSPORT MODELS \n');
fprintf('~~~~~\n');
fprintf('
The gravitational and capillary forces
infiltration \n');
% ##### Parameters for initial and boundary conditions
#####
fprintf('
\n');
fprintf('Enter these parameters for the boundary conditions:
\n');
fprintf('
\n');
wtop=input('The hydraulic pressure head at the top; w-top (L)
: '); %
wbot=input('The hydraulic pressure head at the bottom; w-bottom
(L): '); %
for i=1:1:nnode;
wint(i)=-(0.99999747076322730612195738838237*zdepth(i));
wi(i,1)=wint(i);
end
else;

```

```

    option==2;
    % ##### for infiltration column
    #####

fprintf('~~~~~\n');
    fprintf(' 1-DIMENSIONAL UNSATURATED WATER MOVEMENT&SOLUTE
TRANSPORT MODELS \n');

fprintf('~~~~~\n');
    fprintf('          The gravitational infiltration \n');
    % ##### Parameters for initial and boundary conditions
    #####
    fprintf('
\n');
    fprintf('Enter these parameters for the boundary conditions:
\n');
    fprintf('
\n');
    wtop=input('The hydraulic pressure head at the top; w-top (L)
: '); %
    wbot=input('The hydraulic pressure head at the bottom; w-bottom
(L): '); %
    wint=input('The hydraulic pressure head at any nodes; w-initial
(L): '); %
    wi(:,1)=wint;
end

if wtop>0
    equation=2
elseif wtop > -203.94
    equation=1
else
    equation=3
    deltaL=input('Change in L by consolidation: ');
    wtop = wtop - deltaL
end

%
%=====
% Boundary conditions
% =====
% Dirichlet boundary condition
woldt=zeros(sdof,1);
woldb=zeros(sdof,1);
woldt(1,1)=wtop;
woldb(1,1)=wbot;
wold=woldt+flipud(woldb);
if option==1;
    % ##### for capillary pressure head
    #####
    for i=2:1:nnode;
        wwold(i)=wint(i);
        wold(i)=wwold(i);
        wold(1)=wtop;
        wold(nnode)=wbot;
    end
else;
    option==2;
    %##### for infiltration column #####
    for i=2:1:nnode-1;

```

```

        wold(i)=wint;
    end
end
wnew=zeros(sdof,1);
wnew=wold;
% ### reinstall the initial pressure head for graphical plot ####

intw=zeros(sdof,1);
intw=wold;
% =====
% Neuman boundary condition
% This boundary condition have been inserted in the Darcian velocity
% vector [qqi]
% =====
% 4. MATRIX FOR ELEMENT INTERGRATION
%
% To build the stiffness matrices/vectors for each element.
% =====
% Initialization the stiffness matrices/vector to zero
% =====
aa=zeros(sdof,sdof);
bb=zeros(sdof,sdof);
eei=zeros(sdof,sdof);
bbi=zeros(sdof,1);
qqi=zeros(sdof,1);
%
% =====
% Create the stiffness matices/vectors
% =====
% ##### Step-4: calculate the Unsaturated Soil Hydraulic Properties
#####
clc
clc
fprintf('~~~~~\n');
fprintf(' 1-DIMENSIONAL UNSATURATED WATER MOVEMENT&SOLUTE TRANSPORT
MODELS \n');
fprintf('~~~~~\n');
fprintf('STEP-4: CALCULATE THE NODAL WATER MOVEMENT & SOLUTE
CONCENTRATION \n');
fprintf('                IN UNSATURATED SOIL CONDITION \n');
fprintf('                \n');
fprintf('Unsaturated water movement is calculated using 1-D Richard
equation\n');
fprintf('and solute concentration is estimated using advective-
dispersive \n');
fprintf('equation. \n');
fprintf(' \n');
fprintf('SELECT THE HYDRAULIC PROPERTY MODELS- from the display menu:
\n');
opt=menu('HYDRAULIC PROPERTY MODELS:', 'Van Genuchten', 'Haverkamp', 'Field Data Measurement');
clc
if opt==1;
% ##### VG model #####
fprintf('~~~~~\n');
fprintf(' 1-DIMENSIONAL UNSATURATED WATER MOVEMENT&SOLUTE
TRANSPORT MODELS \n');
fprintf('~~~~~\n');

```

```

fprintf('The selected hydraulic properties model is van Genuchten
model. \n');
fprintf('
\n');
fprintf('Enter these parameters for this hydraulic properties
model. \n');
fprintf('
\n');
Kzz=input('The saturated hydraulic conductivity; Kzz (L/T) :
'); %
zetas=input('The saturated moisture content; zeta-s (L^3/L^3) :
'); %
zetar=input('The residual moisture content; zeta-r (L^3/L^3) :
'); %
n=input('The empirical coefficient p : '); %
ap=input('The empirical coefficient a : '); %
rhoW=input('Water density : '); %
Sstore=input('Specific storativity : '); %
gravity=9.81;
mu=input('Water viscosity : '); %
m=1-1/n;
% =====
% 5. SOLUTE IDENTIFICATION
%
% To show the types of considered solute.
% =====
fprintf('~~~~~\n');
fprintf(' STEP-5: IDENTIFY THE CONSIDERED CONTAMINANTS \n');
fprintf('
\n');
fprintf('The considered contaminant is A Non REACTIVE
CONSTITUENT, or \n');
fprintf('TRACER COMPOUND \n');
fprintf('
\n');
% ~~~~~ Tracer Test mode ~~~~~
%
=====
% 6. INITIAL AND BOUNDARY CONDITION FOR SOLUTE TRANSPORT
%
% To identify the initial and boundary condition for the
considered system.
%
=====
% ##### initial & boundary condition #####
clc
fprintf('~~~~~\n');
fprintf(' 1-DIMENSIONAL UNSATURATED WATER MOVEMENT&SOLUTE
TRANSPORT MODELS \n');
fprintf('~~~~~\n');
fprintf('STEP-6: DEFINE THE INITIAL AND BOUNDARY CONDITIONS FOR
SOLUTE TRANSPORT MODEL\n');
fprintf('
\n');
fprintf('The considered contaminat is the Non-reactive
constituent(tracer). \n');
fprintf('
\n');
fprintf('To identify the initial and boundary condition for the
considered \n');
fprintf('system. \n');
fprintf('
\n');
fprintf('Enter the values for boundary condition: \n');
fprintf('
\n');

```



```

%=====
% Boundary conditions
% =====
Ctop=input('Tracer concentration at the top; C-top (M/L^3)      :
'); %
Cbot=input('Tracer concentration at the bottom; C-bottom (M/L^3):
'); %
% =====
% Initial Condition
% =====
Cint=input('Tracer concentration at any nodes; C-initial (M/L^3):
'); %
%
% ~~~~~~ Dirichlet boundary condition ~~~~~~
Coldt=zeros(sdof,1);
Coldb=zeros(sdof,1);
Coldt(1,1)=Ctop;
Coldb(1,1)=Cbot;
Cold=Coldt+flipud(Coldb);
for i=2:1:nnode-1
    Cold(i)=Cint;
end
Cnew=zeros(sdof,1);
Cnew=Cold;
% =====
% 7. DISPERSION DETERMINATION
%
% To determine the dispersion coefficients for the considered
system.
% =====
% ##### Dispersion coefficients #####
clc
fprintf('~~~~~\n');
fprintf(' 1-DIMENSIONAL UNSATURATED WATER MOVEMENT&SOLUTE
TRANSPORT MODELS \n');
fprintf('~~~~~\n');
fprintf('    STEP-7: DEFINE THE DISPERSION COEFFICIENTS \n');
fprintf(' \n');
fprintf('To determine the dispersion coefficients, these
coefficients are \n');
fprintf('the combination of molecular and mechanical dispersion.
\n');
fprintf(' \n');
fprintf('Enter the values for dispersion determination: \n');
fprintf(' \n');
% #####Dispersion calculation #####
% ~~~~~~ molecular diffusion ~~~~~~
Dmol=zeros(nelem,1);
Dmm=input('The molecular diffusion coefficient; Dmol (L^2/T) :
');%0.07308;%
mfactor=input('The fraction of molecular diffusion; Ff :
');%0.4;%
Dm=Dmm*mfactor;
Dmol(:,:)=Dm;
alpha_T=input('The transverse dispersivity; alpha-T (L)
: ');
Kd=input('Langmuir / Freundlich Adsorption rate;Kd : ');
rhoB=input('Soil bulk density; rho-B (M/L^3) : ');

```

```

% ~~~~~ reinstall the initial matrices ~~~~~
intC=zeros(sdof,1);
intC=Cold;
ppa=zeros(sdof,sdof);
ppb=zeros(sdof,sdof);
QQ=zeros(sdof,sdof);
RR=zeros(sdof,sdof);
SSi=zeros(sdof,1);
kapta=zeros(nnode,nt);
kapta(:,:)=1;
lamda=zeros(nnode,1);

bio_mode=menu('Biological growth model:', 'Simple monod '
, 'Gompertz ');
if bio_mode == 1
    KSO=input('The substrate saturation constant; KSO (M/L^3) :
');
    Rso=input('Biological kinetics rate : ');
else
    bio_ConsumptionRate=input('Specific substrate consumption
rate:');
    bio_delayTime=input('The delay reaction time:');
    bio_asymtote=input('Gompertz asymptote value, A:');
end

% ++++++
% CALCULATION PROCESS IS STARTING HERE.
% ++++++
count=0;
wsol=zeros(sdof,nt);
zsol=zeros(sdof,nt);
ksol=zeros(sdof,nt);
KapTa=zeros(nnode,nt);
TaKap=zeros(nnode,nt);
ssol=zeros(sdof,nt);
qsol=zeros(nelem,nt);
nuesol=zeros(nelem,nt);
dsol=zeros(nelem,nt);
wmw=zeros(1,nt);
Csol=zeros(sdof,nt);
CmC=zeros(1,nt);
time=zeros(1,nt);
% ##### intiialise hydraulic properties#####
[wnew]=intw;
for wx=1:1:nnode;

[krww,smcw,krwz,smcz,Dzeta,zetanew]=hdpVG(wnew,n,zetas,zetar,Kzz,ap,n
node);
end
intzeta=zetanew;
while count<nt;
    ipt=count+1;
    itt=count+1;
    for itt=1:1:nt;
        solw=zeros(sdof,nt);
        solz=zeros(sdof,nt);
        solkrw=zeros(sdof,nt);

```

```

    solsmc=zeros(sdof,nt);
    solq=zeros(nelem,nt);
    solC=zeros(sdof,nt);
    solnue=zeros(nelem,nt);
    sold=zeros(nelem,nt);
    error=1;
    while error>1e-10;
        for i=1:1:nelem;
            nd(1)=nodes(i,1);
            nd(2)=nodes(i,2);
            L1=gcoord(nd(1),1);
            L2=gcoord(nd(2),1);
            leng=(L1-L2);
        end

        for iel=1:1:nnode;
            if equation==3

[krww,smcw,krwz,smcz,Dzeta,zetanew]=hdpVG(wnew,n,zetas,zetar,Kzz,ap,n
node);

[aa]=aai_consolidation(nnel,ndof,sdof,edof,nnode,Kzz,krww,leng,nelem,
aa,rhoW,Sstore,gravity,mu,wnew);

[bb]=cff2(nnel,ndof,nelem,sdof,nnode,smcw,leng,bb);

[eei]=eei_consolidation(nnel,ndof,sdof,edof,nnode,Kzz,krww,leng,nelem
,eei,rhoW,Sstore,gravity,mu,wnew);
            oldval=zeros(sdof,1);
            oldval=[wold];
            [AL]=[aa]*[wold];
            [LA]=[eei]-(0.5.*[AL]);
            [LB]=([bb]./dt)*[wold];
            [BL]=[LA]+[LB];
            [LC]=(0.5.*[aa])+([bb]./dt);
            [CL]=inv([LC]);
            wnew=[CL]*[BL];
            wnew(1)=wtop;
            wnew(nnode)=wbot;
            [wold]=[wnew];
            elseif equation==2

[krww,smcw,krwz,smcz,Dzeta,zetanew]=hdpVG(wnew,n,zetas,zetar,Kzz,ap,n
node);

            %
[aa]=cff1(nnel,ndof,sdof,edof,nnode,Kzz,krww,leng,nelem,aa);

[bb]=bij_darcy(nnel,ndof,nelem,sdof,nnode,smcw,leng,bb,delt1);

[bbi]=bbi_darcy(nnel,ndof,Kzz,krww,nelem,nnode,bbi,wnew);

[qqi]=qqi_darcy(wnew,nnel,ndof,leng,Kzz,krww,nelem,nnode,qqi);
            [eei]=[qqi]-[bbi];
            oldval=zeros(sdof,1);
            oldval=[wold];
            % [AL]=[aa]*[wold];
            [LA]=[eei];
            [LB]=([bb]./dt)*[wold];

```

```

[BL]=[LA]+[LB];
[LC]=( [bb] ./dt);
[CL]=inv([LC]);
wnew=[CL]*[BL];
wnew(1)=wtop;
wnew(nnode)=wbot;
[wold]=[wnew];
else
    % Richard

[krww, smcw, krwz, smcz, Dzeta, zetanew]=hdpVG(wnew, n, zetas, zetar, Kzz, ap, n
node);

[aa]=cff1(nnel, ndof, sdof, edof, nnode, Kzz, krww, leng, nelem, aa);

[bb]=cff2(nnel, ndof, nelem, sdof, nnode, smcw, leng, bb);

[bbi]=cff3(nnel, ndof, Kzz, krww, nelem, nnode, bbi);

[qqi]=cff4(wnew, nnel, ndof, leng, Kzz, krww, nelem, nnode, qqi);
[eei]=[qqi]-[bbi];
oldval=zeros(sdof, 1);
oldval=[wold];
[AL]=[aa]*[wold];
[LA]=[eei]-(0.5.*[AL]);
[LB]=( [bb] ./dt)*[wold];
[BL]=[LA]+[LB];
[LC]=(0.5.*[aa])+( [bb] ./dt);
[CL]=inv([LC]);
wnew=[CL]*[BL];
wnew(1)=wtop;
wnew(nnode)=wbot;
[wold]=[wnew];
end

% ##### check the obtain data #####
check=zeros(nnode, 1);
for i=1:1:nnode;
    check(i)=intw(i)-wold(i);
    if check(i)>0;
        wold(i)=intw(i);
    elseif check(i)==0;
        wold(i)=wold(i);
    elseif check(i)<0;
        wold(i)=wold(i);
    end
end
dcheck=zeros(nnode, 1);
for j=1:1:nnode;
    dcheck(j)=wtop-wold(j);
    if dcheck(j)>0;
        wold(j)=wold(j);
    elseif dcheck(j)==0;
        wold(j)=wold(j);
    elseif dcheck(j)<0;
        wold(j)=intw(j);
    end
end

```

```

        end
        err(iel)=abs(oldval(iel)-wold(iel));
        error2=sum(err(iel));
        error=error2+10e-11;
    end
    krw=krww;
    zeta=zetanew;
    smc=smcw;
    % ##### reinstall value of pressure head
#####
    ww=(1^itt)*[wold];
    solw(:,itt)=ww;
    wsol=wsol+solw;
    www=wsol(nobs,itt);
    wmw(:,itt)=www;
    ttime(itt)=itt*dt;
    time(:,itt)=ttime(itt);
    % ##### reinsall value of moisture content
#####
    zz=(1^itt)*[zeta];
    solz(:,itt)=zz;
    zsol=zsol+solz;
    zww=zsol(nobs,itt);
    wnz(:,itt)=zww;
    ttime(itt)=itt*dt;
    time(:,itt)=ttime(itt);
    % ##### reinsall value of relative permeability
#####
    kk=(1^itt)*[krw];
    solkrw(:,itt)=kk;
    ksol=ksol+solkrw;
    % ### reinsall value of specific soil moisture
capacity ###
    ss=(1^itt)*[smc];
    solsmc(:,itt)=ss;
    ssol=ssol+solsmc;
    DIFFW=zeros(nnode,1);
    WDIFFF=zeros(nelem,1);
    qQ=zeros(nelem,1);
    nN=zeros(nelem,1);
    Avez=zeros(nelem,1);
    Nnue=zeros(nelem,1);
    % ##### Darcy and Pore velocities calculation
#####
    for JJ=1:1:nnode;
        wdifff(JJ)=ww(JJ)-ww(nnode);
        DIFFW(JJ)=wdifff(JJ);
    end
    for JK=1:1:nelem;
        KJ=JK+1;
        Kkrel(JK)=0.5*Kzz.*(kk(JK)+kk(KJ));
        diffw(JK)=0.5*(DIFFW(JK)+DIFFW(KJ))./mcoord(JK);
        WDIFFF(JK)=-Kkrel(JK).*(diffw(JK)+1);
        Avez(JK)=0.5*(zz(JK)+zz(KJ));
        Nnue(JK)=abs(WDIFFF(JK)./Avez(JK));
    end
    qQ=WDIFFF;
    qq=(1^itt)*qQ;

```

```

qz=qq;
solq(:,itt)=qq;
qsol=qsol+solq;
nN=Nnue;
nn=(1^itt)*nN;
solnue(:,itt)=nn;
nuesol=nuesol+solnue;
% ##### Mass Balance calculation #####
MB=zeros(1,nt);
for t=1:1:nt;
    for xa=1:1:nelem-1;
        ax=xa+1;
        zetadiff(xa)=(zsol(xa,t)-zsol(ax,t))*leng;
    end
    mb1=abs(sum(zetadiff));
    mb2=abs((zsol(1,t)-intzeta(1,1))*0.5*leng);
    mb3=abs((zsol(nnode,t)-
intzeta(nnode,1))*0.5*leng);
    mb4=abs((qsol(1,t)-qsol(nelem,t))*dt);
    MB1(t)=(mb1+mb2+mb3)/mb4;
    MB(1,t)=MB1(t);
end
%
+++++
% strating solute transport calculation
%
+++++
Dmec=zeros(nelem,1);
D=zeros(nelem,1);
for HI=1:1:nelem;
    Dme(HI)=nn(HI).*alpha_T;
    Dmec(HI)=Dme(HI);
end
D=Dmec+Dmol;
Dd=(1^itt)*[D];
sold(:,itt)=Dd;
dsol=dsol+sold;
% ##### Adsorption Kinetics Rate #####
kapta=zeros(nnode,1);
kA=(rhoB*Kd);
for RA=1:1:nnode;
    KA(RA)=1+(kA/zeta(RA));
    kapta(RA)=KA(RA);
end

KAPTA=(1^itt)*[kapta];
TaKap(:,itt)=KAPTA;
KapTa=KapTa+TaKap;

for G=1:1:nnode;

    if bio_mode == 1
        RSO(G)=(Rso.*Cnew(G))./(KSO+Cnew(G));
        lamda(G)=RSO(G);
    else
        RSO_EXP(G) = ((bio_ConsumptionRate * 2.718 /
bio_asymtote) * (bio_delayTime - t)) + 1

```

```

                                RSO(G) = bio_ConsumptionRate * 2.718 * exp(-
exp(RSO_EXP(G))) * exp(RSO_EXP(G));
                                lamda(G)=RSO(G);
                                end

                                end;

                                ERROR=1;
                                while ERROR>1e-10;
                                for iel=1:1:nnode;
                                [PP]=cff9(nnode,D,qz,leng,nelem,ppa,ppb);
                                [QQ]=cff10(nnode,nelem,zeta,kapta,leng,QQ);

[RR]=cff11(nnode,nelem,zeta,kapta,lamda,leng,RR);
                                [SSi]=cff12(Cnew,nnel,leng,nelem,nnode,SSi);
                                oldval=zeros(sdof,1);
                                oldval=[Cold];
                                [LA]=0.5.*([PP]+[RR]);
                                [AL]=[LA]*[Cold];
                                [LB]=([QQ]./dt)*[Cold];
                                [BL]=([SSi]-[AL])+[LB];
                                [LC]=([LA])+([QQ]./dt);
                                [CL]=inv([LC]);
                                Cnew=[CL]*[BL];
                                Cnew(1)=Ctop;
                                Cnew(nnode)=Cbot;
                                [Cold]=[Cnew];
                                % ##### check the obtain data #####
                                for i=1:1:nnode;
                                if Cold(i)<0;
                                    Cold(i)=intC(i);
                                elseif Cold(i)>Ctop;
                                    Cold(i)=Ctop;
                                end
                                Check(i)=intC(i)-Cold(i);
                                Dcheck(i)=Ctop-Cold(i);
                                if Check(i)>0
                                    Cold(i)=intC(i);
                                elseif Check(i)==0;
                                    Cold(i)=Cold(i);
                                elseif Check(i)<0;
                                    Cold(i)=Cold(i);
                                end
                                if Dcheck(i)>0;
                                    Cold(i)=Cold(i);
                                elseif Dcheck(i)==0;
                                    Cold(i)=Cold(i);
                                elseif Dcheck(i)<0;
                                    Cold(i)=intC(i);
                                end
                                end
                                err(iel)=abs(oldval(iel)-Cold(iel));
                                ERROR2=sum(err(iel));
                                ERROR=ERROR2+10e-11;
                                end
                                % ## reinstall value of nodal concentration ##
                                CC=(1^itt)*[Cold];
                                solC(:,itt)=CC;

```

```

        Csol=Csol+solC;
        CCC=Csol(nobs,itt);
        CmC(:,itt)=CCC;
        ttime(itt)=itt*dt;
        time(:,itt)=ttime(itt);
    end
    count=count+1;
end
end
end
end
% @@@@ END OF VG MODEL @@@@@@@@@@@@@@@@@@@@@@@@@@@@@@@@@@@@@@@@@@@@@@@@

elseif opt==2;
% ##### HV model #####
fprintf('~~~~~\n');
fprintf(' 1-DIMENSIONAL UNSATURATED WATER MOVEMENT&SOLUTE
TRANSPORT MODELS \n');
fprintf('~~~~~\n');
fprintf('The selected hydraulic property model is Haverkamp
model. \n');
fprintf(' \n');
fprintf('Enter these parameters for this hydraulic properties
model. \n');
fprintf(' \n');
Kzz=input('The saturated hydraulic conductivity; Kzz (L/T) :
'); %
zetas=input('The saturated moisture content; zeta-s (L^3/L^3) :
'); %
zetar=input('The residual moisture content; zeta-r (L^3/L^3) :
'); %
A=input('The empirical coefficient A : ');
%
a=input('The empirical coefficient alpha : ');
%
b=input('The empirical coefficient beta : ');
%
r=input('The empirical coefficient gramar : ');
%
% =====
% 5. SOLUTE IDENTIFICATION
%
% To show the types of considered solute.
% =====
fprintf(' fprintf(' STEP-5: IDENTIFY THE CONSIDERED
CONTAMINANTS \n');
fprintf(' \n');
fprintf('The considered contaminant is A Non REACTIVE
CONSTITUENT, or \n');
fprintf('TRACER COMPOUNDS. \n');
fprintf(' \n');
% ~~~~~ Tracer Test mode ~~~~~
% =====
% 6. INITIAL AND BOUNDARY CONDITION FOR SOLUTE TRANSPORT
%
% To identify the initial and boundary condition for the
considered system.
% =====
% ##### initial & boundary condition #####

```



```

clc
fprintf('~~~~~\n');
fprintf(' 1-DIMENSIONAL UNSATURATED WATER MOVEMENT&SOLUTE
TRANSPORT MODELS          \n');
fprintf('~~~~~\n');
fprintf('STEP-6: DEFINE THE INITIAL AND BOUNDARY CONDITIONS FOR
SOLUTE TRANSPORT MODEL \n');
fprintf('          \n');
fprintf('The considered constituent is the Non-reactive
constituent(tracer)\n');
fprintf('          \n');
fprintf('To identify the initial and boundary condition for the
considered \n');
fprintf('system.          \n');
fprintf('          \n');
fprintf('Enter the values for boundary condition:  \n');
fprintf('          \n');
%=====
% Boundary conditions
% =====
Ctop=input('Tracer concentration at the top; C-top (M/L^3)      :
'); %
Cbot=input('Tracer concentration at the bottom; C-bottom (M/L^3):
'); %
% =====
% Initial Condition
% =====
Cint=input('Tracer concentration at any nodes; C-initial (M/L^3):
'); %
%
% ~~~~~ Dirichlet boundary condition ~~~~~
Coldt=zeros(sdof,1);
Coldb=zeros(sdof,1);
Coldt(1,1)=Ctop;
Coldb(1,1)=Cbot;
Cold=Coldt+flipud(Coldb);
for i=2:1:nnode-1
    Cold(i)=Cint;
end
Cnew=zeros(sdof,1);
Cnew=Cold;
% =====
% 7. DISPERSION DETERMINATION
%
% To determine the dispersion coefficients for the considered
system.
% =====
% ##### Dispersion coefficients #####
clc
fprintf('~~~~~\n');
fprintf(' 1-DIMENSIONAL UNSATURATED WATER MOVEMENT&SOLUTE
TRANSPORT MODELS \n');
fprintf('~~~~~\n');
fprintf(' STEP-7: DEFINE THE DISPERSION COEFFICIENTS          \n');
fprintf('          \n');
fprintf('To determine the dispersion coefficients, these
coefficients are \n');

```

```

fprintf('the combination of molecular and mechanical dispersion.
\n');
fprintf('
\n');
fprintf('Enter the values for dispersion determination:
\n');
fprintf('
\n');
% ##### Dispersion calculation #####
% ~~~~~ molecular diffusion ~~~~~
Dmol=zeros(nelem,1);
Dmm=input('The molecular diffusion coefficient; Dmol (L^2/T) :
');;%0.07308;%
mfactor=input('The fraction of molecular diffusion; Ff (L^2/T)
: ');;%0.4;%
Dm=Dmm*mfactor;
Dmol(:,:)=Dm;
alpha_T=input('The transverse dispersivity; alpha-T (L)
: ');
% ~~~~~ reinstall the initial matrices ~~~~~
intC=zeros(sdof,1);
intC=Cold;
ppa=zeros(sdof,sdof);
ppb=zeros(sdof,sdof);
QQ=zeros(sdof,sdof);
RR=zeros(sdof,sdof);
SSi=zeros(sdof,1);
kapta=zeros(nnode,nt);
kapta(:,:)=1;
lamda=zeros(nnode,1);
% ++++++
% CALCULATION PROCESS IS STARTING HERE.
% ++++++
count=0;
wsol=zeros(sdof,nt);
zsol=zeros(sdof,nt);
ksol=zeros(sdof,nt);
KapTa=zeros(nnode,nt);
TaKap=zeros(nnode,nt);
ssol=zeros(sdof,nt);
qsol=zeros(nelem,nt);
nuesol=zeros(nelem,nt);
dsol=zeros(nelem,nt);
wmw=zeros(1,nt);
Csol=zeros(sdof,nt);
CmC=zeros(1,nt);
time=zeros(1,nt);
% ##### intiialise hydraulic properties#####
[wnew]=intw;
for wx=1:1:nnode;

[krww, smcw, krwz, smcz, Dzeta, zetanew]=hdpHV(A, a, b, r, wnew, zetas, zetar, Kz
z, nnode);
end
intzeta=zetanew;
while count<nt;
ipt=count+1;
itt=count+1;
for itt=1:1:nt;
solw=zeros(sdof,nt);

```

```

solz=zeros(sdof,nt);
solkrw=zeros(sdof,nt);
solsmc=zeros(sdof,nt);
solq=zeros(nelem,nt);
solC=zeros(sdof,nt);
solnue=zeros(nelem,nt);
sold=zeros(nelem,nt);
error=1;
while error>1e-10;
    for i=1:1:nelem;
        nd(1)=nodes(i,1);
        nd(2)=nodes(i,2);
        L1=gcoord(nd(1),1);
        L2=gcoord(nd(2),1);
        leng=(L1-L2);
    end
    for iel=1:1:nnode;

[krww,smcw,krwz,smcz,Dzeta,zetanew]=hdpHV(A,a,b,r,wnew,zetas,zetar,Kz
z,nnode);

[aa]=cff1(nnel,ndof,sdof,edof,nnode,Kzz,krww,leng,nelem,aa);

[bb]=cff2(nnel,ndof,nelem,sdof,nnode,smcw,leng,bb);
    [bbi]=cff3(nnel,ndof,Kzz,krww,nelem,nnode,bbi);

[qqi]=cff4(wnew,nnel,ndof,leng,Kzz,krww,nelem,nnode,qqi);
    [eei]=[qqi]-[bbi];
    oldval=zeros(sdof,1);
    oldval=[wold];
    [AL]=[aa]*[wold];
    [LA]=[eei]-(0.5.*[AL]);
    [LB]=([bb]./dt)*[wold];
    [BL]=[LA]+[LB];
    [LC]=(0.5.*[aa])+([bb]./dt);
    [CL]=inv([LC]);
    wnew=[CL]*[BL];
    wnew(1)=wtop;
    wnew(nnode)=wbot;
    [wold]=[wnew];
    % ##### check the obtain data
#####
check=zeros(nnode,1);
for i=1:1:nnode;
    check(i)=intw(i)-wold(i);
    if check(i)>0;
        wold(i)=intw(i);
    elseif check(i)==0;
        wold(i)=wold(i);
    elseif check(i)<0;
        wold(i)=wold(i);
    end
end
dcheck=zeros(nnode,1);
for j=1:1:nnode;
    dcheck(j)=wtop-wold(j);
    if dcheck(j)>0;
        wold(j)=wold(j);

```

```

elseif dcheck(j)==0;
    wold(j)=wold(j);
elseif dcheck(j)<0;
    wold(j)=intw(j);
end
end
err(iel)=abs(oldval(iel)-wold(iel));
error2=sum(err(iel));
error=error2+10e-11;
end
krw=krww;
zeta=zetanew;
smc=smcw;
% ##### reinstall value of pressure head #####
ww=(1^itt)*[wold];
solw(:,itt)=ww;
wsol=wsol+solw;
www=wsol(nobs,itt);
wmw(:,itt)=www;
ttime(itt)=itt*dt;
time(:,itt)=ttime(itt);
% #### reinsall value of moisture content #####
zz=(1^itt)*[zeta];
solz(:,itt)=zz;
zsol=zsol+solz;
zww=zsol(nobs,itt);
wmz(:,itt)=zww;
ttime(itt)=itt*dt;
time(:,itt)=ttime(itt);
% ### reinsall value of relative permeability ###
kk=(1^itt)*[krw];
solkrw(:,itt)=kk;
ksol=ksol+solkrw;
% ### reinsall value of specific soil moisture
capacity ###
ss=(1^itt)*[smc];
solsmc(:,itt)=ss;
ssol=ssol+solsmc;
DIFFW=zeros(nnode,1);
WDIFF=zeros(nelem,1);
qQ=zeros(nelem,1);
nN=zeros(nelem,1);
Avez=zeros(nelem,1);
Nnue=zeros(nelem,1);
% #### Darcy and Pore velocities calculation #####
for JJ=1:1:nnode;
    wdiff(JJ)=ww(JJ)-ww(nnode);
    DIFFW(JJ)=wdiff(JJ);
end
for JK=1:1:nelem;
    KJ=JK+1;
    Kkrel(JK)=0.5*Kzz.*(kk(JK)+kk(KJ));
    diffw(JK)=0.5*(DIFFW(JK)+DIFFW(KJ))./mcoord(JK);
    WDIFF(JK)=-Kkrel(JK).*(diffw(JK)+1);
    Avez(JK)=0.5*(zz(JK)+zz(KJ));
    Nnue(JK)=abs(WDIFF(JK))./Avez(JK);
end
qQ=WDIFF;

```

```

qq=(1^itt)*qQ;
qz=qQ;
solq(:,itt)=qq;
qsol=qsol+solq;
nN=Nnue;
nn=(1^itt)*nN;
solnue(:,itt)=nn;
nuesol=nuesol+solnue;
% ##### Mass Balance calculation #####
MB=zeros(1,nt);
for t=1:1:nt;
    for xa=1:1:nelem-1;
        ax=xa+1;
        zetadiff(xa)=(zsol(xa,t)-zsol(ax,t))*leng;
    end
    mb1=abs(sum(zetadiff));
    mb2=abs((zsol(1,t)-intzeta(1,1))*0.5*leng);
    mb3=abs((zsol(nnode,t)-
intzeta(nnode,1))*0.5*leng);
    mb4=abs((qsol(1,t)-qsol(nelem,t))*dt);
    MB1(t)=(mb1+mb2+mb3)/mb4;
    MB(1,t)=MB1(t);
end
%
+++++++
% strating solute transport calculation
% ++++++
Dmec=zeros(nelem,1);
D=zeros(nelem,1);
for HI=1:1:nelem;
    Dme(HI)=nn(HI).*alpha_T;
    Dmec(HI)=Dme(HI);
end
D=Dmec+Dmol;
Dd=(1^itt)*[D];
sold(:,itt)=Dd;
dsol=dsol+sold;

for G=1:1:nnode;
    RSO(G)=(Rso.*Cnew(G))./(KSO+Cnew(G));
    lamda(G)=RSO(G);
end;

ERROR=1;
while ERROR>1e-10;
    for iel=1:1:nnode;
        [PP]=cff9(nnode,D,qz,leng,nelem,ppa,ppb);
        [QQ]=cff10(nnode,nelem,zeta,kapta,leng,QQ);

[RR]=cff11(nnode,nelem,zeta,kapta,lamda,leng,RR);
[SSi]=cff12(Cnew,nnel,leng,nelem,nnode,SSi);
oldval=zeros(sdof,1);
oldval=[Cold];
[LA]=0.5.*([PP]+[RR]);
[AL]=[LA]*[Cold];
[LB]=([QQ]./dt)*[Cold];
[BL]=([SSi]-[AL])+[LB];
[LC]=([LA])+([QQ]./dt);

```

```

[CL]=inv([LC]);
Cnew=[CL]*[BL];
Cnew(1)=Ctop;
Cnew(nnode)=Cbot;
[Cold]=[Cnew];
% ##### check the obtain data #####
check=zeros(nnode,1);
for i=1:1:nnode;
    if Cold(i)<0;
        Cold(i)=intC(i);
    elseif Cold(i)>Ctop;
        Cold(i)=Ctop;
    end
    Check(i)=intC(i)-Cold(i);
    Dcheck(i)=Ctop-Cold(i);
    if Check(i)>0
        Cold(i)=intC(i);
    elseif Check(i)==0;
        Cold(i)=Cold(i);
    elseif Check(i)<0;
        Cold(i)=Cold(i);
    end
    if Dcheck(i)>0;
        Cold(i)=Cold(i);
    elseif Dcheck(i)==0;
        Cold(i)=Cold(i);
    elseif Dcheck(i)<0;
        Cold(i)=intC(i);
    end
end
err(iel)=abs(oldval(iel)-Cold(iel));
ERROR2=sum(err(iel));
ERROR=ERROR2+10e-11;
end
% # reinstall value of nodal concentration ###
CC=(1^itt)*[Cold];
solC(:,itt)=CC;
Csol=Csol+solC;
CCC=Csol(nobs,itt);
CmC(:,itt)=CCC;
ttime(itt)=itt*dt;
time(:,itt)=ttime(itt);
end
count=count+1;
end
end
end
% @@@@@@@@@@ END OF HV MODEL @@@@@@@@@@@@@@@@@@@@@@@@@@@@@@@@@@@@@@@@@@@@@@

elseif opt==3;
% =====
% ##### User define mode #####
% =====
clc
fprintf('~~~~~\n');
fprintf('1-DIMENSIONAL UNSATURATED WATER MOVEMENT&SOLUTE
TRANSPORT MODELS\n');
fprintf('~~~~~\n');

```

```

fprintf('The selected hydraulic property model is fields data
measurement. \n');
fprintf('The defined parameters are based on van Genuchten model.
\n');
fprintf('
\n');
fprintf('
Select the soil types from the display menu:
\n');
fprintf('
\n');
stexture=menu('SELECT SOIL TEXTURE:', ' Clay ', ' Clay Loam ', '
Loam ', ' Loam sand ', ' Silt ', ' Silt loam ', ' Silty Clay ', '
Silty Clay Loam ', ' Sand ', ' Sandy clay ', ' Sandy clay loam
', 'Sand Loam');
if stexture==1;
fprintf('Soil texture was classified as "CLAY" \n');
fprintf('The hydraulic parameters are: \n');
fprintf('The saturated hydraulic conductivity;Kzz (cm/hour) =
0.030 \n');
fprintf('The saturated moisture content; zetas = 0.380
\n');
fprintf('The residual moisture content; zetar = 0.068 \n');
fprintf('The coefficient a (1/cm) = 0.008 \n');
fprintf('The coefficient p = 1.090 \n');
Kzz=0.030;
zetas=0.38;
zetar=0.068;
n=1.09;
ap=0.008;
elseif stexture==2;
fprintf('Soil texture was classified as "CLAY LOAM" \n');
fprintf('The hydraulic parameters are: \n');
fprintf('The saturated hydraulic conductivity;Kzz (cm/hour) =
0.100 \n');
fprintf('The saturated moisture content; zetas =
0.410 \n');
fprintf('The residual moisture content; zetar =
0.095 \n');
fprintf('The coefficient a (1/cm) = 0.019 \n');
fprintf('The coefficient p = 1.310 \n');
Kzz=0.1;
zetas=0.41;
zetar=0.095;
n=1.310;
ap=0.019;
elseif stexture==3;
fprintf('Soil texture was classified as "LOAM" \n');
fprintf('The hydraulic parameters are: \n');
fprintf('The saturated hydraulic conductivity;Kzz (cm/hour) =
0.340 \n');
fprintf('The saturated moisture content; zetas =
0.430 \n');
fprintf('The residual moisture content; zetar =
0.078 \n');
fprintf('The coefficient a (1/cm) = 0.036 \n');
fprintf('The coefficient p = 1.560 \n');
Kzz=0.34;
zetas=0.43;
zetar=0.078;
n=1.56;

```

```

    ap=0.036;
    elseif stexture==4;
        fprintf('Soil texture was classified as "LOAM SAND" \n');
        fprintf('The hydraulic parameters are:          \n');
        fprintf('The saturated hydraulic conductivity;Kzz (cm/hour) =
2.990      \n');
        fprintf('The saturated moisture content; zetas           =
0.410      \n');
        fprintf('The residual moisture content; zetar            =
0.057      \n');
        fprintf('The coefficient a (1/cm)          = 0.124          \n');
        fprintf('The coefficient p                  = 2.280          \n');
        Kzz=2.99;
        zetas=0.41;
        zetar=0.057;
        n=2.280;
        ap=0.124;
    elseif stexture==5;
        fprintf('Soil texture was classified as "SILT" \n');
        fprintf('The hydraulic parameters are:          \n');
        fprintf('The saturated hydraulic conductivity;Kzz (cm/hour) =
1.823      \n');
        fprintf('The saturated moisture content; zetas           =
0.460      \n');
        fprintf('The residual moisture content; zetar            =
0.034      \n');
        fprintf('The coefficient a (1/cm)          = 0.106          \n');
        fprintf('The coefficient p                  = 1.370          \n');
        Kzz=1.823;
        zetas=0.46;
        zetar=0.034;
        n=1.37;
        ap=0.106;
    elseif stexture==6;
        fprintf('Soil texture was classified as "SILT LOAM" \n');
        fprintf('The hydraulic parameters are:          \n');
        fprintf('The saturated hydraulic conductivity;Kzz (cm/hour) =
0.650      \n');
        fprintf('The saturated moisture content; zetas           =
0.450      \n');
        fprintf('The residual moisture content; zetar            =
0.067      \n');
        fprintf('The coefficient a(1/cm)          = 0.020          \n');
        fprintf('The coefficient p                  = 1.410          \n');
        Kzz=0.65;
        zetas=0.45;
        zetar=0.067;
        n=1.41;
        ap=0.020;
    elseif stexture==7;
        fprintf('Soil texture was classified as "SILTY CLAY" \n');
        fprintf('The hydraulic parameters are:          \n');
        fprintf('The saturated hydraulic conductivity;Kzz (cm/hour) =
0.050      \n');
        fprintf('The saturated moisture content; zetas           =
0.360      \n');
        fprintf('The residual moisture content; zetar            =
0.070      \n');

```



```

fprintf('The coefficient a (1/cm)      = 0.005      \n');
fprintf('The coefficient p              = 1.090      \n');
Kzz=0.050;
zetas=0.360;
zetar=0.070;
n=1.090;
ap=0.005;
elseif stexture==8;
fprintf('Soil texture was classified as "SILTY CLAY LOAM"
\n');
fprintf('The hydraulic parameters are:      \n');
fprintf('The saturated hydraulic conductivity;Kzz (cm/hour) =
0.100 \n');
fprintf('The saturated moisture content; zetas           =
0.430 \n');
fprintf('The residual moisture content; zetar           =
0.089 \n');
fprintf('The coefficient a (1/cm)      = 0.010      \n');
fprintf('The coefficient p              = 1.230      \n');
Kzz=0.100;
zetas=0.43;
zetar=0.089;
n=1.23;
ap=0.010;
elseif stexture==9;
fprintf('Soil texture was classified as "SAND" \n');
fprintf('The hydraulic parameters are:      \n');
fprintf('The saturated hydraulic conductivity;Kzz (cm/hour) =
11.78 \n');
fprintf('The saturated moisture content; zetas           =
0.430 \n');
fprintf('The residual moisture content; zetar           =
0.045 \n');
fprintf('The coefficient a (1/cm)      = 0.145      \n');
fprintf('The coefficient p              = 2.680      \n');
Kzz=11.78;
zetas=0.43;
zetar=0.045;
n=2.680;
ap=0.145;
elseif stexture==10;
fprintf('Soil texture was classified as "SANDY CLAY" \n');
fprintf('The hydraulic parameters are:      \n');
fprintf('The saturated hydraulic conductivity;Kzz (cm/hour) =
0.060 \n');
fprintf('The saturated moisture content; zetas           =
0.380 \n');
fprintf('The residual moisture content; zetar           =
0.100 \n');
fprintf('The coefficient a (1/cm)      = .027      \n');
fprintf('The coefficient p              = 1.230      \n');
Kzz=0.06;
zetas=0.38;
zetar=0.1;
n=1.230;
ap=0.027;
elseif stexture==11;

```

```

fprintf('Soil texture was classified as "SANDY CLAY LOAM"
\n');
fprintf('The hydraulic parameters are:          \n');
fprintf('The saturated hydraulic conductivity;Kzz (cm/hour) =
0.150      \n');
fprintf('The saturated moisture content; zetas           =
0.390      \n');
fprintf('The residual moisture content; zetar           =
0.100      \n');
fprintf('The coefficient a (1/cm)      = 0.059          \n');
fprintf('The coefficient p      = 1.480          \n');
Kzz=0.15;
zetas=0.39;
zetar=0.1;
n=1.48;
ap=0.059;
elseif stexture==12;
fprintf('Soil texture was classified as "SANY LOAM" \n');
fprintf('The hydraulic parameters are:          \n');
fprintf('The saturated hydraulic conductivity;Kzz (cm/hour) =
1.090      \n');
fprintf('The saturated moisture content; zetas           =
0.410      \n');
fprintf('The residual moisture content; zetar           =
0.065      \n');
fprintf('The coefficient a (1/cm)      = 0.075          \n');
fprintf('The coefficient p      = 1.890          \n');
Kzz=1.890;
zetas=0.41;
zetar=0.065;
n=1.89;
ap=0.075;
end

m=1-1/n;
% =====
% 5. SOLUTE IDENTIFICATION
%
% To show the types of considered solute.
% =====

fprintf('~~~~~\n');
fprintf('          ('STEP-5: SELECT THE CONSIDERED CONTAMINANTS
\n');
fprintf('          \n');
fprintf('The considered contaminant is A Non REACTIVE
CONSTITUENT, or \n');
fprintf('TRACER COMPOUNDS.          \n');
fprintf('          \n');
fprintf('          \n');
% ~~~~~ Tracer Test mode ~~~~~
% =====
% 6. INITIAL AND BOUNDARY CONDITION FOR SOLUTE TRANSPORT
%
% To identify the initial and boundary condition for the
considered system.
% =====
% ##### initial & boundary condition #####

```

```

clc
fprintf('~~~~~ \n');
fprintf(' 1-DIMENSIONAL UNSATURATED WATER MOVEMENT&SOLUTE
TRANSPORT MODELS \n');
fprintf('~~~~~ \n');
fprintf('STEP-6: DEFINE THE INITIAL AND BOUNDARY CONDITIONS FOR
SOLUTE TRANSPORT MODEL \n');
fprintf(' \n');
fprintf('The considered constituent is the Non-reactive
constituent(tracer). \n');
fprintf(' \n');
fprintf('To identify the initial and boundary condition for the
considered \n');
fprintf('system. \n');
fprintf(' \n');
fprintf('Enter the values for boundary condition: \n');
fprintf(' \n');
% Boundary conditions
%
Ctop=input('Tracer concentration at the top; C-top (M/L^3) :
'); %
Cbot=input('Tracer concentration at the bottom; C-bottom (M/L^3):
'); %
%
% Initial Condition
%
Cint=input('Tracer concentration at any nodes; C-initial (M/L^3):
'); %
%
% ~~~~~ Dirichlet boundary condition
Coldt=zeros(sdof,1);
Coldb=zeros(sdof,1);
Coldt(1,1)=Ctop;
Coldb(1,1)=Cbot;
Cold=Coldt+flipud(Coldb);
for i=2:1:nnode-1
    Cold(i)=Cint;
end
Cnew=zeros(sdof,1);
Cnew=Cold;
%
% 7. DISPERSION DETERMINATION
%
% To determine the dispersion coefficients for the considered
system.
%
% ##### Dispersion coefficients
clc
fprintf('~~~~~ \n');
fprintf(' 1-DIMENSIONAL UNSATURATED WATER MOVEMENT&SOLUTE
TRANSPORT MODELS \n');
fprintf('~~~~~ \n');
fprintf(' (STEP-7: DEFINE THE DISPERSION COEFFICIENTS \n');
fprintf('To determine the dispersion coefficients, these
coefficients are \n');
fprintf('the combination of molecular and mechanical dispersion.
\n');

```

```

    fprintf('
\n');
    fprintf('Enter the values for dispersion determination:
\n');
    fprintf('
\n');
    % ##### Dispersion calculation
    % ~~~~~~ molecular diffusion
    Dmol=zeros(nelem,1);
    Dmm=input('The molecular diffusion coefficient; Dmol (L^2/T)   :
');;%0.07308;%
    mfactor=input('The fraction of molecular diffusion; Ff (L^2/T)
:   ');;%0.4;%
    Dm=Dmm*mfactor;
    Dmol(:,:)=Dm;
    alpha_T=input('The transverse dispersivity; alpha-T (L)
:   ');
    % ~~~~~~ reinstall the initial matrices
    intC=zeros(sdof,1);
    intC=Cold;
    ppa=zeros(sdof,sdof);
    ppb=zeros(sdof,sdof);
    QQ=zeros(sdof,sdof);
    RR=zeros(sdof,sdof);
    SSi=zeros(sdof,1);
    kapta=zeros(nnode,nt);
    kapta(:,:)=1;
    lamda=zeros(nnode,1);
+
    % CALCULATION PROCESS IS STARTING HERE.
    %
    count=0;
    wsol=zeros(sdof,nt);
    zsol=zeros(sdof,nt);
    ksol=zeros(sdof,nt);
    KapTa=zeros(nnode,nt);
    TaKap=zeros(nnode,nt);
    ssol=zeros(sdof,nt);
    qsol=zeros(nelem,nt);
    nuesol=zeros(nelem,nt);
    dsol=zeros(nelem,nt);
    wmw=zeros(1,nt);
    Csol=zeros(sdof,nt);
    CmC=zeros(1,nt);
    time=zeros(1,nt);
    % ##### intiialise hydraulic properties
    [wnew]=intw;
    for wx=1:1:nnode;

[krww, smcw, krwz, smcz, Dzeta, zetanew]=hdpVG(wnew,n,zetas,zetar,Kzz,ap,n
node);
    end
    intzeta=zetanew;
    while count<nt;
        ipt=count+1;
        itt=count+1;
        for itt=1:1:nt;
            solw=zeros(sdof,nt);

```

```

solz=zeros(sdof,nt);
solkrw=zeros(sdof,nt);
solsmc=zeros(sdof,nt);
solq=zeros(nelem,nt);
solC=zeros(sdof,nt);
solnue=zeros(nelem,nt);
sold=zeros(nelem,nt);
error=1;
while error>1e-10;
    for i=1:1:nelem;
        nd(1)=nodes(i,1);
        nd(2)=nodes(i,2);
        L1=gcoord(nd(1),1);
        L2=gcoord(nd(2),1);
        leng=(L1-L2);
    end
    for iel=1:1:nnode;
        [krww,smcw,krwz,smcz,Dzeta,zetaneu]=hdpVG(wnew,n,zetas,zetar,Kzz,ap,n
node);
        [aa]=cff1(nnel,ndof,sdof,edof,nnode,Kzz,krww,leng,nelem,aa);
        [bb]=cff2(nnel,ndof,nelem,sdof,nnode,smcw,leng,bb);
            [bbi]=cff3(nnel,ndof,Kzz,krww,nelem,nnode,bbi);
        [qqi]=cff4(wnew,nnel,ndof,leng,Kzz,krww,nelem,nnode,qqi);
        [eei]=[qqi]-[bbi];
        oldval=zeros(sdof,1);
        oldval=[wold];
        [AL]=[aa]*[wold];
        [LA]=[eei]-(0.5.*[AL]);
        [LB]=( [bb] ./dt)*[wold];
        [BL]=[LA]+[LB];
        [LC]=(0.5.*[aa])+( [bb] ./dt);
        [CL]=inv([LC]);
        wnew=[CL]*[BL];
        wnew(1)=wtop;
        wnew(nnode)=wbot;
        [wold]=[wnew];
        % ##### check the obtain data
        check=zeros(nnode,1);
        for i=1:1:nnode;
            check(i)=intw(i)-wold(i);
            if check(i)>0;
                wold(i)=intw(i);
            elseif check(i)==0;
                wold(i)=wold(i);
            elseif check(i)<0;
                wold(i)=wold(i);
            end
        end
        dcheck=zeros(nnode,1);
        for j=1:1:nnode;
            dcheck(j)=wtop-wold(j);
            if dcheck(j)>0;
                wold(j)=wold(j);
            elseif dcheck(j)==0;
                wold(j)=wold(j);
            elseif dcheck(j)<0;
                wold(j)=intw(j);
            end
        end
    end
end
end

```

```

        end
    end
    err(iel)=abs(oldval(iel)-wold(iel));
    error2=sum(err(iel));
    error=error2+10e-11;
end
krw=krww;
zeta=zetanew;
smc=smcw;
% ##### reinstall value of pressure head
ww=(1^itt)*[wold];
solw(:,itt)=ww;
wsol=wsol+solw;
www=wsol(nobs,itt);
wmw(:,itt)=www;
ttime(itt)=itt*dt;
time(:,itt)=ttime(itt);
% ##### reinsall value of moisture content
zz=(1^itt)*[zeta];
solz(:,itt)=zz;
zsol=zsol+solz;
zww=zsol(nobs,itt);
wmz(:,itt)=zww;
ttime(itt)=itt*dt;
time(:,itt)=ttime(itt);
% ##### reinsall value of relative permeability
kk=(1^itt)*[krw];
solkrw(:,itt)=kk;
ksol=ksol+solkrw;
% reinsall value of specific soil moisture capacity
ss=(1^itt)*[smc];
solsmc(:,itt)=ss;
ssol=ssol+solsmc;
DIFFW=zeros(nnode,1);
WDIFF=zeros(nelem,1);
qQ=zeros(nelem,1);
nN=zeros(nelem,1);
Avez=zeros(nelem,1);
Nnue=zeros(nelem,1);
for JJ=1:1:nnode;
    wdiff(JJ)=ww(JJ)-ww(nnode);
    DIFFW(JJ)=wdiff(JJ);
end
% ##### Darcy and Pore velocities calculation
for JK=1:1:nelem;
    KJ=JK+1;
    Kkrel(JK)=0.5*Kzz.*(kk(JK)+kk(KJ));
    diffw(JK)=0.5*(DIFFW(JK)+DIFFW(KJ))./mcoord(JK);
    WDIFF(JK)=-Kkrel(JK).*(diffw(JK)+1);
    Avez(JK)=0.5*(zz(JK)+zz(KJ));
    Nnue(JK)=abs(WDIFF(JK))./Avez(JK);
end
qQ=WDIFF;
qq=(1^itt)*qQ;
qz=qq;
solq(:,itt)=qq;
qsol=qsol+solq;
nN=Nnue;

```

```

nn=(1^itt)*nN;
solnue(:, itt)=nn;
nuesol=nuesol+solnue;
% ##### Mass Balance calculation
MB=zeros(1, nt);
for t=1:1:nt;
    for xa=1:1:nelem-1;
        ax=xa+1;
        zetadiff(xa)=(zsol(xa, t)-zsol(ax, t))*leng;
    end
    mb1=abs(sum(zetadiff));
    mb2=abs((zsol(1, t)-intzeta(1, 1))*0.5*leng);
    mb3=abs((zsol(nnode, t)-
intzeta(nnode, 1))*0.5*leng);
    mb4=abs((qsol(1, t)-qsol(nelem, t))*dt);
    MB1(t)=(mb1+mb2+mb3)/mb4;
    MB(1, t)=MB1(t);
end
%
+++++
%strating solute transport calculation
+++++
Dmec=zeros(nelem, 1);
D=zeros(nelem, 1);
for HI=1:1:nelem;
    Dme(HI)=nn(HI).*alpha_T;
    Dmec(HI)=Dme(HI);
end
D=Dmec+Dmol;
Dd=(1^itt)*[D];
sold(:, itt)=Dd;
dsol=dsol+sold;

for G=1:1:nnode;
    RSO(G)=(Rso.*Cnew(G))./(KSO+Cnew(G));
    lamda(G)=RSO(G);
end;

ERROR=1;
while ERROR>1e-10;
    for iel=1:1:nnode;

        [PP]=cff9(nnode, D, qz, leng, nelem, ppa, ppb);
        [QQ]=cff10(nnode, nelem, zeta, kapta, leng, QQ);

[RR]=cff11(nnode, nelem, zeta, kapta, lamda, leng, RR);
[SSi]=cff12(Cnew, nnel, leng, nelem, nnode, SSi);
oldval=zeros(s dof, 1);
oldval=[Cold];
[LA]=0.5.*([PP]+[RR]);
[AL]=[LA]*[Cold];
[LB]=([QQ]./dt)*[Cold];
[BL]=([SSi]-[AL])+[LB];
[LC]=[LA]+([QQ]./dt);
[CL]=inv([LC]);
Cnew=[CL]*[BL];
Cnew(1)=Ctop;
Cnew(nnode)=Cbot;

```

```

[Cold]=[Cnew];

% ##### check the obtain data
for i=1:1:nnode;
    check(i)=intC(i)-Cold(i);
    if check(i)>0
        Cold(i)=intC(i);
    elseif check(i)==0;
        Cold(i)=Cold(i);
    elseif check(i)<0;
        Cold(i)=Cold(i);
    end
end
for j=1:1:nnode;
    dcheck(j)=Ctop-Cold(j);
    if dcheck(j)>0;
        Cold(j)=Cold(j);
    elseif dcheck(j)==0;
        Cold(j)=Cold(j);
    elseif dcheck(j)<0;
        Cold(j)=Ctop;
    end
end
err(iel)=abs(oldval(iel)-Cold(iel));
ERROR2=sum(err(iel));
ERROR=ERROR2+10e-11;
end
% ##### reinstall value of nodal concentration
CC=(1^itt)*[Cold];
solC(:,itt)=CC;
Csol=Csol+solC;
CCC=Csol(nobs,itt);
CmC(:,itt)=CCC;
ttime(itt)=itt*dt;
time(:,itt)=ttime(itt);
end
count=count+1;
end
end
end
end
% @@@@@@@@ END OF SOLUTE TRANSPORT MODEL @@@@@@@@@@@@@@@@@@@@@@@@@@@@@@@@
fprintf('=====\n');
fprintf(' The Solute transpoprt was completely calculated. \n');
fprintf(' \n');

%
% 5.RESULTS DISPLAY and RESULTS REPORTS
%
% To illustrate the results in Graphical Plot and Table of data
%
% ##### Step-5: Results Display #####
clc
fprintf('~\n');
fprintf(' 1-DIMENSIONAL UNSATURATED WATER MOVEMENT&SOLUTE TRANSPORT MODELS \n');
fprintf('          STEP-8: GRAPHICAL PLOT \n');
fprintf(' These are the obtain results for WATER MOVEMENT \n');

```



```

fpri                & SOLUTE TRANSPORT MODELS. \n');
fprintf('~~~~~\n');
fprintf('Press any key to access the result reports:  ');
pause
% ##### Figure 1 hydraulic pressure head vs depth #####
figure(1);
tt=nt+1;
wsolve=zeros(nnode,tt);
wsolve(:,1)=intw;
for tti=2:1:tt;
    itt=tti-1;
    wsolve(:,tti)=wsol(:,itt);
end
plot(wsolve,gcoord,'*-');
title('NUMERICAL SOLUTION OF WATER MOVEMENT MODEL');
xlabel('HYDRAULIC PRESSURE HEAD; L');
ylabel('DEPTH-above the datum-; L');
% ##### Figure 2 soil moisture content vs depth #####
figure(2);
plot(zsol,gcoord,'*-');
title('NUMERICAL SOLUTION OF WATER MOVEMENT MODEL');
xlabel('SOIL MOISTURE CONTENT; o/o');
ylabel('DEPTH-above the datum-; L');
% ##### Figure 3 concentration vs depth #####
figure(3);
plot(Csol,gcoord,'*-');
title('NUMERICAL SOLUTION OF SOLUTE TRANSPORT MODEL');
xlabel('CONCENTRATION; M/L^3');
ylabel('DEPTH-above the datum-; L');
% ##### Figure 4 nodal Darcian velocity vs depth #####
figure(4);
plot(qsol,mcoord,'+-');
title('NUMERICAL SOLUTION OF WATER MOVEMENT MODEL');
xlabel('NODAL DARCIAN VELOCITY; L/T');
ylabel('DEPTH-above the datum-; L');
% ##### Figure 5 pore velocity vs depth #####
figure(5);
plot(nuesol,mcoord,'+-');
title('NUMERICAL SOLUTION OF WATER MOVEMENT MODEL');
xlabel('PORE VELOCITY; L/T');
ylabel('DEPTH-above the datum-; L');
% ##### Figure 6 relative hydraulic conductivity vs depth #####
figure(6);
plot(ksol,gcoord,'o-');
title('NUMERICAL SOLUTION OF WATER MOVEMENT MODEL');
xlabel('RELATIVE HYDRAULIC CONDUCTIVITY; o/o');
ylabel('DEPTH-above the datum-; L');
% ##### Figure 7 specific moisture capacity vs depth #####
figure(7);
plot(ssol,gcoord,'o-');
title('NUMERICAL SOLUTION OF WATER MOVEMENT MODEL');
xlabel('SPECIFIC SOIL MOISTURE CAPACITY; 1/L');
ylabel('DEPTH-above the datum-; L');
% ##### Figure 8 dispersion vs depth #####
figure(8);
plot(dsol,mcoord,'*-');
title('NUMERICAL SOLUTION OF SOLUTE TRANSPORT MODEL');
xlabel('DISPERSION; L^2/T');

```

```

ylabel('DEPTH-above the datum-; L');
% ##### Figure 9 pressure head vs time #####
figure(9);
plot(time,wmw,'-b');
title('NUMERICAL SOLUTION OF WATER MOVEMENT MODEL');
xlabel('TIME; T');
ylabel('HYDRAULIC PRESSURE HEAD- at the observation node; L');
% ##### Figure 10 moisture content vs time #####
figure(10);
plot(time,wmz,'-b');
title('NUMERICAL SOLUTION OF WATER MOVEMENT MODEL');
xlabel('TIME; T');
ylabel('VOLUMETRIC MOISTURE CONTENT- at the observation node');
% ##### Figure 11 pressure head vs time #####
figure(11);
plot(time,CmC,'-b');
title('NUMERICAL SOLUTION OF WATER MOVEMENT MODEL');
xlabel('TIME; T');
ylabel('CONCENTRATION- at the observation node; M/L^3');
% ##### Figure 12 accumulated mass vs time #####
figure(12);
plot(time,MB,'-b');
title('NUMERICAL SOLUTION OF WATER MOVEMENT MODEL');
xlabel('TIME; T');
ylabel('WATER BALANCE');

% ##### Calculate the Darcy's velocity #####
% ##### Average Darcian Velocity #####
fprintf('~~~~~ \n');
fprintf('1-DIMENSIONAL UNSATURATED WATER MOVEMENT & SOLUTE TRANSPORT
MODELS \n');
fprintf('~~~~~\n');
sum_q=sum(qsol);
q_sum=sum(sum_q);
ndata=nelem*nt;
qAV=q_sum/ndata;
sum_zeta=sum(zsol);
zeta_sum=sum(sum_zeta);
zAV=zeta_sum/ndata;
sum_d=sum(dsol);
d_sum=sum(sum_d);
DAV=d_sum/ndata;
if option==1;
    fprintf('THE TOTAL WATER MOVEMENT (Gravitational&Capillary
Forces)\n');
    fprintf(' \n');
    if opt==1;
        fprintf('The selected hydraulic properties model is van
Genuchten Model\n');
        fprintf('.....\n');
        fprintf('The hydraulic properties parameters are: \n');
        fprintf('The saturated soil conductivity; Kzz (L/T) =
%.5f\n',Kzz);
        fprintf('The saturated moisture content; zeta-s (L^3/L^3)=
%.5f\n',zetas);
        fprintf('The residual moisture content; zeta-r (L^3/L^3) =
%.5f\n',zetar);
        fprintf('The empirical coefficient p = %.5f\n',n);

```

```

    fprintf('The empirical coefficient a (1/L) = %.5f\n',ap);
  elseif opt==2;
    fprintf('The selected hydraulic property model is Haverkamp
model.\n');
    fprintf('.....\n');
    fprintf('The hydraulic properties parameters are: \n');
    fprintf('The saturated hydraulic conductivity; Kzz (L/T) =
%.5f\n',Kzz);
    fprintf('The saturated moisture content; zeta-s (L^3/L^3)=
%.5f\n',zetas);
    fprintf('The residual moisture content; zeta-r (L^3/L^3) =
%.5f\n',zetar);
    fprintf('The empirical coefficient A = %.5f\n',A);
    fprintf('The empirical coefficient alpha = %.5f\n',a);
    fprintf('The empirical coefficient beta = %.5f\n',b);
    fprintf('The empirical coefficient gamma = %.5f\n',r);
  elseif opt==3;
    fprintf('The selected hydraulic properties model is Field
Data Measurement\n');
    fprintf('.....\n');
    fprintf('The hydraulic properties parameters are estimated
from van Genuchten Model\n');
    if stexture==1;
      fprintf('Soil was classified as "CLAY"\n');
      fprintf('The saturated soil conductivity; Kzz (L/T)
= %.5f\n',Kzz);
      fprintf('The saturated moisture content; zeta-s
(L^3/L^3)= %.5f\n',zetas);
      fprintf('The residual moisture content; zeta-r (L^3/L^3)
= %.5f\n',zetar);
      fprintf('The empirical coefficient p = %.5f\n',n);
      fprintf('The empirical coefficient a (1/L)
= %.5f\n',ap);
    elseif stexture==2;
      fprintf('Soil was classified as "CLAY LOAM"\n');
      fprintf('The saturated soil conductivity; Kzz (L/T)
= %.5f\n',Kzz);
      fprintf('The saturated moisture content; zeta-s
(L^3/L^3)= %.5f\n',zetas);
      fprintf('The residual moisture content; zeta-r (L^3/L^3)
= %.5f\n',zetar);
      fprintf('The empirical coefficient p = %.5f\n',n);
      fprintf('The empirical coefficient a (1/L)
= %.5f\n',ap);
    elseif stexture==3;
      fprintf('Soil was classified as "LOAM"\n');
      fprintf('The saturated soil conductivity; Kzz (L/T)
= %.5f\n',Kzz);
      fprintf('The saturated moisture content; zeta-s
(L^3/L^3)= %.5f\n',zetas);
      fprintf('The residual moisture content; zeta-r (L^3/L^3)
= %.5f\n',zetar);
      fprintf('The empirical coefficient p = %.5f\n',n);
      fprintf('The empirical coefficient a (1/L)
= %.5f\n',ap);
    elseif stexture==4;
      fprintf('Soil was classified as "LOAM SAND"\n');

```

```

        fprintf('The saturated soil conductivity; Kzz (L/T)
= %.5f\n',Kzz);
        fprintf('The saturated moisture content; zeta-s
(L^3/L^3)= %.5f\n',zetas);
        fprintf('The residual moisture content; zeta-r (L^3/L^3)
= %.5f\n',zetar);
        fprintf('The empirical coefficient p = %.5f\n',n);
        fprintf('The empirical coefficient a (1/L) = %.5f\n',ap);
    elseif stexture==5;
        fprintf('Soil was classified as "SILT"\n');
        fprintf('The saturated soil conductivity; Kzz (L/T)
= %.5f\n',Kzz);
        fprintf('The saturated moisture content; zeta-s
(L^3/L^3)= %.5f\n',zetas);
        fprintf('The residual moisture content; zeta-r (L^3/L^3)
= %.5f\n',zetar);
        fprintf('The empirical coefficient p = %.5f\n',n);
        fprintf('The empirical coefficient a (1/L)
= %.5f\n',ap);
    elseif stexture==6;
        fprintf('Soil was classified as "SILT LOAM"\n');
        fprintf('The saturated soil conductivity; Kzz (L/T)
= %.5f\n',Kzz);
        fprintf('The saturated moisture content; zeta-s
(L^3/L^3)= %.5f\n',zetas);
        fprintf('The residual moisture content; zeta-r (L^3/L^3)
= %.5f\n',zetar);
        fprintf('The empirical coefficient p = %.5f\n',n);
        fprintf('The empirical coefficient a (1/L)
= %.5f\n',ap);
    elseif stexture==7;
        fprintf('Soil was classified as "SILTY CLAY"\n');
        fprintf('The saturated soil conductivity; Kzz (L/T)
= %.5f\n',Kzz);
        fprintf('The saturated moisture content; zeta-s
(L^3/L^3)= %.5f\n',zetas);
        fprintf('The residual moisture content; zeta-r (L^3/L^3)
= %.5f\n',zetar);
        fprintf('The empirical coefficient p = %.5f\n',n);
        fprintf('The empirical coefficient a (1/L)
= %.5f\n',ap);
    elseif stexture==8;
        fprintf('Soil was classified as "SILTY CLAY LOAM"\n');
        fprintf('The saturated soil conductivity; Kzz (L/T)
= %.5f\n',Kzz);
        fprintf('The saturated moisture content; zeta-s
(L^3/L^3)= %.5f\n',zetas);
        fprintf('The residual moisture content; zeta-r (L^3/L^3)
= %.5f\n',zetar);
        fprintf('The empirical coefficient p = %.5f\n',n);
        fprintf('The empirical coefficient a (1/L)
= %.5f\n',ap);
    elseif stexture==9;
        fprintf('Soil was classified as "SAND"\n');
        fprintf('The saturated soil conductivity; Kzz (L/T)
= %.5f\n',Kzz);
        fprintf('The saturated moisture content; zeta-s
(L^3/L^3)= %.5f\n',zetas);

```

```

        fprintf('The residual moisture content; zeta-r (L^3/L^3)
= %.5f\n', zetar);
        fprintf('The empirical coefficient p = %.5f\n', n);
        fprintf('The empirical coefficient a (1/L)
= %.5f\n', ap);
        elseif stexture==10;
            fprintf('Soil was classified as "SANDY CLAY"\n');
            fprintf('The saturated soil conductivity; Kzz (L/T)
= %.5f\n', Kzz);
            fprintf('The saturated moisture content; zeta-s
(L^3/L^3)= %.5f\n', zetas);
            fprintf('The residual moisture content; zeta-r (L^3/L^3)
= %.5f\n', zetar);
            fprintf('The empirical coefficient p = %.5f\n', n);
            fprintf('The empirical coefficient a (1/L)
= %.5f\n', ap);
            elseif stexture==11;
                fprintf('Soil was classified as "SANDY CLAY LOAM"\n');
                fprintf('The saturated soil conductivity; Kzz (L/T)
= %.5f\n', Kzz);
                fprintf('The saturated moisture content; zeta-s
(L^3/L^3)= %.5f\n', zetas);
                fprintf('The residual moisture content; zeta-r (L^3/L^3)
= %.5f\n', zetar);
                fprintf('The empirical coefficient p = %.5f\n', n);
                fprintf('The empirical coefficient a (1/L)
= %.5f\n', ap);
            elseif stexture==12;
                fprintf('Soil was classified as "SANDY LOAM"\n');
                fprintf('The saturated soil conductivity; Kzz (L/T)
= %.5f\n', Kzz);
                fprintf('The saturated moisture content; zeta-s
(L^3/L^3)= %.5f\n', zetas);
                fprintf('The residual moisture content; zeta-r (L^3/L^3)
= %.5f\n', zetar);
                fprintf('The empirical coefficient p = %.5f\n', n);
                fprintf('The empirical coefficient a (1/L)
= %.5f\n', ap);
            end
        end
    elseif option==2;
        fprintf('THE GRAVITATIONAL WATER MOVEMENT (Free Flow
Infiltration)\n');
        fprintf('
        \n');
        if opt==1;
            fprintf('The selected hydraulic properties model is van
Genuchten Model\n');
            fprintf('.....\n');
            fprintf('The hydraulic properties parameters are:
        \n');
            fprintf('The saturated soil conductivity; Kzz (L/T)
=
%.5f\n', Kzz);
            fprintf('The saturated moisture content; zeta-s (L^3/L^3)=
%.5f\n', zetas);
            fprintf('The residual moisture content; zeta-r (L^3/L^3) =
%.5f\n', zetar);
            fprintf('The empirical coefficient p = %.5f\n', n);
            fprintf('The empirical coefficient a (1/L)
=
%.5f\n', ap);

```

```

    elseif opt==2;
        fprintf('The selected hydraulic property model is Haverkamp
model.\n');
        fprintf('.....\n');
        fprintf('The hydraulic properties parameters are: \n');
        fprintf('The saturated hydraulic conductivity; Kzz (L/T) =
%.5f\n',Kzz);
        fprintf('The saturated moisture content; zeta-s (L^3/L^3)=
%.5f\n',zetas);
        fprintf('The residual moisture content; zeta-r (L^3/L^3) =
%.5f\n',zetar);
        fprintf('The empirical coefficient A      = %.5f\n',A);
        fprintf('The empirical coefficient alpha  = %.5f\n',a);
        fprintf('The empirical coefficient beta   = %.5f\n',b);
        fprintf('The empirical coefficient gamma  = %.5f\n',r);
    elseif opt==3;
        fprintf('The selected hydraulic properties model is Field
Data Measurement\n');
        fprintf('.....\n');
        fprintf('The hydraulic properties parameters are estimated
from van Genuchten Model\n');
        if stexture==1;
            fprintf('Soil was classified as "CLAY"\n');
            fprintf('The saturated soil conductivity; Kzz (L/T)
= %.5f\n',Kzz);
            fprintf('The saturated moisture content; zeta-s
(L^3/L^3)= %.5f\n',zetas);
            fprintf('The residual moisture content; zeta-r (L^3/L^3)
= %.5f\n',zetar);
            fprintf('The empirical coefficient p   = %.5f\n',n);
            fprintf('The empirical coefficient a (1/L)
= %.5f\n',ap);
            elseif stexture==2;
                fprintf('Soil was classified as "CLAY LOAM"\n');
                fprintf('The saturated soil conductivity; Kzz (L/T)
= %.5f\n',Kzz);
                fprintf('The saturated moisture content; zeta-s
(L^3/L^3)= %.5f\n',zetas);
                fprintf('The residual moisture content; zeta-r (L^3/L^3)
= %.5f\n',zetar);
                fprintf('The empirical coefficient p = %.5f\n',n);
                fprintf('The empirical coefficient a (1/L)
= %.5f\n',ap);
            elseif stexture==3;
                fprintf('Soil was classified as "LOAM"\n');
                fprintf('The saturated soil conductivity; Kzz (L/T)
= %.5f\n',Kzz);
                fprintf('The saturated moisture content; zeta-s
(L^3/L^3)= %.5f\n',zetas);
                fprintf('The residual moisture content; zeta-r (L^3/L^3)
= %.5f\n',zetar);
                fprintf('The empirical coefficient p = %.5f\n',n);
                fprintf('The empirical coefficient a (1/L)
= %.5f\n',ap);
            elseif stexture==4;
                fprintf('Soil was classified as "LOAM SAND"\n');
                fprintf('The saturated soil conductivity; Kzz (L/T)
= %.5f\n',Kzz);

```

```

        fprintf('The saturated moisture content; zeta-s
(L^3/L^3)= %.5f\n', zetas);
        fprintf('The residual moisture content; zeta-r (L^3/L^3)
= %.5f\n', zetar);
        fprintf('The empirical coefficient p = %.5f\n', n);
        fprintf('The empirical coefficient a (1/L)
= %.5f\n', ap);
        elseif stexture==5;
            fprintf('Soil was classified as "SILT"\n');
            fprintf('The saturated soil conductivity; Kzz (L/T)
= %.5f\n', Kzz);
            fprintf('The saturated moisture content; zeta-s
(L^3/L^3)= %.5f\n', zetas);
            fprintf('The residual moisture content; zeta-r (L^3/L^3)
= %.5f\n', zetar);
            fprintf('The empirical coefficient p = %.5f\n', n);
            fprintf('The empirical coefficient a (1/L)
= %.5f\n', ap);
            elseif stexture==6;
                fprintf('Soil was classified as "SILT LOAM"\n');
                fprintf('The saturated soil conductivity; Kzz (L/T)
= %.5f\n', Kzz);
                fprintf('The saturated moisture content; zeta-s
(L^3/L^3)= %.5f\n', zetas);
                fprintf('The residual moisture content; zeta-r (L^3/L^3)
= %.5f\n', zetar);
                fprintf('The empirical coefficient p= %.5f\n', n);
                fprintf('The empirical coefficient a (1/L)
= %.5f\n', ap);
                elseif stexture==7;
                    fprintf('Soil was classified as "SILTY CLAY"\n');
                    fprintf('The saturated soil conductivity; Kzz (L/T)
= %.5f\n', Kzz);
                    fprintf('The saturated moisture content; zeta-s
(L^3/L^3)= %.5f\n', zetas);
                    fprintf('The residual moisture content; zeta-r (L^3/L^3)
= %.5f\n', zetar);
                    fprintf('The empirical coefficient p = %.5f\n', n);
                    fprintf('The empirical coefficient a (1/L)
= %.5f\n', ap);
                    elseif stexture==8;
                        fprintf('Soil was classified as "SILTY CLAY LOAM"\n');
                        fprintf('The saturated soil conductivity; Kzz (L/T)
= %.5f\n', Kzz);
                        fprintf('The saturated moisture content; zeta-s
(L^3/L^3)= %.5f\n', zetas);
                        fprintf('The residual moisture content; zeta-r (L^3/L^3)
= %.5f\n', zetar);
                        fprintf('The empirical coefficient p = %.5f\n', n);
                        fprintf('The empirical coefficient a (1/L)
= %.5f\n', ap);
                        elseif stexture==9;
                            fprintf('Soil was classified as "SAND"\n');
                            fprintf('The saturated soil conductivity; Kzz (L/T)
= %.5f\n', Kzz);
                            fprintf('The saturated moisture content; zeta-s
(L^3/L^3)= %.5f\n', zetas);

```

```

        fprintf('The residual moisture content; zeta-r (L^3/L^3)
= %.5f\n', zetar);
        fprintf('The empirical coefficient p = %.5f\n', n);
        fprintf('The empirical coefficient a (1/L)
= %.5f\n', ap);
        elseif stexture==10;
            fprintf('Soil was classified as "SANDY CLAY"\n');
            fprintf('The saturated soil conductivity; Kzz (L/T)
= %.5f\n', Kzz);
            fprintf('The saturated moisture content; zeta-s
(L^3/L^3)= %.5f\n', zetas);
            fprintf('The residual moisture content; zeta-r (L^3/L^3)
= %.5f\n', zetar);
            fprintf('The empirical coefficient p= %.5f\n', n);
            fprintf('The empirical coefficient a (1/L)
= %.5f\n', ap);
            elseif stexture==11;
                fprintf('Soil was classified as "SANDY CLAY LOAM"\n');
                fprintf('The saturated soil conductivity; Kzz (L/T)
= %.5f\n', Kzz);
                fprintf('The saturated moisture content; zeta-s
(L^3/L^3)= %.5f\n', zetas);
                fprintf('The residual moisture content; zeta-r (L^3/L^3)
= %.5f\n', zetar);
                fprintf('The empirical coefficient p = %.5f\n', n);
                fprintf('The empirical coefficient a (1/L)
= %.5f\n', ap);
                elseif stexture==12;
                    fprintf('Soil was classified as "SANDY LOAM"\n');
                    fprintf('The saturated soil conductivity; Kzz (L/T)
= %.5f\n', Kzz);
                    fprintf('The saturated moisture content; zeta-s
(L^3/L^3)= %.5f\n', zetas);
                    fprintf('The residual moisture content; zeta-r (L^3/L^3)
= %.5f\n', zetar);
                    fprintf('The empirical coefficient p = %.5f\n', n);
                    fprintf('The empirical coefficient a (1/L) = %.5f\n', ap);
                end
            end
        end

% ##### Display the qz and zeta #####
fprintf('.....\n');
fprintf('Average Darcian Velocity; qz (L/T) = %.10f\n', qAV);
fprintf('Average Soil Moisture Content; zeta (o/o) = %
.10f\n', zAV);
fprintf('Constant Flux of upper boundary; qtop (L/T) =
%.10f\n', qsol(1, nt));
fprintf('Constant Flux of lower boundary; qbot (l/T) =
%.10f\n', qsol(nelem, nt));
fprintf('
\n');
wfinal=wsol(:, nt);
zfinal=zsol(:, nt);
kfinal=ksol(:, nt);
Cfinal=Csol(:, nt);
wresult=wmw(:, :);
zresult=wmz(:, :);
resultw=intw;

```



```

MassBalance=MB(:,:);
fprintf('~~~~~\n');
fprintf(' The considered contaminant is non-reactive
constituents(tracer).\n');
fprintf('.....\n');
fprintf(' The dispersion -diffusion parameters are:      \n');
fprintf('          \n');
fprintf('The molecular diffusion coefficient; Dm (L^2/T)      =
%.10f\n', Dmm);
fprintf('The fraction of molecular diffusion; Ff (L^2/T)      =
%.10f\n', mfactor);
fprintf('Average dispersion-diffusion coefficient; D (L^2/T)  =
%.10f\n', DAV);
fprintf('.....\n');
fprintf('The kinetics reaction rates are:          \n');
fprintf('The retardation coefficient; kapta      \ = %.10f\n', 1);
fprintf('The decay rate constant; lamda (1/T)    = %.10f\n', 0);
fprintf('.....\n');
fprintf('Constant concentration of upper boundary; Ctop (M/L^3) =
%.10f\n', Ctop);
fprintf('Constant concentration of lower boundary; Cbot (M/L^3) =
%.10f\n', Cbot);
fprintf('          \n');
fprintf('          \n');
fprintf('##### THE WATER MOVEMENT AND SOLUTE TRANSPORT RESULTS
#####\n');
fprintf('          \n');
fprintf(' The final time for this calculation; tf (T)      =
%.4f\n', tf);
fprintf('          \n');
watersolute_res=zeros(nnode,4);
for i=1:1:nnode;
    watersolute(i,1)=gcoord(i,:);
    watersolute(i,2)=wfinal(i,:);
    watersolute(i,3)=zfinal(i,:);
    watersolute(i,4)=Cfinal(i,:);
end
fprintf(' DEPTH   Pressure   Volumetric   Conc. \n');
fprintf(' -above   Head       Moisture   Tracer\n');
fprintf(' datum-   Content     \n');
fprintf(' (L)      (L)          (M/L^3)\n');
fprintf('===== ===== ===== =====\n');
format short e
watersolute

```

APPENDIX B

Water retention curve of sand and soil



B.1 Water retention curve

Dimension of testing Zeolite column: Inner diameter 6.50 cm, Cross section area 33.2 cm², Total volume 663.325 cm³

Table B.1 Observation data of hydraulic properties in zeolite sample

Volume of water (cm ³)	weight (g)	Packing in bulk density (g/cm ³)	Moisture content (%)	Volumetric water content (%)	Pressure head (centibar)	Pressure head (cmH ₂ O)
0	113.4	1.286	0.000	0.00	-20.0	-203.94
0.5	113.4	1.286	0.493	0.00	-14.0	-142.76
1	113.4	1.286	0.764	0.01	-13.0	-132.56
1.5	113.4	1.286	1.111	0.01	-10.5	-107.07
2	113.4	1.286	1.459	0.01	-9.0	-91.77
4	113.4	1.286	5.473	0.05	-5.0	-50.99
6	113.4	1.286	6.274	0.06	-4.5	-45.89
8	113.4	1.286	8.115	0.08	-4.0	-40.79
10	113.4	1.286	12.469	0.12	-3.0	-30.59
15	113.4	1.286	11.034	0.11	-3.0	-30.59
20	113.4	1.286	14.718	0.15	-3.0	-30.59
20	113.4	1.286	19.927	0.20	-3.0	-30.59
25	113.4	1.286	27.918	0.28	-2.5	-25.49
30	113.4	1.286	23.917	0.24	-2.5	-25.49
40	113.4	1.286	31.853	0.32	-2.0	-20.39
50	113.4	1.286	40.192	0.40	-0.5	-5.10
>50	113.4	1.286	44.827	0.45	0.0	0.00

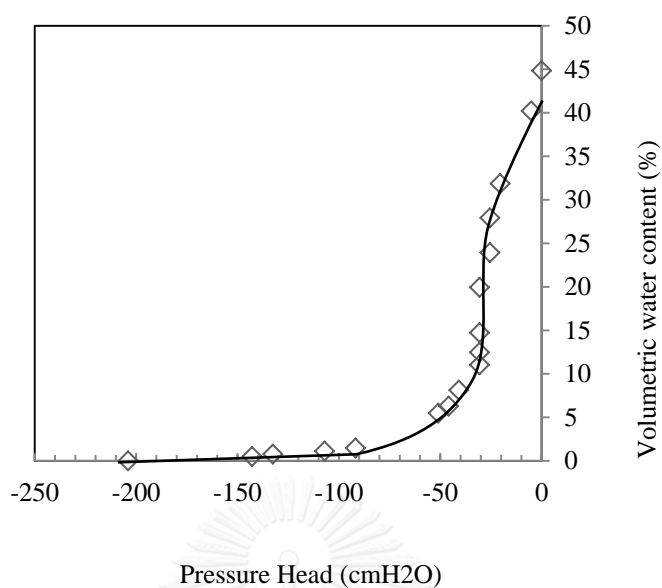


Figure B.1 Water retention curve of zeolite

van Genuchten hydraulic properties coefficients were determined. The mid point of water content; θ_p , was evaluated as follows.

$$\theta_p = \frac{\theta_s + \theta_r}{2}$$

The slope; S at point p was determined graphically from the experimental sand-water retention curve. The dimensionless slope; S_p was calculated graphically from the water retention curve.

$$S_p = \frac{S}{\theta_s - \theta_r}$$

The coefficient m was determined from the value of S_p with this given formula.

$$m = 1 - \exp(-0.8S_p) \text{ with } 0 < S_p \leq 1 \text{ or}$$

$$m = \frac{0.5755}{S_p} + \frac{0.1}{S_p^2} + \frac{0.025}{S_p^3} \text{ with } S_p > 1$$

Then the coefficients, p and a were analysed by using the bubbling pressure. The equations were provided as follows.

$$p = \frac{1}{1-m} \text{ and } a = \frac{1}{h_b} (2^{1/m} - 1)^{1-m}$$

Determinations of hydraulic properties coefficients are given in Figure B.2.

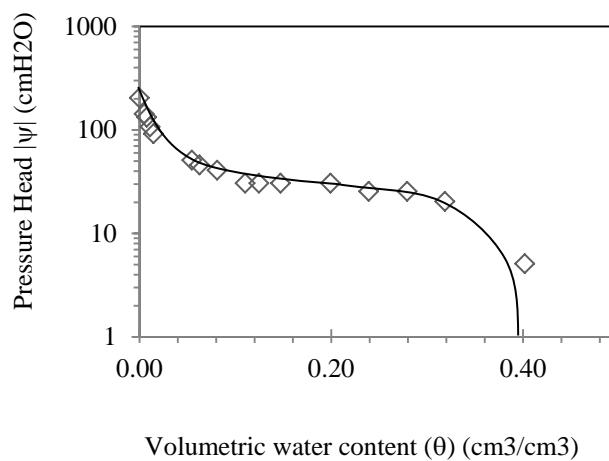


Figure C.2 zeolite water retention curve

At the middle volumetric water content, θ_p , the slope of the curve, S is 0.069. The term Sp is 0.069. The bubbling pressure; $\log h_b$ is 5.1. The coefficients of m , p and a are 0.054, 1.057 and 0.148, respectively.

Dimension of testing sand-manure column: Inner diameter 6.50 cm, Cross section area 33.2 cm², Total volume 663.325 cm³

Table B.2 Observation data of hydraulic properties in sand-manure sample

Volume of water (cm ³)	weight (g)	Packing in bulk density (g/cm ³)	Moisture content (%)	Volumetric water content (%)	Pressure head (centibar)	Pressure head (cmH ₂ O)
0	46.7	0.529	1.45	0.01	-22	-224.34
0.5	46.7	0.529	2.51	0.03	-22	-224.34
1	46.7	0.529	3.46	0.03	-20	-203.94
1.5	46.7	0.529	5.67	0.06	-18	-183.55
2	46.7	0.529	7.48	0.07	-14	-142.76
4	46.7	0.529	9.53	0.10	-12	-122.37
6	46.7	0.529	10.79	0.11	-5	-50.99
8	46.7	0.529	16.41	0.16	-5	-50.99
10	46.7	0.529	21.13	0.21	-4	-40.79
15	46.7	0.529	25.95	0.26	-3	-30.59
20	46.7	0.529	31.17	0.31	-3	-30.59
25	46.7	0.529	34.74	0.35	-2	-20.39
30	46.7	0.529	43.38	0.43	-1	-10.20
40	46.7	0.529	42.57	0.43	-1	-10.20
50	46.7	0.529	42.14	0.42	-0.5	-5.10
>50	46.7	0.529	44.000	0.44	0.0	0.00

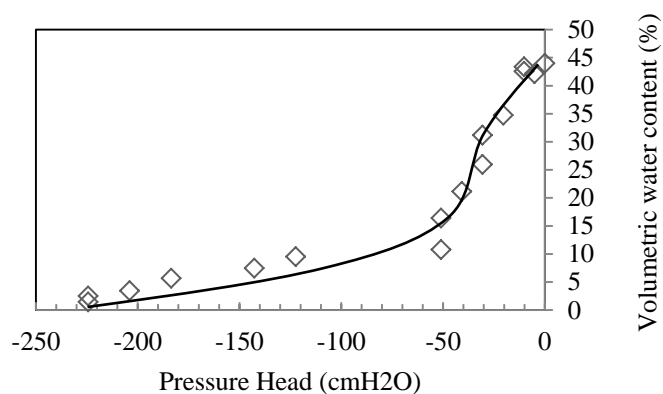


Figure B.3 Water retention curve of sand-manure

van Genuchten model applied to the data observed in the soil column. The soil water retention curve is given in Figure B.4. The saturated volumetric water content; θ_s is 0.441 and residual moisture content; θ_r is 0.014. The volumetric moisture content at P ; θ_p is 0.208, and the slope; S is 0.223. The S_p is 0.507. $\text{Log}(h_b)$ is 2.5. The coefficients of m , p and a are 0.180, 1.040 and 0.052, respectively.

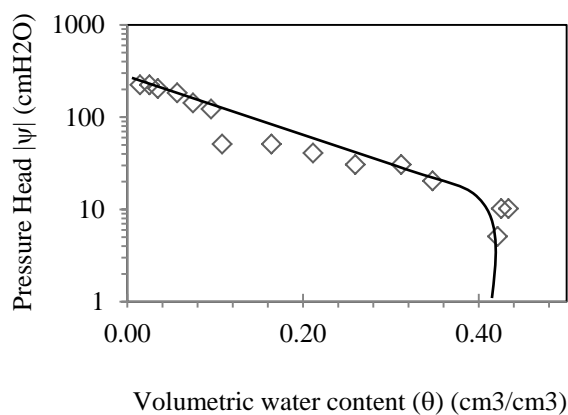


Figure B.4 Sand-manure water retention curve

APPENDIX C

Sequential Extraction

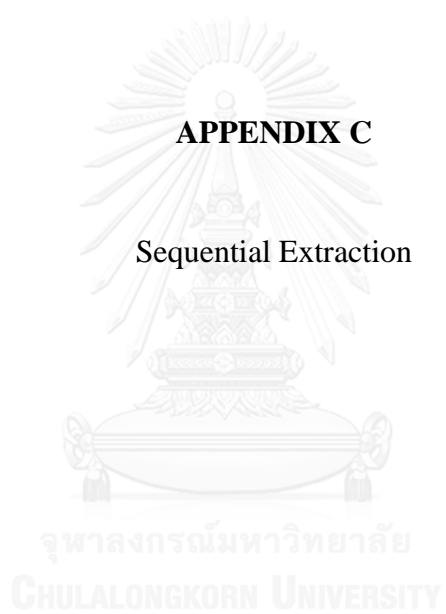


Table C.1 Sequential Extraction of manure

Chemical form (%)	manure (mg/L)			Avg
Water soluble fraction	0.14	0.150	0.13	0.140
Exchangeable	0.12	0.089	0.06	0.090
Bound-to-carbonates	0.104	0.079	0.086	0.090
Bound-to-Fe & Mn oxides	0.08	0.030	0.1	0.070
Bound-to-organic matter	0.21	0.190	0.2	0.200
Residual	0.258	0.205	0.257	0.240

Table C.2 Sequential Extraction of biosorbent: 0-3.5 cm of manure column

Chemical form (%)	0-3.5 cm (mg/L)			Avg
Water soluble fraction	0.156	0.180	0.145	0.160
Exchangeable	0.15	0.069	0.23	0.150
Bound-to-carbonates	0.22	0.260	0.239	0.240
Bound-to-Fe & Mn oxides	0.2	0.220	0.21	0.210
Bound-to-organic matter	0.1	0.150	0.2	0.150
Residual	0.5	0.500	0.5	0.500

Table C.3 Sequential Extraction of biosorbent : 3.5-7 cm of manure column

Chemical form (%)	3.5-7 cm(mg/L)			Avg
Water soluble fraction	0.103	0.150	0.047	0.100
Exchangeable	0.149	0.155	0.145	0.150
Bound-to-carbonates	0.24	0.260	0.22	0.240
Bound-to-Fe & Mn oxides	0.2	0.210	0.22	0.210
Bound-to-organic matter	0.19	0.100	0.159	0.150
Residual	0.54	0.600	0.36	0.500

Table C.4 Sequential Extraction of biosorbent: 7.5-11 cm of manure column

Chemical form (%)	7.5-11 cm (mg/L)			Avg
Water soluble fraction	0.09	0.100	0.079	0.090
Exchangeable	0.18	0.170	0.13	0.160
Bound-to-carbonates	0.036	0.054	0.029	0.040
Bound-to-Fe & Mn oxides	0.13	0.150	0.11	0.130
Bound-to-organic matter	0.22	0.220	0.19	0.210
Residual	0.45	0.52	0.5	0.490

Table C.5 Sequential Extraction of biosorbent: 11-14.5 cm of manure column

Chemical form (%)	11-14.5 cm (mg/L)			Avg
Water soluble fraction	0.063	0.080	0.038	0.060
Exchangeable	0.21	0.220	0.2	0.210
Bound-to-carbonates	0.208	0.225	0.198	0.210
Bound-to-Fe & Mn oxides	0.21	0.210	0.21	0.210
Bound-to-organic matter	0.41	0.400	0.42	0.410
Residual	0.5	0.50	0.5	0.500

Table C.6 Sequential Extraction of zeolite

Chemical form (%)	Zeolite (mg/L)			Avg
Water soluble fraction	0.033	0.024	0.043	0.033
Exchangeable	0.040	0.025	0.056	0.040
Bound-to-carbonates	0.010	0.012	0.009	0.010
Bound-to-Fe & Mn oxides	0.021	0.031	0.01	0.021
Bound-to-organic matter	0.077	0.088	0.065	0.077
Residual	0.390	0.440	0.32	0.383

Table C.7 Sequential Extraction of biosorbent: fed Pb(II) only to zeolite column

Chemical form (%)	Zeolite column fed Pb(II) only (mg/L)			Avg
Water soluble fraction	0.028	0.030	0.027	0.028
Exchangeable	0.157	0.170	0.145	0.157
Bound-to-carbonates	0.040	0.052	0.02	0.037
Bound-to-Fe & Mn oxides	0.064	0.031	0.06	0.052
Bound-to-organic matter	0.730	0.810	0.65	0.730
Residual	2.197	2.080	1.9	2.059

Table C.8 Sequential Extraction of biosorbent fed molasses + Pb(II) to zeolite column

Chemical form (%)	Biobarrier			Avg
Water soluble fraction	0.023	0.030	0.027	0.027
Exchangeable	0.115	0.170	0.145	0.143
Bound-to-carbonates	0.28	0.052	0.02	0.117
Bound-to-Fe & Mn oxides	0.033	0.031	0.06	0.041
Bound-to-organic matter	0.347	0.810	0.65	0.602
Residual	2.055	2.10	1.98	2.045

APPENDIX D

Microbial analysis

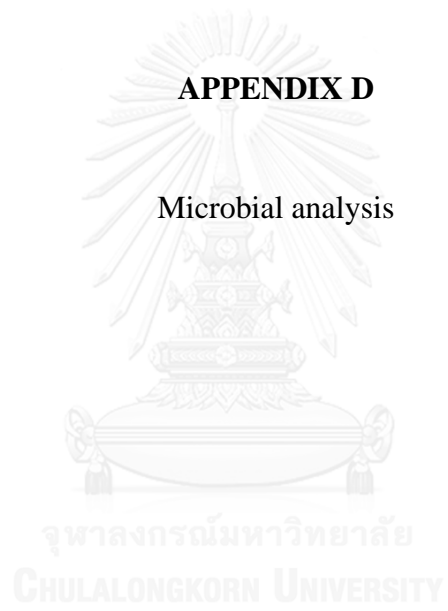


Table D.1 Nucleotide sequences of primers used in this study

Primer name	Nucleotide sequences (5' - 3')	Reference
341F	CCTACGGGAGGCAGCAG	Muyzeret <i>al.</i> , 1993
520R	ACCGCGGCTGCTGGC	
ITS1	TCCGTAGGTGAACCTGCGG	White <i>et al.</i> , 1990
ITS4	TCCTCCGCTTATTGATATGC	
GC clamp	CGCCCGCCGCGCCCCGCGCCCGTCCCG CCGCCCCCGCCCCG	Kim et al, 2002

Table D.2 Sequencing of bacterial from manure as biobarrier

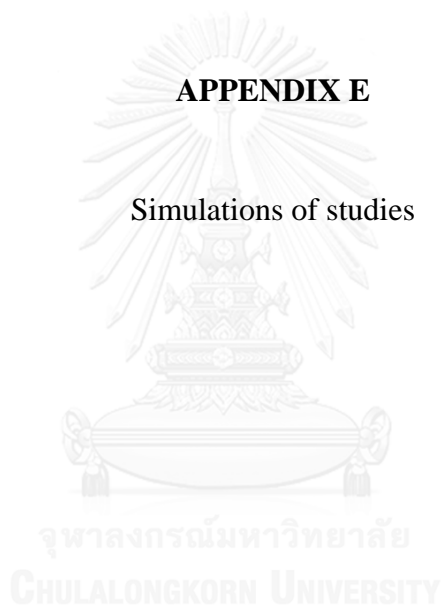
Band	Matching	Sequences
B2	<i>Bacillus sp.</i>	CGGGAGGCAGCAGTGGGGAATATTGCACAATGGGCGAA AGCCTGATGCAGCAACGCCGCGTGAGTGATGAAGGTCT TCGGATTGTAAAGCTCTGTTGTTAGGGAAGAACAAGTA CAAGAGTAACTGCTTGTACCTTGACGGTACCTAACCAG AAAGCCACGGCTAACTACGTGCCAGCAG
B3	<i>Bacillus sp.</i>	CGGCTGCTGGCACGTAGTTAGCCGTGGCTTTCTGGTTAG GTACCGTCAAGGTACGAGCAGTTACTCTCGTACTTGTTC TTCCCTAACAAACAGAGTTTTACGATCCGAAAACCTTCAT CACTCACGCGGCGTTGCTCCGTCAGACTTTCGTCCATTG CGGAAGATTCCCTACTGCTGCCTCC
B4	<i>Clostridium sp.</i>	TCTACGGGAGGCAGCAGTGGGGAATATTGCACAATGGG CGAAAGCCTGATGCAGCAACGCCGCGTGAGTGATGAAG GTCTTCGGATTGTAAAACCTGTCTTTTGGGACGATAAT GACGGTACCAAAGGAGGAAGCCACGGCTAACTACGTGC CAGCAGCCGCGGTAAT
B5	<i>Sporolactobacillus nakayamae</i>	TTCCTACGGGAGGCAGCAGTAGGGAATCTTCCACAATG GACGAAAGTCTGATGGAGCAACGCCGCGTGAGCGAAGA AGGTTTTTCGGATCGTAAAGCTCTGTTGCCGGAGAAGAA TGAGTATGAGAGGAAATGCTTGTACTGTGACGGTATCC GGCCAGAAAGCCACGGCTAACTAC
B6	<i>Clostridium sp.</i>	GATTACCGCGGCTGCTGGCACGTAGTTAGCCGTGGCTTC CTCCTTTGGTACCGTCATTATCGTCCCAGAAGACAGAGC TTTACAATCCGAAGACCTTCATCACTCACGCGGCGTTGC TGCATCAGAGTTTCCTCCATTGTGCAATATTCCCCACTG CTGCCTCCCGTAGGAATCA
B7	<i>Clostridium pasteurianum</i>	CGATTCTACGGGAGGCAGCAGTGGGGAATATTGCACA ATGGGCGAAAGCCTGATGCAGCAACGCCGCGTGAGTGA TGACGGTCTTCGGATTGTAAAGCTCTGTCTTCAGGGACG ATAATGACGGTACCAAAGGAGGAAGCCACGGCTAACTA CGTGCCAGCAGCCGCGGTAAT

Table D.3 Sequencing of bacterial from zeolite as biobarrier

Band	Matching	Sequences
B1	<i>Nostoc sp.</i>	ATTACCGCGGCTGCTGGCACAGAGTTAGCC GATACTTATTCCTTAGATACTGTCATTTTTTT CATTTCTAAGAAAAGACCTTTACGACTTAG CCTTCTTCGGTCACGTGGTATGGCTCCGTCA AGCTTTCGCTCATTGCGGAATATTCCTCACT GCTGCCTCCCGTAGGAA
B8	<i>Bradyrhizobium sp.</i>	ATTACCGCGGCTGCTGGCACGAAGTTAGCC GGGGCTTATTCTTGCGGTACCGTCATTATCT TCCCGCACAAAAGAGCTTTACAACCCTAGG GCCTTCATCACTCACGCGGCATGGCTGGAC CAGGCTTGCGCCCATGTCCAATATTCCCA CTGCTGCCTCCCGTAGG
B9	<i>Bacillus sp.</i>	TTACCGCGGCTGCTGGCACGTAGTTAGCCG TGGCTTTCTGGTTAGGTACCGTCAAGGTACG AGCAGTACTCTCGTACTTGTTCTTCCCTAA CAACAGAGTTTTACGATCCGAAAACCTTCA TCACTCACGCGGCGTTGCTCCGTCAGACTTT CGTCCATTGCGGAAGATTCCCT
B10	<i>Nostoc sp.</i>	TTCGATTCCCTACGGGAGGCAGCAGTGAGGA ATATTCCGCAATGAGCGAAAGCTTGACGGA GCCATACCACGTGACCGAAGAAGGCTAAGT CGTAAAGGTCTTTTCTTAGAAATGAAAAAA ATGACAGTATCTAAGGAATAAGTATCGGCT AACTCTGTGCCAGCAGCCGCGGTAATCACT

APPENDIX E

Simulations of studies



E.1 Transport of Pb(II) movement in sand-manure column

hrs	0 cm (bottom)	5 cm	7.5 cm	10 cm	15 cm	16 cm (top)
	Pb(II) conc. (mg/L)	Pb(II) conc. (mg/L)	Pb(II) conc. (mg/L)	Pb(II) conc. (mg/L)	Pb(II) conc. (mg/L)	Pb(II) conc. (mg/L)
	Simulation	Simulation	Simulation	Simulation	Simulation	Simulation
0	0.0000	0.0000	0.0000	0.0000	0.0000	0.2100
1	0.0000	0.0000	0.0000	0.0000	0.0000	0.2100
2	0.0000	0.0000	0.0000	0.0000	0.0000	0.2100
4	0.0000	0.0000	0.0000	0.0000	0.0000	0.2100
8	0.0000	0.0000	0.0000	0.0000	0.0000	0.2100
12	0.0000	0.0000	0.0000	0.0000	0.0590	0.2100
24	0.0000	0.0000	0.0000	0.0000	0.1200	0.2100
48	0.0000	0.0000	0.0000	0.0370	0.1440	0.2100
60	0.0000	0.0000	0.0010	0.0740	0.1530	0.2100
72	0.0000	0.0000	0.0020	0.0800	0.1500	0.2100
96	0.0000	0.0000	0.0030	0.0850	0.1600	0.2100
120	0.0000	0.0002	0.0034	0.0913	0.1700	0.2100
144	0.0000	0.0003	0.0036	0.1000	0.1800	0.2100
168	0.0000	0.0005	0.0038	0.1100	0.1900	0.2100
192	0.0000	0.0006	0.0040	0.1200	0.2000	0.2100
216	0.0000	0.0007	0.0047	0.1250	0.2100	0.2100
240	0.0000	0.0008	0.0050	0.1300	0.2100	0.2100
264	0.0000	0.0009	0.0110	0.1350	0.2100	0.2100
288	0.0000	0.0010	0.0120	0.1400	0.2100	0.2100
312	0.0000	0.0011	0.0130	0.1450	0.2100	0.2100
336	0.0000	0.0012	0.0135	0.1500	0.2100	0.2100
360	0.0000	0.0015	0.0138	0.1550	0.2100	0.2100
480	0.0000	0.0017	0.0140	0.1600	0.2100	0.2100
600	0.0000	0.0019	0.0142	0.1700	0.2100	0.2100
624	0.0000	0.0019	0.0200	0.1800	0.2100	0.2100
648	0.0000	0.0019	0.0300	0.1800	0.2100	0.2100
672	0.0000	0.0019	0.0400	0.1800	0.2100	0.2100
696	0.0000	0.0020	0.0480	0.1800	0.2100	0.2100
720	0.0000	0.0037	0.0490	0.1800	0.2100	0.2100
840	0.0000	0.0100	0.0500	0.1800	0.2100	0.2100
960	0.0000	0.0200	0.0600	0.1800	0.2100	0.2100
1200	0.0000	0.0380	0.0690	0.1800	0.2100	0.2100
1440	0.0000	0.0480	0.0700	0.1800	0.2100	0.2100
1680	0.0480	0.0480	0.0800	0.1800	0.2100	0.2100
1920	0.0480	0.0480	0.0900	0.1800	0.2100	0.2100

E.2 Pb(II) movement pass through zeolite column: transport part and retardation
(continued)

hrs	0 cm (bottom)	5 cm	7.5 cm	10 cm	15 cm	17.5 cm	20 cm (top)
	Pb(II) conc. (mg/L)	Pb(II) conc. (mg/L)	Pb(II) conc. (mg/L)	Pb(II) conc. (mg/L)	Pb(II) conc. (mg/L)	Pb(II) conc. (mg/L)	Pb(II) conc. (mg/L)
	Simulati on	Simulati on	Simulati on	Simulati on	Simulati on	Simulati on	Simulati on
0	0.0000	0.0000	0.0000	0.0000	0.0000	0.0000	0.2000
1	0.0000	0.0000	0.0000	0.0000	0.0000	0.0000	0.2000
2	0.0000	0.0000	0.0000	0.0000	0.0000	0.0000	0.2000
4	0.0000	0.0000	0.0000	0.0000	0.0000	0.0000	0.2000
8	0.0000	0.0000	0.0000	0.0000	0.0000	0.0000	0.2000
12	0.0000	0.0000	0.0000	0.0000	0.0000	0.0000	0.2000
24	0.0000	0.0000	0.0000	0.0000	0.0000	0.0000	0.2000
48	0.0000	0.0000	0.0000	0.0000	0.0000	0.0000	0.2000
60	0.0000	0.0000	0.0000	0.0000	0.0000	0.0000	0.2000
72	0.0000	0.0000	0.0000	0.0000	0.0000	0.0230	0.2000
96	0.0000	0.0000	0.0000	0.0000	0.0029	0.0530	0.2000
120	0.0000	0.0000	0.0000	0.0000	0.0051	0.0528	0.2000
144	0.0000	0.0000	0.0000	0.0000	0.0072	0.0518	0.2000
168	0.0000	0.0000	0.0000	0.0000	0.0091	0.0517	0.2000
192	0.0000	0.0000	0.0000	0.0000	0.0103	0.0516	0.2000
216	0.0000	0.0000	0.0000	0.0000	0.0119	0.0523	0.2000
240	0.0000	0.0000	0.0000	0.0001	0.0128	0.0528	0.2000
264	0.0000	0.0000	0.0000	0.0002	0.0142	0.0534	0.2000
288	0.0000	0.0000	0.0000	0.0003	0.0146	0.0545	0.2000
312	0.0000	0.0000	0.0000	0.0004	0.0156	0.0552	0.2000
336	0.0000	0.0000	0.0000	0.0005	0.0161	0.0560	0.2000
360	0.0000	0.0000	0.0000	0.0006	0.0168	0.0570	0.2000
480	0.0000	0.0000	0.0000	0.0007	0.0191	0.0611	0.2000
600	0.0000	0.0000	0.0000	0.0008	0.0211	0.0648	0.2000
624	0.0000	0.0000	0.0000	0.0010	0.0231	0.0700	0.2000
648	0.0000	0.0000	0.0000	0.0011	0.0250	0.0750	0.2000
672	0.0000	0.0000	0.0000	0.0012	0.0270	0.0800	0.2000
696	0.0000	0.0000	0.0000	0.0013	0.0290	0.0700	0.2000
720	0.0000	0.0000	0.0000	0.0014	0.0200	0.0800	0.2000

E.2 Pb(II) movement pass through zeolite column: transport part and retardation

(continued)

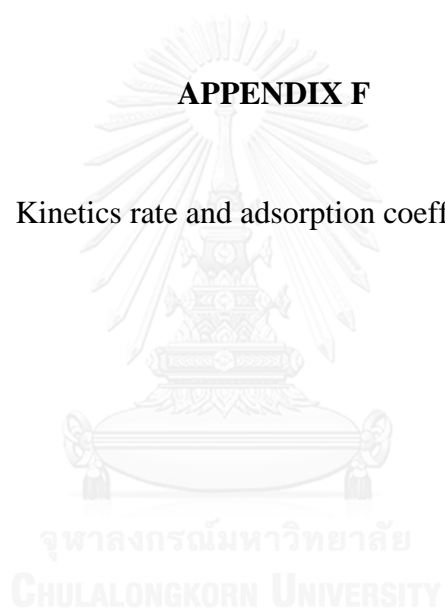
hrs	0 cm (bottom)	5 cm	7.5 cm	10 cm	15 cm	17.5 cm	20 cm (top)
	Pb(II) conc. (mg/L)	Pb(II) conc. (mg/L)	Pb(II) conc. (mg/L)	Pb(II) conc. (mg/L)	Pb(II) conc. (mg/L)	Pb(II) conc. (mg/L)	Pb(II) conc. (mg/L)
	Simulation	Simulation	Simulation	Simulation	Simulation	Simulation	Simulation
840	0.0000	0.0000	0.0000	0.0015	0.0300	0.0900	0.2000
960	0.0000	0.0000	0.0000	0.0016	0.0350	0.1000	0.2000
1200	0.0000	0.0000	0.0000	0.0017	0.0400	0.1200	0.2000
1440	0.0000	0.0000	0.0000	0.0018	0.0500	0.1600	0.2000
1680	0.0000	0.0000	0.0000	0.0020	0.0560	0.1800	0.2000
1920	0.0000	0.0000	0.0001	0.0027	0.0800	0.2000	0.2000
2160	0.0000	0.0015	0.0002	0.0050	0.0800	0.2000	0.2000
2400	0.0000	0.0017	0.0004	0.0080	0.1200	0.2000	0.2000
2640	0.0000	0.0017	0.0021	0.0100	0.1800	0.2000	0.2000
2880	0.0000	0.0018	0.0045	0.0150	0.2000	0.2000	0.2000
3120	0.0000	0.0020	0.0050	0.0170	0.2000	0.2000	0.2000
3360	0.0000	0.0022	0.0060	0.0190	0.2000	0.2000	0.2000
3600	0.0000	0.0030	0.0070	0.0210	0.2000	0.2000	0.2000
3840	0.0000	0.0035	0.0080	0.0230	0.2000	0.2000	0.2000
4080	0.0000	0.0040	0.0088	0.0250	0.2000	0.2000	0.2000
4320	0.0000	0.0045	0.0089	0.0270	0.2000	0.2000	0.2000
4560	0.0000	0.0046	0.0090	0.0290	0.2000	0.2000	0.2000
4800	0.0000	0.0050	0.0095	0.0310	0.2000	0.2000	0.2000
5040	0.0000	0.0055	0.0100	0.0450	0.2000	0.2000	0.2000
5280	0.0000	0.0060	0.0120	0.0480	0.2000	0.2000	0.2000
5520	0.0000	0.0070	0.0130	0.0500	0.2000	0.2000	0.2000
5760	0.0000	0.0080	0.0140	0.0550	0.2000	0.2000	0.2000
6000	0.0000	0.0120	0.0160	0.0600	0.2000	0.2000	0.2000
6240	0.018	0.0180	0.0180	0.0700	0.2000	0.2000	0.2000
6480	0.018	0.0180	0.0180	0.0800	0.2000	0.2000	0.2000

E.2 Pb(II) movement pass through zeolite column: transport part and retardation
(continued)

hrs	0 cm (bottom)	5 cm	7.5 cm	10 cm	15 cm	17.5 cm	20 cm (top)
	Pb(II) conc. (mg/L)	Pb(II) conc. (mg/L)	Pb(II) conc. (mg/L)	Pb(II) conc. (mg/L)	Pb(II) conc. (mg/L)	Pb(II) conc. (mg/L)	Pb(II) conc. (mg/L)
	Simulation	Simulation	Simulation	Simulation	Simulation	Simulation	Simulation
6720	0.018	0.0180	0.0180	0.0800	0.2000	0.2000	0.2000
6960	0.018	0.0180	0.0180	0.0800	0.2000	0.2000	0.2000
7200	0.018	0.0180	0.0180	0.0800	0.2000	0.2000	0.2000
7440	0.018	0.0180	0.0180	0.0800	0.2000	0.2000	0.2000
7680	0.018	0.0180	0.0180	0.0800	0.2000	0.2000	0.2000
7920	0.018	0.0180	0.0180	0.0800	0.2000	0.2000	0.2000
8160	0.018	0.0180	0.0180	0.0800	0.2000	0.2000	0.2000
8400	0.018	0.0180	0.0180	0.0800	0.2000	0.2000	0.2000
8640	0.018	0.0180	0.0180	0.0800	0.2000	0.2000	0.2000
8880	0.018	0.0180	0.0180	0.0800	0.2000	0.2000	0.2000
9120	0.018	0.0180	0.0180	0.0800	0.2000	0.2000	0.2000
9360	0.018	0.0180	0.0180	0.0800	0.2000	0.2000	0.2000
9600	0.018	0.0180	0.0180	0.0800	0.2000	0.2000	0.2000
9840	0.018	0.0180	0.0180	0.0800	0.2000	0.2000	0.2000
10080	0.018	0.0180	0.0180	0.0800	0.2000	0.2000	0.2000
10320	0.018	0.0180	0.0180	0.0800	0.2000	0.2000	0.2000
10560	0.018	0.0180	0.0180	0.0800	0.2000	0.2000	0.2000
10800	0.018	0.0180	0.0180	0.0800	0.2000	0.2000	0.2000

APPENDIX F

Kinetics rate and adsorption coefficients



F.1 Adsorption: Batch studies

P SAT +pb	Mass (mg)	Co (mg/L)	Ct (mg/L)	Blank (mg/L)
0.1	0.5084	10	0.74	0.003
0.1	1.0136	10	1.00	0.003
0.1	2.0334	10	1.40	0.003
0.1	5.0364	10	0.20	0.003
0.1	10.0231	10	0.08	0.003
0.1	20.0091	10	1.28	0.003

Pb only	Mass (mg)	Co (mg/L)	Ct (mg/L)	Blank (mg/L)
0.1	0.5015	10	4.28	0.003
0.1	1.0092	10	0.85	0.003
0.1	2.0208	10	3.54	0.003
0.1	5.0307	10	1.48	0.003
0.1	10.0101	10	0.92	0.003
0.1	20.0171	10	0.63	0.003

P + Pb	Mass (mg)	Co (mg/L)	Ct (mg/L)	Blank (mg/L)
0.1	0.502	10	0.85	0.003
0.1	1.0059	10	0.52	0.003
0.1	2.0249	10	0.18	0.003
0.1	5.0448	10	0.01	0.003
0.1	10	10	0.01	0.003
0.1	20.0132	10	0.01	0.003

F.2 Adsorption: Column studies of biobarrier (continued)

Days	Volumn			Pb(II) +molasses	
	volumn (mL)	volumn (L)	Accum Vol (L)	Co (mg/L)	C (mg/L)
161	400	0.40	28.101	0.255	0.018
162		-	28.10		
163		-	28.10		
164		-	28.10		
165		-	28.10		
166	375	0.38	28.48	0.255	0.011
167	300	0.30	28.78	0.255	0.012
168	400	0.40	29.18	0.308	0.012
169		-	29.18		
170		-	29.18		
171		-	29.18		
172		-	29.18		
173	375	0.38	29.55	0.308	0.013
174	-	-	29.55	0.308	0.013
175	500	0.50	30.05		
176	100	0.10	30.15	0.308	0.015
177	30	0.03	30.18	0.308	0.015
178	160	0.16	30.34	0.308	0.015
179	250	0.25	30.59	0.308	0.011
180	125	0.13	30.72	0.308	0.016
181	160	0.16	30.88	0.270	0.010
182	160	0.16	31.04		
183	180	0.18	31.22		
184	110	0.11	31.33		
185	105	0.11	31.43	0.271	0.013
186	105	0.11	31.54	0.204	0.008
187	100	0.10	31.64	0.204	0.007
188	110	0.11	31.75	0.204	0.001
189	100	0.10	31.85	0.204	0.014
190	100	0.10	31.95		
191	100	0.10	32.05		
192	100	0.10	32.15		
193	150	0.15	32.30		
194	125	0.13	32.42	0.204	0.008
195	100	0.10	32.52	0.204	0.006

F.2 Adsorption: Column studies of biobarrier (continued)

Days	Volumn			Pb(II) +molasses	
	volumn (mL)	volumn (L)	Accum Vol (L)	Co (mg/L)	C (mg/L)
207	175	0.18	33.76	0.204	0.004
208	175	0.18	33.93		
209	175	0.18	34.11	0.204	0.007
210	175	0.18	34.28		
211	125	0.13	34.41	0.204	0.007
212	150	0.15	34.56	0.204	0.009
213	115	0.12	34.67		
214	150	0.15	34.82		
215	110	0.11	34.93	0.204	0.009
216	110	0.11	35.04	0.204	0.009
217	110	0.11	35.15	0.204	0.008
218	120	0.12	35.27		
219	110	0.11	35.38		
220	120	0.12	35.50		
221	110	0.11	35.61	0.204	0.007
222	110	0.11	35.72	0.204	0.010
223	110	0.11	35.83	0.204	0.009
224	110	0.11	35.94		
225	115	0.12	36.06		
226	125	0.13	36.18	0.204	0.009
227	125	0.13	36.31		
228	145	0.15	36.45		
229	150	0.15	36.60	0.203	0.010
230	125	0.13	36.73		
231	135	0.14	36.86	0.185	0.009
232	125	0.13	36.99	0.185	0.009
233	125	0.13	37.11		
234	125	0.13	37.24	0.203	0.017

F.2 Adsorption: Column studies of biobarrier (continued)

Days	Volumn			Pb(II) +molasses	
	volumn (mL)	Volumn (L)	Accum Vol (L)	Co (mg/L)	C (mg/L)
246	125	0.13	38.74	0.22	0.022
247	125	0.13	38.86		
248	125	0.13	38.99		
249	125	0.13	39.11		
250	125	0.13	39.24		
251	125	0.13	39.36	0.22	0.022
252	125	0.13	39.49	0.22	0.022
253	125	0.13	39.61		
254	125	0.13	39.74		
255	125	0.13	39.86		
256	125	0.13	39.99		
257	125	0.13	40.11		
258	125	0.13	40.24	0.22	0.022
259	125	0.13	40.36		
260	125	0.13	40.49	0.22	0.028
261	125	0.13	40.61	0.22	0.028
262	125	0.13	40.74		
263	125	0.13	40.86		
264	125	0.13	40.99		
265	125	0.13	41.11		
266	125	0.13	41.24	0.22	0.028
267	125	0.13	41.36		
268	125	0.13	41.49		
269	125	0.13	41.61	0.22	0.028
270	125	0.13	41.74	0.22	0.03
271	125	0.13	41.86		
272	125	0.13	41.99	0.22	0.034

F.3 Monod constant

Sand-manure biobarrier

hr	COD (mg/L)		COD (mg/L)		
	1 NC pH ๗.๓		1 NC pH 4	1 NC pH 7	1 NC pH 9
	5 g	10 g	5 g	5 g	5 g
0	5130.43	4260.87	4260.87	4173.91	4434.78
1	4173.91	4086.96	4086.96	4086.96	4173.91
13	4173.91	3826.09	4173.91	4260.87	4173.91
48	4100.00	3826.09	4090.43	4175.65	4090.43
72	4000.00	3826.09	3913.04	3739.13	3739.13
96	3920.00	3749.57	3834.78	3664.35	3664.35
120	3841.60	3674.57	3850.00	3652.17	3652.17
144	3073.28	2939.66	3080.00	2921.74	2921.74
168	2458.62	2351.73	2464.00	2337.39	2337.39

hr	COD (mg/L)		COD (mg/L)		
	3 NC pH ๗.๓		3 NC pH 4	3 NC pH 7	3 NC pH 9
	5 g	10 g	5 g	5 g	5 g
0	4260.87	4173.91	4260.87	4260.87	4173.91
1	4086.96	4173.91	4434.78	4000.00	4173.91
13	4086.96	4260.87	4086.96	4260.87	4086.96
48	4005.22	4175.65	4005.22	4175.65	4005.22
72	3913.04	3865.22	3739.13	3739.13	3739.13
96	3834.78	3787.91	3664.35	3664.35	3664.35
120	4000.00	3526.09	3652.17	3478.26	3478.26
144	3200.00	2820.87	2921.74	2782.61	2782.61
168	2560.00	2256.70	2337.39	2226.09	2226.09

hr	COD (mg/L)		COD (mg/L)		
	4 NC pH ๗.๓		4 NC pH 4	4 NC pH 7	4 NC pH 9
	5 g	10 g	5 g	5 g	5 g
0	3652.17	3478.26	3652.17	3826.09	3043.48
1	4000.00	3913.04	4173.91	4173.91	4260.87
13	3913.04	4000.00	4000.00	4086.96	4000.00
48	3834.78	3920.00	3920.00	4005.22	3920.00
72	3565.22	3678.26	3652.17	3739.13	3478.26
96	3493.91	3604.70	3579.13	3664.35	3408.70
120	3478.26	3552.17	3552.17	3565.22	3278.26
144	2782.61	2841.74	2841.74	2852.17	2622.61
168	2226.09	2273.39	2273.39	2281.74	2098.09

Zeolite

COD (mg/L)

hr	Adjust pH				
	1 NC pH ๗.๓		1 NC pH 4	1 NC pH 7	1 NC pH 9
	5 g	10 g	5 g	5 g	5 g
0	5130.43	4260.87	4260.87	4173.91	4434.78
1	4173.91	4086.96	4086.96	4086.96	4173.91
13	4173.91	3826.09	4173.91	4260.87	4173.91
48	4100.00	3826.09	4090.43	4175.65	4090.43
72	4000.00	3826.09	3913.04	3739.13	3739.13
96	3920.00	3749.57	3834.78	3664.35	3664.35
120	3841.60	3674.57	3850.00	3652.17	3652.17
144	3764.77	3601.08	3080.00	2921.74	2921.74
168	3689.47	3529.06	2464.00	2337.39	2337.39

Biobarrier

COD (mg/L)

hr	Adjust pH				
	3 NC pH ๗.๓		3 NC pH 4	3 NC pH 7	3 NC pH 9
	5 g	10 g	5 g	5 g	5 g
0	4260.87	4173.91	4260.87	4260.87	4173.91
1	4086.96	4173.91	4434.78	4000.00	4173.91
13	4086.96	4260.87	4086.96	4260.87	4086.96
48	4005.22	4175.65	4005.22	4175.65	4005.22
72	3913.04	3865.22	3739.13	3739.13	3739.13
96	3834.78	3787.91	3664.35	3664.35	3664.35
120	4000.00	3526.09	3652.17	3478.26	3478.26
144	3200.00	2820.87	2921.74	2782.61	2782.61
168	2560.00	2256.70	2337.39	2226.09	2226.09

